THE THERMAL CONDUCTIVITY AND SPECIFIC HEAT CAPACITY OF A SEMI-CRYSTALLINE POLYMER BELOW 2K

A thesis presented by

PHILIP JAMES MASON, BSc.

to the University of St Andrews

in application for the degree of

Doctor of Philosophy.

CERTIFICATE

I certify that Philip James Mason, BSc, has spent nine terms at research work in the School of Physical Sciences in the University of St Andrews under my direction, that he has fulfilled the conditions of the Resolution of the University Court, 1967, No 1, and that he is qualified to submit the accompanying thesis in application for the Degree of Doctor of Philosophy.

D. M. Finlayson

Research Supervisor

DECLARATION

I hereby certify that this thesis has been composed by me, and is a record of work done by me, and has not previously been presented for a higher degree. The research was carried out in the School of Physical Sciences in the University of St Andrews, under the supervision of Dr. D. M. Finlayson.

P. J. Mason

ABSTRACT

The specific heat capacity of an isotropic polyethylene sample, and 3 extruded polyethylene samples, was measured over the temperature range 0.15K to 1.3K. The specific heat capacity of the isotropic and extruded samples was found to be the same. The temperature dependence of the specific heat capacity was of the form $c(T) = aT + bT^3$. The linear component of the specific heat capacity, was explained in terms of the localised tunnelling states, proposed by Anderson et Al (1972) and by Phillips (1972), present within the amorphous regions of the semi-crystalline polymer. It was concluded that the density of these localised tunnelling states is not affected by extrusion.

The thermal conductivity of 3 of the polyethylene samples was measured over the temperature range 0.08K to 1.8K. It was found that the thermal conductivity has an approximately linear temperature dependence over a significant range of temperature, and that this range of temperature is different for the isotropic and extruded samples. This behaviour is quite different to that observed for purely amorphous materials and cannot be explained solely in terms of tunnelling state scattering theory. It was explained by assuming that the long wavelength phonons dominant at very low temperatures, are scattered by the localised tunnelling states; while the phonons dominant at higher temperatures are scattered by the structure of the semi-crystalline polymer. The phonon mean free path due to structure scattering is obtained using the theory developed by Morgan & Smith (1974), which introduces correlation lengths a_s & a_c, which are related to the dimensions of the structural units present within the amorphous and crystalline regions of the polymer respectively. The differences between the conductivity curves obtained for the isotropic and extruded samples, have been explained using different values of the correlation length a_c, which have been related to the change in the orientation of the crystalline lamellae, which occurs as a result of extrusion.

ACKNOWLEDGEMENTS

I should like to thank both my supervisor Dr. D. M. Finlayson and my wife Hilary Mason, for their encouragement and patience during the preparation of this work.

TABLE OF CONTENTS

CHAPTER I

INTRODUCTION

This work deals with the specific heat capacity and the thermal conductivity of amorphous and semi-crystalline dielectric materials at low temperatures. The specific heat capacity of these materials, which is observed at low temperatures, can be explained in terms of the heat capacity associated with a set of phonons, combined with the heat capacity associated with the localised tunnelling states proposed by Anderson et Al (1972) and by Phillips (1972). As in crystalline dielectric materials, it is assumed that heat is carried through amorphous and semi-crystalline dielectric materials by the phonons, which contribute to the specific heat capacity. Thus the thermal conductivity of these materials depends on the phonon density of states, and on the phonon mean free path, which is determined by the scattering processes which occur in amorphous and semi-crystalline materials.

The thermal conductivity of amorphous materials at very low temperatures, can be explained using either tunnelling state scattering or structure scattering. Tunnelling state scattering is the resonant scattering of phonons by the localised tunnelling states, which contribute to the specific heat capacity. Structure scattering is the scattering of phonons by fluctuations in the properties of disordered materials. Structure scattering theories have been developed by Walton (1974) and by Morgan & Smith (1974).

Semi-crystalline materials such as polyethylene, contain regions of both amorphous and crystalline material. The temperature dependence of the thermal conductivity of semi-crystalline materials, which is observed at low temperatures, differs from that which is observed for purely amorphous materials. The explanation of the conductivity of semi-crystalline materials, provides an obvious test for the theories

developed to explain the conductivity of amorphous materials.

Obvious links exist between the thermal conductivity and the specific heat capacity of amorphous and semi-crystalline dielectric materials. These are: (1) the density of states of the phonons, which carry the heat current and which contribute to the specific heat capacity; (2) the density of the localised tunnelling states, which contribute to the specific heat capacity and which may scatter phonons. Thus any investigation of thermal conductivity at low temperatures, is incomplete without a parallel investigation of the specific heat capacity.

Burgess & Greig (1975) measured the thermal conductivity of 4 polyethylene samples, over the temperature range 3K to 100K. They also measured the specific heat capacity of one polyethylene sample, over the temperature range 10K to 100K. Sample SH0 was an isotropic polyethylene sample, while samples SH1, SH2 & SH3 were extruded. Rogers (1980) measured the thermal conductivity of 2 of these polyethylene samples (SH0 & SH2) over the temperature range 0.14K to 2.9K. Rogers (1980) explained the thermal conductivity of polyethylene, observed over the temperature range 0.14K to 100K, including the differences between the conductivity of the isotropic and extruded samples, using the structure scattering theory developed by Morgan & Smith (1974).

The work reported in this thesis, completes the work begun by Burgess & Greig and continued by Rogers. It consists of the measurements of the specific heat capacity of all 4 polyethylene samples, over the temperature range 0.15K to 1.3K; and the measurement of the thermal conductivity of three of the polyethylene samples (SH0, SH2 & SH3), over the temperature range 0.08K to 1.8K. The measurement of the conductivity of samples SH0 & SH2 performed by Rogers, was repeated; because a change in the slope of the conductivity curve obtained for sample SH3, which occurred at 0.2K, did not occur in the curve obtained for sample SH2 by

Rogers. The extension of the measurements to lower temperatures, and the improvements in experimental technique, which led to a reduction in the experimental scatter, revealed that a change in the slope of the curve obtained for sample SH2, did exist at 0.2K.

Chapter II describes in more detail, the behaviour of the thermal conductivity and the specific heat capacity, of amorphous and semi-crystalline dielectric materials at low temperatures, and the theories which attempt to explain this behaviour. A description of the He^3/He^4 dilution refrigerator used to cool the samples is given in Chapter III. The thermometry techniques required to measure the thermal conductivity and specific heat capacity, at very low temperatures, are discussed in chapter IV. Chapters V & VI describe the experimental measurement of the specific heat capacity, and the analysis of the data generated by this experiment. Chapter VII describes the experimental measurement of the thermal conductivity. Chapter VIII contains a consideration of the experimental results in terms of theory. The conclusions are presented in chapter IX.

CHAPTER II

AN INTRODUCTION TO THE LOW TEMPERATURE THERMAL PROPERTIES OF AMORPHOUS AND SEMI-CRYSTALLINE DIELECTRIC MATERIALS

2.1 An Outline of the Experimental Observations

2.1.1 Thermal Conductivity

Considerable interest in the low temperature thermal properties of amorphous dielectric materials, has arisen from the observation made by Zeller & Pohl (1971), that the thermal conductivities of a wide range of these materials, with very different structures (such as glasses and polymers), exhibit striking similarities both in temperature dependence and in actual values. The variation in the values of the thermal conductivity, obtained using different samples of the same material, is generally less than the experimental error associated with the measurements (Stephens 1976). This observation is in sharp contrast with the fact that for crystalline materials, differences of several orders of magnitude exist between the thermal conductivities of different materials, and also between different samples of the same material. These similarities suggest that any explanation of the thermal conductivity of amorphous materials, should be applicable to all amorphous materials, and independent of the detailed atomic structure of these materials (Zeller & Pohl 1971). It is these similarities, which theoretical models find most difficult to explain.

The thermal conductivity of amorphous materials is in general much smaller than that of crystalline materials, except at high temperatures where they are comparable. At very low temperatures ($T<1K$), the thermal conductivity (k) is found to be related to temperature (T) by the equation $k=bT^n$ where $1.8 < n < 2.0$ and $10^3 < b < 10^4$ and, the conductivity is measured in erg s^{-1} cm^{-1} K^{-1} (Stephens 1973 & 1976, Stephens et Al 1972). As temperature increases the temperature

dependence of k decreases, until between 5K and 10K the conductivity becomes independent of temperature, giving rise to a plateau region. Above 10K, the conductivity starts to increase again with increasing temperature (see figure 2.1). In contrast with crystalline materials, the thermal conductivity of amorphous materials does not decrease with increasing temperature, at any point within the temperature range of interest (0.1K to 100K).

There are distinct differences between the thermal conductivity of semi-crystalline polymers and purely amorphous ones. At low temperatures (below 10K), amorphous polymers have the greater conductivity, while at high temperatures the reverse is true. The conductivity of a semi-crystalline polymer exhibits a temperature dependence between T and T^2 . The plateau and the $T^{1.8}$ dependence below 1K, associated with amorphous materials, do not occur in the conductivity of semi-crystalline materials (Kolouch & Brown 1968, Scott et Al 1973). Some of the more crystalline polymers, such as highly crystalline polyethylene, have a maximum at about 100K. The conductivity of semi-crystalline polymers is found to be sample dependent, both in values and temperature dependence. In particular, changes in manufacture, which alter either the degree of crystallinity or the orientation of the crystalline regions, produce significant changes in the conductivity, which may also be anisotropic (Burgess & Greig 1975, Choy & Greig 1975 & 1977, Gibson et Al 1977).

2.1.2 Specific Heat Capacity

It has been found experimentally, that the variation of the specific heat capacity of an amorphous material with temperature, below 2K, can best be described by the equation $c = aT + bT^3$ (Stephens 1973). Not only is the experimentally observed temperature dependence different to that predicted by the Debye theory at these temperatures; but the cubic term bT^3 is larger (by an arbitrary factor between 1.2

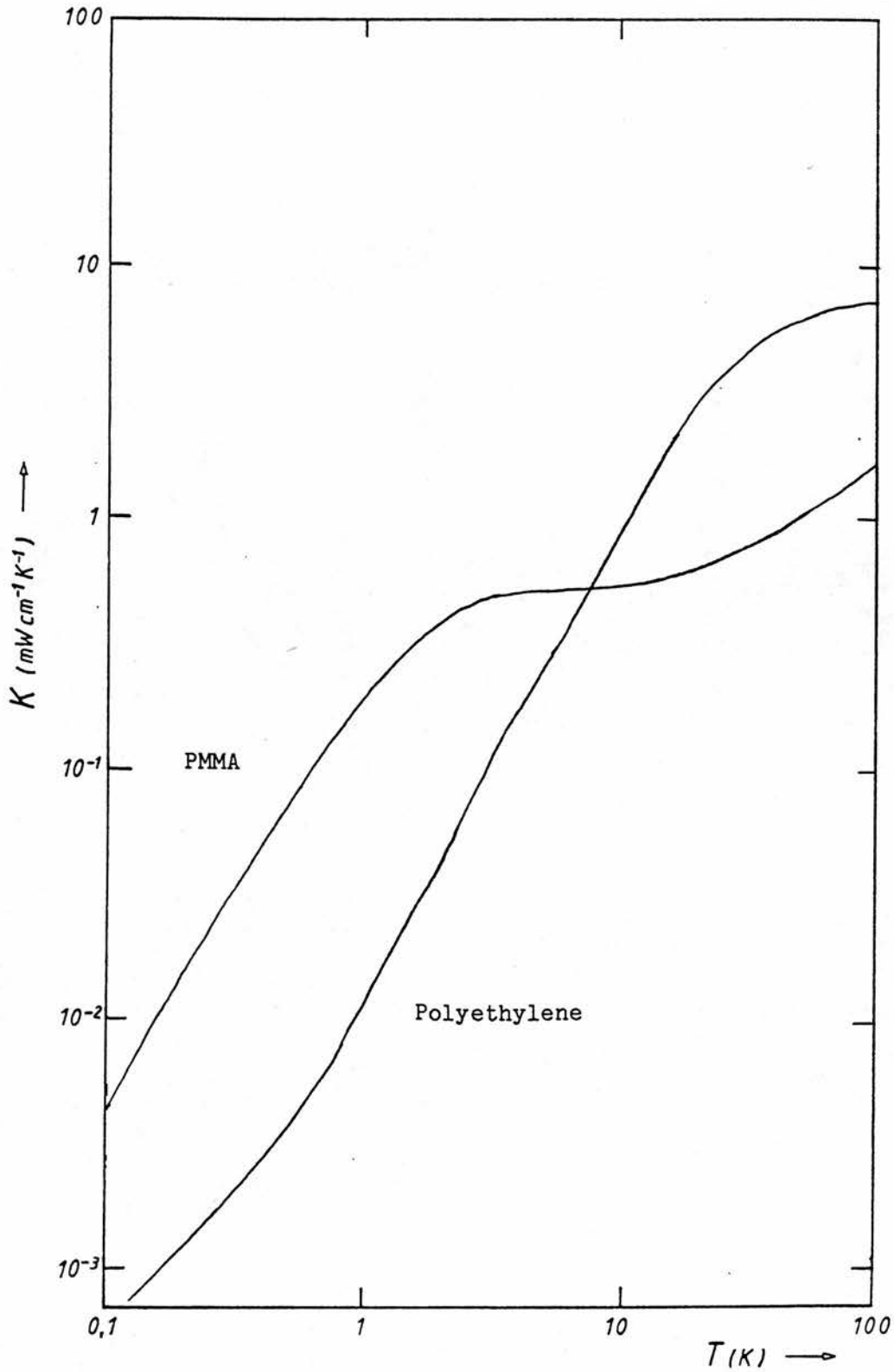

Figure 2.1

The variation of thermal conductivity with temperature for an amorphous polymer, PMMA, and a semi-crystalline polymer, polyethylene.

(taken from Rogers 1980)

and 3.0) than the heat capacity $c_D T^3$ calculated from the Debye theory, with parameter values determined from acoustic measurements. The excess specific heat capacity ($aT + (b-c_D)T^3$) is referred to as the specific heat anomaly. Partially crystalline polymers such as polyethylene also exhibit a similar specific heat anomaly below 2K (Scott et Al 1973), although it is smaller than the anomaly exhibited by amorphous materials.

Tucker & Reese (1967) found that the specific heat capacity of polyethylene over the temperature range 2.5K to 30K, varied linearly with the fractional crystallinity of the samples. From these results, it was possible to deduce the specific heat capacity of purely amorphous and purely crystalline polyethylene. It is not known whether this relationship, between fractional crystallinity and specific heat capacity, exists at lower temperatures. Tucker & Reese observed that while the specific heat of the crystalline phase displayed a T^3 dependence between 2.5K and 12K, an anomaly existed in the specific heat capacity c_A of the amorphous material. This anomaly consisted of a distinct hump in the variation of (c_A/T^3) with temperature, centred at 5K. A very similar anomaly was found in the specific heat capacity of the amorphous polymers PMMA and polystyrene by Choy, Hunt & Salinger (1970). Reese (1969) notes that similar anomalies have been observed in other amorphous materials, such as vitreous silica and germania; and that the size of the anomaly at 4K in polymers, can be reduced by sample irradiation. No such effect has been reported for the low temperature anomaly, suggesting that the anomaly above 1K is distinct from that below 1K (Phillips 1972).

2.2 Theoretical Basis

The low temperature thermal properties of crystalline materials are comparatively well understood. The specific heat capacity can be predicted reasonably well using the Debye theory; and the thermal

conductivity can be explained in terms of the heat carried by a phonon current in conjunction with a variety of scattering mechanisms. Using the relaxation time method to solve the Boltzmann equation, and the assumptions of the Debye theory, it can be shown that the thermal conductivity is given by:

$$k(T) = \frac{1}{3} v \int_0^{x_D} c(x)\, L(x)\, dx \qquad 2.1$$

where the heat capacity per unit volume is given by:

$$c(T) = \int_0^{x_D} c(x)\, dx = \frac{3 K_B^4 T^3}{2\pi^2 v^3 \hbar^3} \int_0^{x_D} \frac{x^4 e^x}{(e^x - 1)^2} dx \qquad 2.2$$

where $x = \frac{\hbar v q}{K_B T}$ and $x_D = \frac{\theta_D}{T} = \frac{\hbar v q_D}{K_B T}$,

$L(x)$ is the phonon mean free path,

v is the phonon velocity averaged over 3 polarizations, and assumed independent of frequency or direction,

K_B is the Boltzmann constant,

$2\pi\hbar$ is Planck's constant,

q is phonon wave number,

θ_D is the Debye temperature and

q_D is the cut-off wave number introduced by the Debye theory.

In general the same approach is used to explain the low temperature properties of amorphous materials. Scattering mechanisms peculiar to amorphous and semi-crystalline materials, are used in conjunction with equation 2.1 to explain the thermal conductivity. These mechanisms are discussed in detail in sections 2.3 to 2.5. Experiments justifying the assumption, that the heat current is carried in amorphous materials by phonons with a Debye density of states, are described in section 2.6, although this assumption was made prior to these experiments. Similarly the heat capacity of an amorphous material is assumed to be the sum of contributions from a Debye set of phonons and other states associated with the movement of atoms or groups of atoms in amorphous materials.

As yet the behaviour of amorphous and semi-crystalline materials is not well understood, in that no one description of the amorphous state and the processes which occur in it, can explain all the experimental observations. A good introduction to the theories of thermal conduction in both crystalline and amorphous materials is given by Berman (1976).

The dominant phonon approximation is particularly useful in the analysis of thermal conductivity data (Zeller & Pohl 1971). In this approximation, the phonon mean free path at a given temperature, is assumed initially to be independent of frequency so that:

$$k(T) = \tfrac{1}{3} v\, L(T) \int_0^{\frac{\theta_D}{T}} c(x)\, dx = \tfrac{1}{3} v\, c(T)\, L(T)$$

The mean free path obtained in this manner from the experimental data, is assumed to correspond to the mean free path of those phonons which contribute most to the specific heat capacity. These phonons are referred to as the dominant phonons, and their frequency is given by:

$$w_{DOM} = \frac{4\, K_B T}{\hbar} \quad \text{for} \quad T < \frac{\theta_D}{4} \quad \text{and} \quad w_{DOM} = \frac{K_B \theta_D}{\hbar} \quad \text{for} \quad T \geqslant \frac{\theta_D}{4} \ .$$

Using this approximation, the relationship between phonon frequency and mean free path can be deduced without any knowledge of the scattering mechanism involved.

2.3 Early Theories

Klemens (1951) suggested that phonons travelling through amorphous material, should be scattered by fluctuations in the properties of the material, and obtained using this model a mean free path for phonons $L(q) \propto q^{-2}$. Klemens assumed that transverse waves were scattered much more strongly than longitudinal waves, which therefore dominated the low temperature conductivity. At higher temperatures, longitudinal waves are scattered into transverse waves as a result of anharmonic normal processes, limiting the mean free path of the longitudinal phonons, giving rise to the conductivity plateau. At

higher temperatures, the conductivity increases again, following the increasing heat capacity of the phonon system. The high frequency phonons dominant at these temperatures, have a constant mean free path, comparable to the dimensions of the structural units found within the material (Kittel scattering).

The Klemens theory of structure scattering predicts that at very low temperatures the conductivity (k) should be proportional to temperature (T). In order to explain the temperature dependence ($k \propto T^n$ where $n > 1$), observed at low temperatures for glasses and polymers, Chang & Jones (1962) suggested that an extra scattering mechanism existed, which introduced a frequency independent mean free path, so that the total mean free path was given by: $\frac{1}{L(q)} = \frac{a\,q^2}{A} + \frac{1}{L_c}$. This extra scattering length was assumed to be the result of phonon scattering by internal boundaries present within glasses and polymers. Reese & Tucker (1965) found some correlation between this scattering length and the dimensions of the spherulites present in a variety of polymer samples. However Kolouch & Brown (1968) found a correlation between this parameter and the thickness of the lamellae found in the semi-crystalline polymer, polyethylene (see section 2.7.1). Although the Chang-Jones theory was used to explain the thermal conductivity of glasses, no firm evidence for the existence of these internal boundaries in glasses was forthcoming.

Measurements of the conductivity of polyethylene revealed a change in the temperature dependence of the conductivity; between 4K and 1K the conductivity varied as $T^{1.9}$, while between 0.5K and 0.15K it varied as $T^{1.1}$ (Giles & Terry 1969, Scott et Al 1973). Modifications to the Chang Jones model were suggested in an attempt to explain these observations. Scott et Al (1973) modified the phonon density of states, while Phillips (1971) used a modified expression for the phonon mean free path. Both theories were based on a consideration of the

microscopic structure of polyethylene and provided an adequate description of the experimental data. This illustrates the importance of specific heat data in any consideration of the conductivity.

The heat capacity of amorphous materials was assumed to be the sum of a Debye specific heat, and a specific heat contributed by modes of vibration, characterised by a single frequency w_E , and hence by an Einstein temperature ($\Theta_E = \hbar w_E/K_B$), introduced in order to explain the specific heat anomaly found at 4K (Tucker & Reese 1967, Choy, Hunt & Salinger 1970, Reese 1969). A variety of explanations of these Einstein modes were advanced, such as the vibration of pendant groups within cavities present in amorphous polymers. This idea was supported by the reduction in the excess heat capacity observed when crosslinking by irradiation occurred.

Zeller & Pohl (1971) reviewed both the experimental observations made on a wide variety of amorphous materials, and the theories advanced to explain these observations. They pointed out the difficulties associated with any theory based on the microscopic structure of amorphous materials, since materials with very different structures exhibited very similar thermal properties.

2.4 Tunnelling States

Anderson et Al (1972) and Phillips (1972) have independently proposed theories, based on the existence of tunnelling states within amorphous material, in order to explain the specific heat anomaly observed below 2K. The model assumes the existence of atoms or groups of atoms within the disordered material, which can sit in one of two equilibrium positions, separated by a potential energy barrier, which is large enough to prevent resonant tunnelling between these positions, but small enough to allow phonon assisted tunnelling to occur during a heat capacity measurement. The difference in the energies associated with these equilibrium positions (ε), leads to an extra contribution to the

heat capacity, which is proportional to temperature:

$c \approx \frac{\pi^2 K_B^2}{6} n_o T$ where $n_o d\varepsilon$ equals the number of atoms (or groups of atoms) per unit volume which can tunnel between states with an energy difference between ε and $\varepsilon + d\varepsilon$.

Anderson et Al and Phillips consider the resonant scattering of phonons by these tunnelling states, and show that the phonon mean free path (L) as a result of this scattering mechanism is proportional to q^{-1}. If the heat current is carried by phonons with a Debye density of states and the dominant scattering mechanism is that described above, then it follows that the thermal conductivity varies as T^2. In order to explain the behaviour of the conductivity at higher temperatures (i.e. the plateau), other scattering mechanisms, such as Rayleigh scattering ($L \propto q^{-4}$) and Kittel scattering ($L=L_o$), must be introduced to limit the mean free path of the high frequency phonons dominant at these temperatures (Zaitlin & Anderson 1975a).

The effect of this scattering mechanism on the thermal conductivity depends on the strength of the coupling between the tunnelling states and the phonon system. Stephens (1973) and Walton (1974) point out that for tunnelling states in crystalline materials, the strength of this coupling varies significantly. Therefore assuming that this mechanism controls the conductivity of amorphous materials below 1K, it is difficult to see why significant differences in the conductivities of these materials do not exist.

Zaitlin & Anderson (1975b) and Stephens (1973) note that any explanation of the specific heat anomaly, must include a quadratic term in the excess density of states function, in order to explain the anomalously large T^3 term found in the specific heat below 2K. Alternatively Pohl et Al (1973) suggest that the increase in the quadratic density of states could be explained by bending of the w-q curve, as a result of dispersion becoming important in a glass at lower

frequencies than in crystalline materials.

Stephens (1976) has investigated the effect of impurities found in glasses, and has shown that while the size of the specific heat anomaly can be reduced by careful sample preparation, the thermal conductivity is sample independent. In order to explain these experimental results, it is necessary to assume that the heat capacity anomaly has two components. The first is related to the density of impurities. The second is sample independent and is related to the density of the tunnelling states, which scatter the phonons and control the conductivity below 1K. From a calculation of the number of states, required to explain the specific heat anomaly associated with the purest samples, and assuming that the thermal conductivity is controlled by these states, Stephens deduces that the coupling between these states and the phonon system must be considerably stronger than any such coupling found in crystalline materials.

Similar effects have been observed by Lasjaunias et Al (1975), who measured the thermal conductivity and specific heat capacity of samples of vitreous silica, with different densities of hydroxyl ions, over the temperature range 0.025K to 0.5K. They found that:

(1) below 0.1K, the specific heat had a temperature dependence greater than T (which is the expected dependence since the T^3 contribution is negligible at these temperatures);

(2) both the magnitude and the temperature dependence of the specific heat was sample dependent;

(3) the samples had identical conductivities with $k \propto T^{1.95}$ over the whole temperature range.

2.5 Structure Scattering Theories

Structure scattering theories, which can explain the conductivity of amorphous materials over the temperature range 0.1K to 100K, including the $T^{1.8}$ dependence, have been advanced by Walton (1974)

and also by Morgan & Smith (1974). These theories do not attempt to explain the existence of the specific heat anomaly, since there is no necessary connection between this anomaly and the scattering mechanism which controls the conductivity.

Walton (1974) uses a relatively simple model, which assumes that a fraction p of the volume of an amorphous material is empty, and that this empty volume is randomly distributed throughout the material, giving rise to density fluctuations, which scatter the long wavelength phonons dominant at low temperatures. Using the results obtained by Rayleigh, for the scattering of sound waves by a region of density $(\rho + \Delta\rho)$ within a medium of density ρ, in conjunction with this model; Walton obtains the mean free path of a phonon as a result of structure scattering: $L(q)^{-1} \approx \left(\frac{p}{1-p}\right) \frac{q}{4}$.

Walton also assumes the existence of regions of short range order of volume V_o (such as the tetrahedra found in vitreous silica); which scatter the short wavelength phonons dominant at higher temperatures. The phonon mean free path, which results from the combination of these two scattering processes is then:

$$L(q)^{-1} = \left(\frac{p}{1-p}\right) \frac{q}{4} + A\, q^4 V_o \quad , \quad q\, V_o^{\frac{1}{3}} < 1$$

$$= A\, V_o^{-\frac{1}{3}} \quad , \quad q\, V_o^{\frac{1}{3}} \geqslant 1 \quad \text{where} \quad V_o^{\frac{1}{3}} \approx 5\text{Å} .$$

Using this expression for the mean free path, which contains 3 fitting parameters (p, A & V_o) and assuming: (1) a Debye density of states, (2) the longitudinal and 2 transverse polarizations contribute equally to the conductivity; Walton obtains an expression for the conductivity, which fits the observed behaviour of the conductivity of an amorphous material between 0.1K and 100K. This theory is based on structural features common to all amorphous materials, and so provides an adequate description of the similarities observed in the conductivities of these materials.

Morgan & Smith (1974) use a model of amorphous materials, which assumes that fluctuations in the properties of the material exist which scatter phonons. These fluctuations can be characterised by a correlation length (a) and a parameter Δ^2. On a microscopic level, these parameters are defined by the way in which the pair distribution function $P(\underline{x},\underline{s})$ (the probability of finding atoms at $\underline{x}$ and $\underline{s}$) varies within the material:

$$P(\underline{x},\underline{s}) = (1 + \Delta(\underline{x}))\, P(\underline{s})$$

$$\Omega^{-1} \int \Delta(\underline{x})\, \Delta(\underline{x}+\underline{r})\, \underline{dx} = \Delta^2 \exp(-r/a)$$

$$\Omega^{-1} \int \Delta^2(\underline{x})\, \underline{dx} = \Delta^2$$

where Ω is the volume of the system. On a macroscopic level, Δ^2 is related to the size of the fluctuations in the properties of the material, and the correlation length (a) is related to the distance over which they occur.

Morgan (1968) calculated the transition rate between phonon states $(\underline{q},p)$ and $(\underline{q}',p')$ (where p represents polarization), which results from the elastic scattering of phonons by structure within a disordered material. Using this transition rate and the model described above, Morgan & Smith solve the Boltzmann equation to obtain two "universal" relaxation curves, one for the transverse waves and one for the longitudinal waves. The mean free path of a phonon of wave number q, due to scattering within a material characterised by parameters a and Δ^2, can be determined from these curves.

Morgan & Smith propose that amorphous materials can be characterised by two correlation lengths: (1) a short correlation length a_S ($5\text{Å} < a_S < 15\text{Å}$), which is related to the dimensions of the regions of order, which exist within disordered materials; (2) a long correlation length a_L ($1000\text{Å} < a_L < 3000\text{Å}$), which is required to predict the low temperature behaviour of the conductivity. Light

scattering experiments have revealed fluctuations in the dielectric constant of amorphous PMMA, which have a correlation length $a \sim 2500\text{Å}$, and are cited by Morgan & Smith as evidence for the existence of long correlation lengths. Phonons with wavelengths much longer than the correlation length a_L are only weakly scattered (for $\lambda >> a_L$, $L \propto \lambda^4$), and so Morgan & Smith introduce boundary scattering in order to limit the mean free path of these phonons and avoid infinite conductivities. The phonon mean free path $L_p(q)$ is now given by:

$$\frac{1}{L_p(q)} = \frac{1}{L_B} + \frac{1}{v_p\, t_p(q, a_L, \Delta_L^2)} + \frac{1}{v_p\, t_p(q, a_S, \Delta_S^2)} \qquad 2.3$$

where v_p is the velocity of sound for polarization p,

L_B is the minimum sample dimension and

$t_p(q, a, \Delta^2)$ is the relaxation time obtained from the MS relaxation curve appropriate to polarization p. The conductivity due to each polarization can be calculated by assuming a Debye density of states in the usual manner. When fitting a curve obtained using the MS theory, to the observed conductivity of an amorphous material, physically reasonable values of correlation length are chosen, and the values of Δ_L^2 and Δ_S^2 are chosen so as to obtain the best fit.

At high temperatures, when short wavelength phonons are dominant, the mean free path of these phonons is smaller than the long correlation length a_L, and so these phonons will not be affected by the presence of long range correlation. However equation 2.3 can still be used, as the term which involves the short correlation length is much larger than the others, and controls the conductivity. When the dominant phonon wavelength exceeds the short correlation length, the scattering due to short range order decreases, giving rise to the decrease in the temperature dependence of the conductivity, which is observed in the plateau region. Eventually scattering due to long range correlation dominates the conductivity giving rise to the $T^{1.8}$ region below 1K.

Morgan & Smith point out that a range of values of the parameters a_L and Δ_L^2 can be used to obtain the $T^{1.8}$ dependence of the conductivity, and so this theory can explain the similarities in the behaviour of different materials, without assuming similarities in their microscopic structure.

2.6 The Role of Debye Phonons

Stephens (1973) suggested that the systems, which give rise to the low temperature specific heat anomaly, might be sufficiently numerous and extended in space, to allow transfer of energy between these systems, and so contribute directly to the conductivity. Experiments to investigate this possibility, and the role of Debye phonons, have been performed; and involved the introduction of boundaries which would scatter phonons, thereby reducing their contribution to the conductivity, without affecting any contribution from the localised systems. Boundary scattering lengths were chosen, which were smaller than the mean free path of the phonons dominant at low temperatures (calculated assuming that the heat current is carried entirely by phonons).

Pohl et Al (1973) measured the thermal conductivity of etched glass fibres (diameter 60 μm) and found that it was less than the thermal conductivity of bulk glass. They found that the observed conductivities could be predicted assuming a Debye density of states, and a mean free path obtained by combining the mean free path of phonons in the bulk material with an additional scattering length, equal to the diameter of the fibres. Pohl et Al also performed Brillouin scattering experiments, which confirmed the existence of phonons in amorphous materials, with frequencies which are dominant at low temperatures.

Zaitlin & Anderson (1975a) measured the conductivity of samples of glass, which contained a large number of holes. They found that at very low temperatures (below 0.15K), for sufficiently small values of

the mean free path due to holes ($\sim 5\ \mu m$), the thermal conductivity varied as T^3; and that its magnitude could be calculated assuming a constant mean free path, equal to that due to holes, and a Debye heat capacity calculated from acoustic data. They also observed changes in the conductivity at higher temperatures, in particular that the plateau tended to disappear as the boundary scattering length decreased. Zaitlin & Anderson demonstrated that the observed effects could be explained using either the tunnelling states model of Anderson et Al or the structure scattering theory of Walton. Substitution of the values of the boundary scattering length (L_B) used by Zaitlin & Anderson, into a calculation of the conductivity using the MS theory, gives rise to curves with the same features as those observed experimentally.

These experiments confirm the idea that the heat current in an amorphous material is carried by phonons with a Debye density of states. Also a calculation of the mean free path of these phonons from observed conductivities, shows that these phonons are well defined excitations (Walton 1974).

2.7 Semi-crystalline Polymers

2.7.1 Structure of Semi-crystalline Polymers

The available information on the structure of the partially crystalline polymer polyethylene, has been reviewed and summarised by Phillips (1971) and Burgess & Greig (1975). It is generally accepted that polyethylene contains lamellar regions of ordered or crystalline material, which are typically 100Å thick. The molecular chains, which may be 1 μm long, are folded back on themselves within the lamellae a large number of times. In a melt crystallized sample, these lamellae join end to end to form ribbon like structures, which grow out from nucleating centres in three dimensions, to form spherulites with a typical diameter of 10 μm. The lamellae are randomly orientated with respect to any chosen direction, giving rise to an isotropic structure.

Between the lamellae, regions of disorder (amorphous material) exist, which have a lower density and are less stiff than the crystalline regions.

The fractional crystallinity of a sample (X) may be determined from its density (ρ), by assuming values for the density of completely amorphous material (ρ_A) and of completely crystalline material (ρ_c). Originally crystallinity was determined using x-ray scattering techniques, from which these values of density have been determined:

$\rho = X\rho_c + (1-X)\rho_A$ where $\rho_c = 1.00$ g cm^{-3} and $\rho_A = 0.85$ g cm^{-3} .

When a sample crystallizes during extrusion, the lamellae grow out with cylindrical symmetry from the nucleating centres, which lie close together on a line parallel to the stress direction. The molecular chains within the lamellae are also closely aligned with the extrusion direction.

The extruded polyethylene samples used in this research, have been extruded and characterised by the Leeds University polymer physics group. The results obtained using x-ray diffraction techniques, indicate a roof top structure, such that the lamellae are orientated at about 48° to the extrusion direction, and the molecular chains are aligned with the extrusion direction to within 5°.

2.7.2 The Thermal Conductivity of Semi-crystalline Polymers

Choy & Greig (1975) measured the conductivity of samples of polyethylene terephthalate (PET) with different fractional crystallinities, over the temperature range 1.5K to 70K. The behaviour of the least crystalline sample (X=0.015) was typical of a purely amorphous polymer. At temperatures above 20K, the conductivity of the samples increased with increasing crystallinity, while below this temperature the reverse was true. They also observed that as crystallinity increased, the plateau tended to disappear, and the

temperature dependence of the conductivity at low temperature increased.

Choy & Greig interpreted their results using a simple model of a semi-crystalline polymer and the acoustic mismatch theory proposed by Little (1959). This theory assumes that a phonon approaching a boundary, between materials with different densities and sound velocities, can either be reflected or refracted, giving rise to a thermal resistance at the boundary, which varies as T^{-3} . Thus the resistance, which arises at a boundary between the crystalline lamellae and the amorphous regions, is most important at low temperatures. Thus at low temperatures, increasing the crystallinity increases both the number of boundaries and the thermal resistance of the sample. This approach is only valid when the dominant phonon wavelength is small compared with the dimensions of the lamellae. The intrinsic resistance of the crystalline regions is small compared with that of the amorphous regions, so that at high temperatures, the conductivity increases with increasing crystallinity.

Burgess & Greig (1975) measured the thermal conductivity of isotropic and extruded polyethylene samples, over the temperature range 2K to 100K. The work reported in this thesis, is a continuation of the work of Burgess & Greig, which is therefore of particular interest. Burgess & Greig found that extrusion had very little effect at the low temperature end of the measurements, but introduced a significant anisotropy at high temperatures. Extrusion increased both the values and the temperature dependence of the conductivity parallel to the extrusion direction ($k_{//}$), relative to the conductivity of the isotropic sample (k_{iso}). The reverse was true for the conductivity measured perpendicular to the extrusion direction ($k_{\perp}$).

The structure scattering theory, developed by Morgan & Smith to explain the conductivity of amorphous materials, was adapted by Burgess & Greig in order to explain the conductivity of semi-crystalline materials. The expression for the mean free path used by Burgess & Greig

is as follows:

$$\frac{1}{L_p(q)} = \frac{1}{L_B} + \frac{1}{v_p\, t_p(q, a_c, \Delta_c^2)} + \frac{(1-X)}{v_p\, t_p(q, a_s, \Delta_s^2)} + \frac{X}{L_u(q)} \qquad 2.4$$

where X is the fractional crystallinity of the sample and

$$L_u(q) = \frac{A}{q^2} \exp\left(\frac{\theta_D}{2T}\right) \qquad \text{(Klemens 1951)} \qquad 2.5$$

Included in this expression for the mean free path are the effects of: (1) boundary scattering; (2) scattering as a result of the fluctuations in the properties of the material, arising from the arrangement of amorphous and crystalline regions within the sample, giving rise to a correlation length $a_c \sim 100\text{Å}$; (3) the scattering within the amorphous regions as a result of short range order, characterised by a correlation length $a_s \sim 8\text{Å}$; (4) Umklapp processes, which occur in the crystalline regions of the sample, giving rise to the phonon mean free path $L_u(q)$. The scattering due to long range correlation within the amorphous material has not been included, as this process is important only at very low temperatures.

It was assumed that extrusion aligned the molecular chain axes in the crystalline regions parallel to the extrusion direction, without significantly affecting the amorphous regions or the dimensions of the lamellae. Strong covalent bonding exists along the polymer chains, while weak Van der Waals forces exist in directions perpendicular to the chain axes. As a result of these differences, the velocity of phonons propagating parallel to the chain axes, is much larger than the velocity of phonons propagating in a direction perpendicular to the chain axes. Thus assuming the existence of a cut-off wave number, which is independent of polarization and direction of propagation; it follows that the value of Debye temperature appropriate to a phonon propagating parallel to the chain axes, is much larger than the value appropriate to a phonon propagating normal to the chain axes ($\theta_{D\parallel}$ = 1300K, $\theta_{D\perp}$ = 150K). It can be seen from equation 2.5, that the effect of U

processes within the crystalline regions, is negligible if the direction of propagation is parallel to the chain axes; but significant at the high temperature end of the measurements, for phonons propagating normal to the chain axes. Thus the term in equation 2.4 arising from U processes is assumed to be zero, for measurements parallel to the extrusion direction. In the case of the isotropic sample, where the chain axes have random orientations relative to the direction of the measurement, the effect of U processes is significant. Thus at high temperatures, the conductivity of the isotropic sample is less than the conductivity of the extruded samples measured parallel to the extrusion direction.

Burgess & Greig also measured the specific heat capacity of an isotropic polyethylene sample, over the temperature range 10K to 100K. They fitted their experimental data using a Debye density of states, in order to obtain a value for the cut-off wave number, required in the analysis of the conductivity.

Rogers (1980) measured the conductivity of two of the samples used by Burgess & Greig, over the temperature range 0.14K to 2.9K. This work is closely related to that reported in this thesis, and is discussed in section 8.3.

Choy & Greig (1977) have measured the conductivity of a variety of extruded and isotropic polymers over the temperature range 2K to 100K. They were able to explain their results qualitatively using the models described above, for the effect of crystallinity and extrusion on the conductivity of a polymer.

CHAPTER III

THE DILUTION REFRIGERATOR

3.1 Introduction

The principal tool of this research is a "Harwell" He^3/He^4 dilution refrigerator built by the Oxford Instrument Company Ltd. Its dilution unit was replaced by a more modern version in 1971 and again in 1978. When the existing dilution unit (designed to reach 50mK) was replaced, several modifications had to be made to the remaining equipment, in order to accommodate the new dilution unit (designed to reach 12mK). At the same time the system was modified so that it would run continuously once started. The following sections include a brief description of the refrigerator, descriptions of the modifications made to the system and a description of the operation of the refrigerator.

Lounasmaa (1974) describes the design and theory of operation of a dilution refrigerator and discusses many of the problems associated with low temperature experiments.

3.2 Description of the Refrigerator

The principal components of the refrigerator are as follows:

(1) The Outer Vacuum Chamber (OVC) isolates thermally the helium bath and the nitrogen reservoirs from each other, and from the outside world.

(2) The liquid nitrogen reservoir is an annular container made from aluminium, which cools the nitrogen shield suspended below it by conduction. The function of this shield is to cool by radiative transfer of heat, the sections of the refrigerator which it encloses, from room temperature to a sufficiently low temperature, to permit the transfer of liquid helium into the helium bath. It also prevents the radiation from the room temperature parts of the apparatus from reaching the helium bath.

(3) The helium bath (or helium chamber) holds about 25 litres of liquid

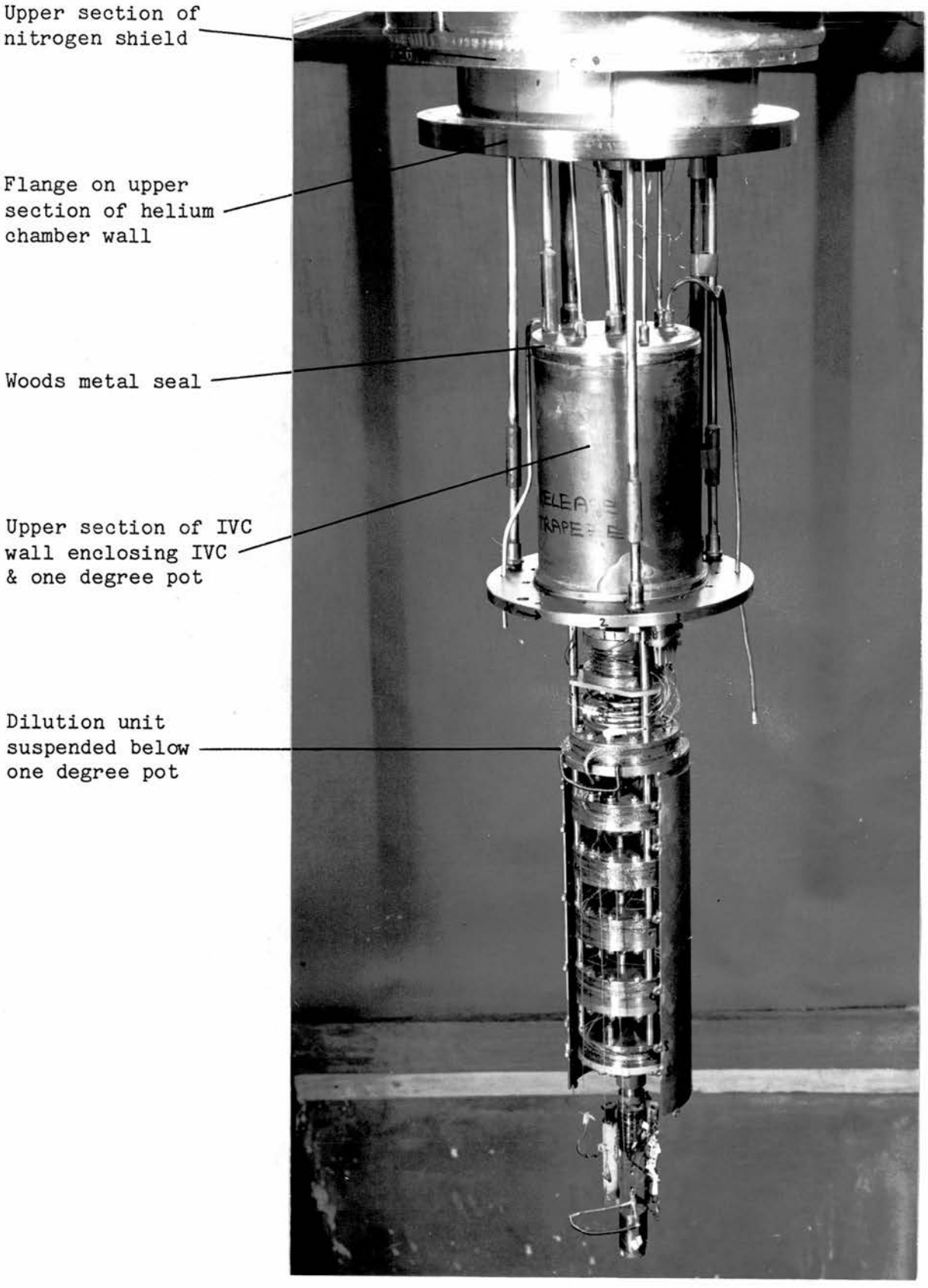

Plate 1 Lower section of cryostat

The lower sections of the walls of the OVC, helium chamber & IVC and the radiation shields have been removed to allow access to the experiment.

helium.

(4) The Inner Vacuum Chamber (IVC) provides thermal isolation between the one degree pot, the dilution unit and the surrounding helium bath.

The outer walls of the OVC, helium chamber and IVC are all in two sections, for ease of access to the experiment. The low temperature seals between the upper and lower sections of the walls of the helium chamber and IVC are made by compressing indium wire between heavy steel flanges. The seal between the top plate of the IVC and the upper section of the IVC wall is made of Woods metal. This seal is difficult to make and is only broken and remade when access is required to the one degree pot, either to repair a leak or to replace wiring.

(5) The one degree pot is a copper vessel with a capacity of 250cc, which is filled with liquid helium and then pumped to reach a temperature in the region of 1K. The one degree pot is linked to the helium chamber by the one degree pot filling line, which permits liquid helium from the helium chamber to enter the one degree pot. The line can be closed by means of a needle valve.

(6) The dilution unit itself is suspended below the one degree pot. Its component parts listed in order are the still, a continuous counterflow heat exchanger, five step heat exchangers and the mixing chamber.

When the refrigerator is operating, two distinct phases exist in the mixing chamber, which is the coldest part of the system. The upper phase consists of almost pure He^3 and the lower phase consists of a dilute solution of He^3 in He^4. Cooling is produced by the movement of He^3 atoms across the phase boundary, from the concentrated to the dilute phases. An osmotic pressure gradient drives the He^3 atoms in the dilute phase from the mixing chamber through the heat exchangers to the still. This osmotic pressure gradient is maintained by removing He^3 from the still. The He^3 vapour is pumped away via the refrigerator pumping line, by a combination of an oil diffusion pump and a rotary pump. A diaphragm

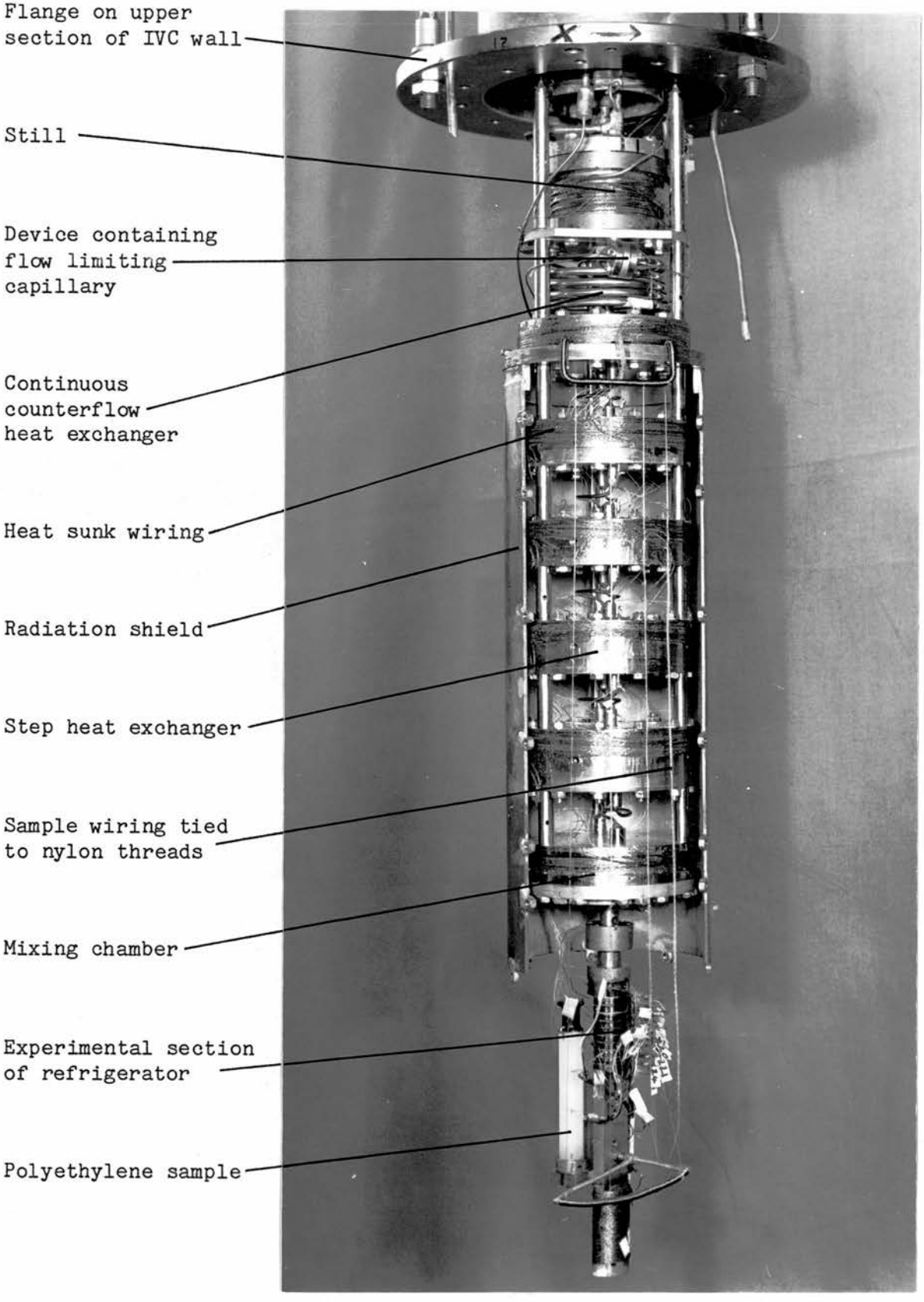

Plate 2 The dilution unit

at the neck of the still reduces He^4 film flow, this combined with the still temperature (approximately 0.7K) minimises the amount of He^4 circulating around the system. The He^3 gas is passed through an oil trap, and a charcoal trap cooled using liquid nitrogen, in order to prevent oil or air from reaching the dilution unit and blocking it. The He^3 is then returned to the low temperature part of the system via the condensing line. The He^3 gas condenses in a spiral copper tube inside the one degree pot, and the liquid He^3 then cools as it passes through a copper pipe wrapped around the still. A length of capillary tubing limits the flow rate, so that the pressure in the condenser is sufficiently high for condensation to occur. The He^3 then cools as it passes through the heat exchangers and is finally returned to the upper phase of the mixing chamber.

The capillary bypass line permits the mixture to reach the dilution unit, without passing through the flow limiting capillary. This line is only used during the initial condensation of the mixture into the dilution unit. A radiation shield is suspended from the warmest step heat exchanger and encloses the remaining heat exchangers and the mixing chamber. The experimental section, which is constructed entirely of copper, is attached to the bottom of the mixing chamber.

3.3 Modifications to the Refrigerator

3.3.1 Installation of the New Dilution Unit

The lower section of the IVC, and the flanges on both the upper and lower sections of the IVC had to be replaced, because the diameter of the new dilution unit was greater than that of the old one. The new can was made from 16 gauge copper tube with an outside diameter of 4".

Three stainless steel rods were used to support the weight of the new dilution unit, which is much heavier than the old unit, which was supported entirely by the refrigerator pumping line. The lower ends of the rods were attached to a plate on the bottom of the still, and the

upper ends were attached to a permali collar, which was attached to the one degree pot. The collar was made from permali, in order to reduce the thermal link introduced between the one degree pot and the still.

The new unit required a larger quantity of He^3/He^4 mixture than the old one. A new 20 litre dump had to be made and installed, in order to contain this extra mixture. The extra mixture was created by introducing pure He^3 and pure He^4 separately into the system, in the quantities recommended by the Oxford Instrument Company Ltd, the manufacturers of the new unit.

The actual installation of the new unit was relatively simple, involving the connection of the three refrigerator lines and the three support rods, while ensuring that the unit was aligned with the wall of the IVC. The new unit had to be wired. This process is described in chapter IV.

Initial problems in cooling the increased heat capacity of the new unit to 4K, were overcome by the following changes: The pressure of the helium inside the IVC acting as exchange gas during the cooling period, was increased from 0.5 torr to 50 torr. The length of time, during which the system was cooled using liquid nitrogen, prior to the transfer of liquid helium, was increased from 24 to 48 hours. The refrigerator then operated successfully, reaching temperatures well below 45mK, which is the lowest temperature on the calibration curves of the germanium resistance thermometers.

3.3.2 The Overnight Running System

It takes from four to six hours for the refrigerator to cool from helium temperature to its lowest temperature. If the refrigerator could run continuously once started, it is obvious that large savings in time could be made, increasing the time available for experimentation. In order to achieve this, two problems had to be solved. The first was to render the equipment safe while unsupervised. This involved providing

a mechanism, such that if the refrigerator started to warm up, or if a blockage in the circulating system developed for any reason, the mixture would be allowed to pass into the dumps, before any dangerously high pressures built up in the circulating system. This was achieved by installing a pressure switch behind the circulating rotary pump which controlled a solenoid valve via a relay (see figure 3.1). The pressure switch was set so that the solenoid valve opened, allowing the mixture to flow into the dumps, if the pressure behind the circulating rotary pump reached 600 torr. The relay ensured that the valve remained open and that the diffusion pump was switched off. A spring release valve was installed in parallel with the solenoid valve, in case the solenoid valve stuck in the closed position.

A second solenoid valve was installed, which linked the inlet of the rotary pump to its outlet, so that in the event of a mains power failure, the valve opened equalising the pressure on each side of the pump. A relay was installed, in the power supply of the rotary pump and its solenoid bypass valve, which prevented the pump from restarting when the power was restored. If during a mains failure, the refrigerator had warmed up, and the pump had then restarted with the pressure in the circulating system close to an atmosphere, a dangerously high pressure surge would have occurred at the pump outlet.

The new sections of pipeline which were installed had to be carefully leak tested. Air entering the circulating system in significant quantities, would eventually find its way through the charcoal trap, and freeze out in the condensing line and block it.

The other problem, which required solution before the refrigerator could operate continuously, was to find a way of preventing the one degree pot from running dry. As soon as the one degree pot is empty, condensation of He^3 gas within the one degree pot stops, and the pressure in the circulating system starts to build up. The size of the

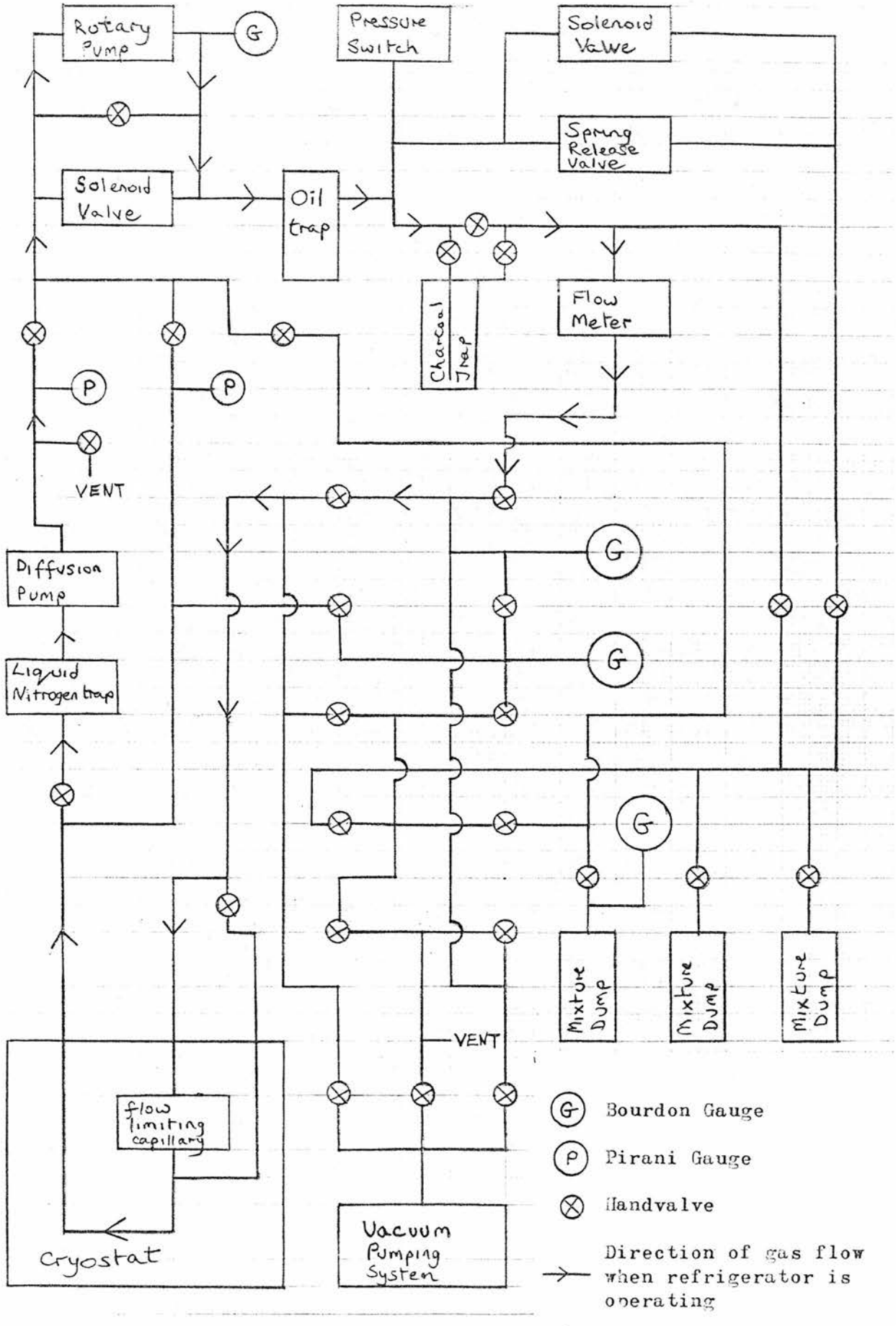

Figure 3.1

The system used to circulate the gas around the refrigerator.

one degree pot was such, that with the old unit it lasted for 24 hours. With the increased circulation of He^3 through the new unit, the load on the one degree pot would increase and so it would run dry more frequently. In order to fill the one degree pot using the existing filling line, a needle valve had to be opened manually and then reclosed when the one degree pot was full.

A continuous filling line was installed, so that liquid helium could pass continuously from the helium bath into the one degree pot. An impedance had to be included in this line, such that a pressure gradient and a temperature gradient can be maintained across it. The flow rate through the impedance is important. If it is too small, then the one degree pot will eventually run dry. If the flow rate is too high, then too much warm helium enters through the impedance, and the pumping system will be unable to remove evaporating helium fast enough to maintain the required temperature and pressure. A suitable flow rate for our system (0.8 torr/minute into 1 litre at room temperature) was suggested by the Oxford Instrument Company. Two types of impedance were tried.

The first device, designed by the Oxford Instrument Company was essentially a needle valve. The needle and its housing were threaded, so that the impedance of the device could be adjusted, by tightening and loosening the screw. It was found that the device frequently became blocked, and for this reason it was abandoned without ever being tried out at low temperatures. A possible explanation of this tendency to block, is that helium passing through the device flowed along a very small number of channels, which were in fact microscopic scratches on the surface of the needle and the valve seat.

The second device was a powder impedance constructed by John Armitage, a lecturer in the department. The impedance consisted of a german silver tube of internal diameter 1.55mm and about 5cm long,

crimped at two places about 2.5cm apart. A section of the tube 1.5cm long, was tightly packed with fine silicon carbide powder (1000 grade), which provided the impedance. The powder was prevented from escaping through the crimps by two layers (one at each end) of coarse powder, whose particles were too large to pass through the crimps. It is virtually impossible to block this device, because of the large number of possible paths through the device. The device cannot be adjusted once made, and a suitable flow rate is obtained by trial and error; variable parameters being the length and cross-sectional area of the impedance and the particle size of the powder.

It is important that the section of the continuous fill line inside the IVC (which includes the powder impedance) should be leak tight. The first powder impedance installed had to be replaced, because helium leaked from one of the crimps.

When the refrigerator is running, two liquid nitrogen traps have to be kept cold. The first a charcoal trap, freezes out any air present in the mixture. The second condenses oil vapour from the circulating diffusion pump, preventing it from reaching the refrigerator unit. In order to run the refrigerator unsupervised, automatic liquid nitrogen filling devices had to be connected to each of these traps. The laboratory already possessed one of these devices so that a second had to be constructed. A 2.2kΩ resistor, with a resistance at liquid nitrogen temperature of about 3.3kΩ , was placed inside the traps. When the liquid nitrogen level falls below the position of the resistor, it warms and the change in its resistance is detected by an electronic system, which operates a liquid nitrogen pump for a preset length of time. The pump consists of a pipe which reaches to the bottom of a 25 litre liquid nitrogen dewar. A solenoid valve is closed, preventing the escape of gas boiling off from the dewar, the volume of which is increased by passing a current through a resistor immersed in the liquid

nitrogen. The gas pressure builds up forcing liquid up the filling pipe into the trap.

3.4 A Typical Refrigerator Run

After the installation of the sample and the reconstruction of the cryostat, which involves making the two indium seals mentioned earlier, a series of room temperature tests are made to ensure the successful operation of the refrigerator. First, the wiring inside the cryostat is checked to ensure that both the leads and their insulation are undamaged (see section 4.1). The IVC & OVC are pumped using a small diffusion pump for at least 12 hours, before being leak tested in the following manner. The one degree pot, helium chamber and dilution unit are pumped using a rotary pump, while a mass spectrometer (tuned to detect He^4) is connected in front of the diffusion pump, which is pumping the IVC & OVC. The mass spectrometer monitors the level of helium inside these two chambers. Helium is then allowed into the one degree pot and helium chamber and later into the dilution unit; the presence of a leak is registered by a change in the mass spectrometer leak rate reading. The pressure inside the vacuum chambers is not critical, provided no helium leak exists, since cryopumping will occur when the system is cooled. The minimum pressure inside the helium chamber produced by the rotary pump is also of interest, as a significant air leak into this chamber can lead to the one degree pot filling lines being blocked by frozen air.

The flow rate of helium through both the powder impedance on the one degree pot continuous filling line and the flow limiting capillary on the refrigerator condensing line is checked. In order to displace any air trapped in the powder impedance, the flow of helium through it is maintained for some time. If no faults are found, then the IVC is isolated from the pumping system, and helium at a pressure of 50 torr is allowed into it, to act as exchange gas. The pumping of the OVC by the

diffusion pump is continued. The dilution unit is pumped using a second diffusion pump.

The system is now ready to be cooled. The nitrogen reservoir, which holds 10 litres of liquid nitrogen, is filled and topped up as necessary by the automatic nitrogen transferring system described earlier. During the nitrogen precooling stage, which lasts 48 hours, about 100 litres of liquid nitrogen boil off from the cryostat.

The dilution unit is isolated from its pumping system, which is now used to pump the line connected to the circulating rotary and diffusion pumps. This line includes the oil and charcoal traps. Liquid helium can now be transferred into the helium chamber. The needle valve on the original one degree pot filling line is open at this stage, so that the one degree pot is also filled during the helium transfer. The transfer takes four hours and about 50 litres of liquid helium are transferred, of which 25 litres remain in the cryostat.

The OVC is now isolated from the pumping system, which is then used to pump the helium out of the IVC. After pumping the IVC for at least 15 hours, the mass spectrometer is used to measure the level of the helium inside the IVC; if this is sufficiently low then an attempt to run the refrigerator can be made.

The system pumping the circulating pumps is closed off. The mixture is then allowed to flow out of the dumps, through the charcoal trap immersed in liquid nitrogen, into the dilution unit, in such a way that the flow rate of the mixture through the flow limiting capillary can be measured, to ensure that it is not blocked. The mixture is now condensed into the dilution unit by pumping the one degree pot. In order to speed up this process, the circulating rotary pump is used to pump the mixture out of the dumps, into the dilution unit via the capillary bypass line. A valve on the inlet side of the rotary pump is used to control the pressure of the condensing mixture, which is held just below

600 torr until the dumps are empty. When condensation is nearly complete, the needle valve on the original one degree pot filling line is opened slightly, and then closed again, when the one degree pot is full of liquid helium. At the end of the condensation period of 1 hour, the pressure of the condensing mixture is about 100 torr and the mixing chamber has cooled to about 2.5K.

After closing the capillary bypass valve, circulation of the mixture around the refrigerator using the rotary pump begins. Initially the flow rate is controlled by a valve on the inlet side of the pump. Rapid cooling results leading to further condensation of the mixture. The flow rate soon drops off due to the reduction in the temperature of the still. The diffusion pump is now introduced to increase the pumping speed of the system. At this stage the still is the coldest part of the dilution unit and the mixing chamber is the warmest. In order to maintain a suitable rate of circulation, power (about 1 milliwatt) is supplied to the still heater. The flow rate of the mixture around the system is monitored using a Kronburger flow meter, and various pressure gauges.

The unit cools steadily until phase separation occurs, when the temperature gradient of the unit is reversed and the cooling of the mixing chamber accelerates. The flow rate increases and the still heater power supply is switched off; it is not required again. The mixing chamber reaches its lowest temperature about 4 hours after starting the circulation.

The refrigerator will now operate continuously, provided that the level of the liquid helium is not allowed to fall below the flange on the IVC, and the traps and cryostat are kept topped up with liquid nitrogen. The system uses about 50 litres of liquid nitrogen per day and 20 litres of liquid helium every 2 days. The refrigerator has been run continuously for 300 hours and there seems to be no reason why it should

not run for longer periods if required.

At the end of a run after the refrigerator has warmed up, the mixture is returned to the dumps using a cryopump. The charcoal trap which contains frozen air, is only allowed to warm up after the mixture has been returned to the dumps.

CHAPTER IV

THERMOMETRY

4.1 The Wiring of the Refrigerator

The installation of the wiring from the top of the cryostat, to just below the mixing chamber was done in two stages. During the first stage, 30 leads were installed between the top of the cryostat and two 15 pin connecting plugs hung just below the one degree pot. These leads pass along the IVC pumping line, so that all the wiring within the cryostat, is contained within the IVC. During the second stage, 22 leads were installed between the connectors below the one degree pot and a single 25 pin connecting plug hung just below the mixing chamber. Leads from the still heater and five carbon resistors were connected to the other 8 pins on the one degree pot connecting plug.

44 SWG eureka wire was used for all but 5 of the leads, for which 44 SWG copper wire was used. The eureka wire was preferred in general because of its low thermal conductivity, which minimised the extra thermal link created by the leads between different sections of the refrigerator. The copper leads were used where low electrical resistance was important. One of the copper leads was the common lead, which linked one side of all the carbon resistors. The other 4 copper leads were installed in case they were required for use with a CMN thermometer. All the wires were insulated with double silk as well as enamel, as it has been observed that the enamel tends to dissolve in the varnish (General Electric 7031) used to attach these wires. Once the varnish has hardened, the silk impregnated with varnish provides adequate insulation.

In order to reduce the effect of external fields, the leads between the top of the cryostat and the one degree pot, and between the one degree pot and the mixing chamber, were twisted in pairs prior to

installation. The wires were then connected so that the link between the low temperature and room temperature sections of a circuit was via one or more twisted pairs.

The connections at the one degree pot were made using 15 pin plugs and sockets made by RS, from which the metal cases had been removed. The connections at the mixing chamber were made using a similar 25 pin socket into which the individual pins (taken from a plug) could be inserted. This permitted the leads from the experimental section to be connected to the rest of the wiring easily and one at a time, making the installation of the sample wiring and trouble shooting considerably easier.

All the wiring installed, was carefully heat-sunk throughout its length, in order to minimise the heat input to the low temperature sections of the apparatus. The leads were heat-sunk to: a copper tube attached to the wall of the IVC, the one degree pot, the still, all five step heat exchangers and finally the mixing chamber, by passing the leads two or three times around each of these bodies. Varnish held the wires in position and improved the thermal contact between the wires and their heat sink. As a result of this, about 6 metres of wire per lead were required to link the top of the cryostat to the mixing chamber. Care had to be taken to include sufficient slack to allow wires to contract when the system was cooled.

Extreme care had to be taken to avoid damage to the wiring, during the soldering operations required to repair leaks. The insulation of the wiring also appears to age, possibly the GE varnish becomes too brittle and cracks when touched. Consequently before every experiment, careful tests of the wiring were performed to ensure that both the wiring and its insulation was undamaged. This was done by checking the resistance between a lead and every other lead and also between every lead and earth. The resistance between independent leads should be at

least 10^7 ohms, measured using a potential difference of 15 volts.

Two complete sets of wiring were installed, during the period of this research, as well as temporary wiring sets used during tests of the refrigerator.

4.2 Carbon Thermometers

Carbon thermometers were used to monitor the temperature of the different sections of the dilution unit, because they are cheap and simple to install and use. A two terminal AC measurement of the resistance of these thermometers, was made using a resistance bridge designed and built by the Oxford Instrument Company Ltd. This bridge operated at a frequency of 225 Hz, and was balanced manually by means of five thumbwheel switches, which enabled the selection of resistances of up to 10^5 ohms to be made in 1Ω steps. The bridge could monitor the resistance of up to 12 resistors, with a nominal accuracy of 0.1%. The rms voltage across a resistor could be set to nominal values of 10μV, 30μV, 100μV, 300μV & 1000μV and the gain of the system could be increased by factors of 1, 3, 10, 30 & 100. The sensitivity of the bridge could be increased, by increasing either the sensor voltage or the gain setting.

A 470Ω Speer resistor was mounted on the one degree pot, and proved useful during both the initial helium transfer, and the condensation of the mixture into the dilution unit. Speer 220Ω, 1/2 watt resistors were mounted on the still, heat exchangers, mixing chamber and the experimental section of the dilution unit. The thermometer on the experimental section was used to stabilise its temperature (see section 4.6). The resistors were placed in holes, drilled in the body whose temperature the thermometer measured. The diameter of the holes was only slightly greater than the diameter of the resistor; thermal contact between the resistor and the surrounding metal being improved by a layer of Apiezon grease. Where a suitable hole was

not available, a copper tube was attached with solder or Woods metal to the relevant body and the resistor placed in the tube. A common lead linked one side of all the resistors together, the other side of the resistors being linked to the bridge by means of independent leads. In order to minimise the effect of external fields, the leads inside the cryostat were twisted in pairs and shielded by the cryostat itself. Screened multicore cables were used outside the cryostat.

The calibration of these resistors was not important; as the relative temperatures of the different sections of the dilution unit, during the period between commencing circulation and reaching the minimum temperature, were of interest rather than any absolute values of temperature. A rough calibration of one of these thermometers against magnetic temperature, performed by the Oxford Instrument Company, was used when necessary.

At low temperatures, self heating of the thermometers occurred, even when the minimum value of sensor voltage was used. This self heating was evident, because of the noticeable drift in the resistance of a thermometer, which occurred during the period just after the bridge was switched to the thermometer in question. At 0.05K, the values obtained for the resistance of a conventionally mounted thermometer, using the Oxford bridge and the potentiometric conductance bridge (see section 4.4), differ by a factor of 10. However at 0.05K, both bridges obtain the same value for the resistance of the carbon thermometer, which was mounted in the experimental section, in such a way as to reduce the thermal resistance between it and the experimental section (see section 4.6). Thus it is clear that this self heating is the result of a significant thermal resistance between the thermometer and its heat sink, combined with the high values of sensor voltage used by the Oxford bridge, which are significantly higher than the nominal voltage values. As the thermometers mounted on the dilution unit were not used to obtain

absolute values of temperature, no attempt was made to reduce the levels of self heating.

4.3 Germanium Thermometers

Germanium resistance thermometers (GRT's) were used to measure the temperatures of both the sample and the experimental section of the refrigerator, for both the heat capacity and thermal conductivity experiments. GRT's were used for the following reasons: their small physical size, small heat capacity, low levels of self heating, their high degree of reproducibility, the speed of their response to temperature changes and the speed with which changes in their conductance can be measured. A GRT is superior to a carbon thermometer with respect to several of these properties. All of these properties were essential to the heat capacity experiment described in chapter V.

A GRT manufactured by Lake Shore Cryotronics Inc. consists of a sensing element, which is a suitably doped germanium crystal, to which four contacts have been made, permitting a 4 terminal resistance measurement. The crystal is mounted on a base made of beryllium oxide and enclosed by a gold plated copper can. The thermometer has a diameter of 3.2 mm and is 8.5 mm long. The leads emerge from the thermometer through an epoxy seal. The sensing element is isolated electrically and almost isolated thermally from the thermometer case. Consequently both electrical and thermal contact to the thermometer is via the leads. In an attempt to improve the thermal link between the sensing element and the case, the capsule is filled with He^4 during manufacture. GRT's manufactured by Scientific Instruments Inc. were also used in this research.

The temperature range of any particular GRT, is very sensitive to the levels of the dopants used in the manufacture of the germanium crystal. The only reliable way of determining the useful temperature range of the thermometer is to measure it experimentally. The lower

temperature limit corresponds to the maximum resistance of the thermometer, which can be accurately measured by the instrument monitoring the resistance of the GRT. The upper temperature limit is less critical and is determined by the minimum required sensitivity, as the slope of the calibration curve (dR/dT) decreases as temperature increases. The useful temperature range of the GRT required by this research was from 0.05K to 2.0K. Some of the thermometers used in this research, were bought as calibrated thermometers and so their temperature range was known, the others were uncalibrated when bought and several proved to have a temperature range which was too small.

It is necessary to heat sink the leads of a GRT when soldering wires to these leads, in order to avoid an excessive heat input to the germanium crystal, which may alter the thermometer calibration. It is also necessary to avoid contact between a GRT and fresh GE varnish, as it contains a solvent which attacks the epoxy seal.

4.4 The Potentiometric Conductance Bridge

The conductance of a GRT was measured using a potentiometric conductance bridge (PCB) manufactured by the SHE corporation of California. The PCB is a self balancing, four terminal, AC conductance bridge with a digital readout and a nominal accuracy of 0.1%. It is specifically designed for use with GRT's. The conductance of the GRT's was always obtained using a 4 terminal measurement, in order to eliminate the resistance of the leads. The sensor excitation is a 27.5 Hz square wave. The use of an AC measurement technique, eliminates the effect of the thermal EMF's, which develop when a wire is positioned in a thermal gradient due to inhomogeneity along the wire. The voltage across the sensor is constant, and can be altered in order to avoid self heating of the thermometers by the excitation current. Possible values of RMS voltage are 10μV, 30μV, 100μV & 300μV. The bridge has four conductance ranges, the maximum values of conductance of these ranges

are 200μMho, 2.0mMho, 20mMho & 200mMho.

The analogue to digital conversion is performed by a digital voltmeter incorporated into the instrument, which uses a dual slope integration technique. The length of time taken to perform each analogue to digital conversion, depends on the value of the voltage being measured, and is typically about 0.25 seconds. The noise seen on the PCB readout arises because consecutive conversions give different results. Each result is obtained by averaging the noise in the analogue circuitry over the length of the signal integration period (33ms). The noise seen on the digital display can be reduced by altering the time constant of a filter placed between the analogue circuitry and the panel meter. Increasing the time constant of the filter, increases the response time of the instrument. Possible time constants are 0.3 s, 1.0 s, 3.0 s & 10.0 s. The noise seen on the digital display, can also be reduced by increasing the sensor excitation voltage and so increasing the ratio of the signal to the noise input to the panel meter.

The PCB also has a differential analogue output voltage, which is proportional to the fractional change in the conductance of the sensor, from a reference value of conductance, set by means of a ten turn potentiometer. This output is unaffected by either the panel meter or the filters in the panel meter input. The only way in which the noise on this output can be reduced is by increasing the sensor excitation voltage. This output is essential to the experimental measurement of heat capacity and is discussed in section 6.2.

4.5 Self heating of Germanium Resistance Thermometers

Self heating of the GRT's occurs as a result of the power dissipated in the sensor, by the measuring current and the noise current flowing within the sensor. The heating caused by the measuring current, can be reduced by reducing the sensor excitation voltage, at the expense of a reduction in the signal to noise ratio. In order to obtain a

suitable compromise, the sensor excitation voltage was set to the maximum value, which did not cause the observed values of thermometer conductance to alter. This value of excitation voltage varied with temperature.

The noise current is a combination of currents associated with the bridge circuitry, Johnson noise and external fields. The noise current inherent in the bridge circuitry can be minimised by selecting the lowest conductance range, which includes the conductance of the thermometer. Measurements performed by the manufacturers, have shown that provided this condition is fulfilled, the heating effect of the noise current generated by the bridge circuitry, will not exceed the heating effect of the sensor excitation voltage. Usually the former effect is negligible compared with the latter.

The effect of external fields was minimised as far as possible by careful shielding of the thermometer leads and the grounding of these shields. Screened multicore cables were used to connect the PCB via a screened switch box to the cryostat. The leads inside the cryostat were twisted in pairs and screened by the cryostat itself. The thermometers were connected so that both the current leads and the voltage leads constituted a twisted pair.

During the calibration experiment, the thermometers are linked by a relatively small thermal resistance to the specimen block, which has a very large heat capacity; while the low temperatures at which thermometer self heating is seen, did not occur during the heat capacity experiment. For these reasons, thermometer self heating was only observed during the thermal conductivity measurements (see section 7.6).

4.6 Temperature Stabilisation

All the experiments performed, including thermometer calibration and the measurement of both heat capacity and thermal conductivity, require that the temperature of the experimental section of the

refrigerator T_{ES}, should be held as nearly constant as possible. This is achieved by means of a system which consists of a carbon thermometer, the Oxford AC resistance bridge, an electronic device referred to as the stabiliser and the stabiliser heater.

The carbon thermometer is a 220Ω Speer resistor, which was covered with a thin film of apiezon grease, and forced into a hole drilled in the experimental section. The diameter of the hole was fractionally smaller than the diameter of the resistor, ensuring a tight fit between the resistor and the hole. Consequently the thermal resistance at very low temperatures, between this resistor and the experimental section, is noticeably smaller than the equivalent resistance for the other carbon thermometers, which are mounted in holes large enough to allow the resistor to be inserted without difficulty. The effects of this reduction in thermal resistance are as follows:

(1) The self heating which has been observed in conventionally mounted resistors (see section 4.2) is not observed in the stabilising resistor.

(2) The time taken by the stabilising thermometer to respond to a temperature change is shorter than the response time of the other carbon thermometers.

(3) At very low temperatures, the electrical resistance of a conventionally mounted thermometer tends to drift slightly with respect to the temperature measured by a GRT. The resistance of the stabilising thermometer does not drift in this manner.

Once the refrigerator had reached its minimum temperature, the resistance values of the other carbon resistors were of no further interest and so the Oxford bridge could be used to monitor the resistance of the stabilising thermometer continuously. A DC output voltage from the Oxford bridge, which was proportional to the difference between the thermometer resistance and the resistance of the balancing resistor, was used as input to the stabiliser. The stabiliser based on a

design by Rochlin (1970), was built by the electronics workshop staff. Its output was connected to the stabiliser heater which had a resistance of about 1000Ω. The heater was formed by: twisting together the two sides of a loop of 44 SWG eureka wire; this twisted pair was then wound around part of the experimental section of the refrigerator and covered with GE varnish.

The stabiliser had two modes of operation. In the manual mode, it behaves as a constant voltage power supply. In this mode the current supplied to the stabiliser heater is adjusted manually, until the temperature of the experimental section, monitored by a GRT, is close to the desired temperature. The Oxford bridge is then balanced and the stabiliser switched to the automatic mode of operation. In this mode, the stabiliser adjusts the current flowing through the stabiliser heater, in response to changes in thermometer resistance, in such a way as to reverse these changes. The time constant of the stabiliser is controlled by altering the value of an integrating capacitor. The rate of change of stabiliser current is a function of: the sensor voltage and the gain of the Oxford bridge, the gain and time constant of the stabiliser, as well as the difference between the resistances of the thermometer and balancing resistor. These parameters need careful adjustment. If the response of the stabiliser is too slow, it is unable to compensate for a change in the refrigerator cooling power, permitting T_{ES} to drift unchecked. If on the other hand the response of the stabiliser is too fast, it over compensates for a change in cooling power, and T_{ES} starts to oscillate with an increasing amplitude. The optimum time constant for the stabilising system decreases with increasing temperature.

Once successful operation of the stabiliser has been established, to alter T_{ES} it is sufficient to adjust the value of the balancing resistor of the Oxford bridge. Adjustment of the other

parameters is only occasionally required. When the stabiliser is operating normally, the short term fluctuations in the value of T_{ES} are small, and can be averaged out, by using a PCB filter with a long time constant. Over long periods of time, the variation in the value of T_{ES} is also small, typically this variation is less than 1% over a 24 hour period at very low temperatures (T_{ES} =0.07K).

When stabilising at the higher temperatures (above 0.7K), the flow rate of the mixture around the refrigerator increases considerably, and large erratic changes in its cooling power occur, which make it difficult to maintain a steady value of T_{ES}. This difficulty can be overcome by using the rotary pump to circulate the mixture by itself. This has the effect of decreasing both the flow rate of the mixture around the refrigerator and its cooling power, while improving the stability of the system. Under these conditions, T_{ES} can be held steady at temperature values of up to 2.0K.

4.7 Thermometer Calibration

One of the GRT's used in this research (Ge5), had been calibrated against magnetic temperature by the manufacturers. This thermometer was used to measure the temperature of the experimental section during the experimental measurement of heat capacity and thermal conductivity. The thermometers Ge1 & Ge3, which were used to measure the sample temperature, were calibrated against Ge5. This calibration was repeated, after defects in the thermometer calibration became apparent, during the calculation of the experimental values of heat capacity. These defects and the changes in the calibration procedure are described in section 4.9.

The thermometers were attached to the experimental section of the refrigerator using Woods metal, which provided a thermal link between the case of the thermometer and the experimental section. The electrical link between the thermometer leads and the connecting socket

below the mixing chamber, was made using 28 SWG enamelled copper wire. These wires were attached to the experimental section using GE varnish and passed around it at least three times, forming the principal thermal link between the thermometers and the experimental section.

The temperature of the experimental section (T_{ES}) was held as nearly constant as possible, using the stabiliser. The value of the conductance of each thermometer, which corresponds to the current value of T_{ES}, was then determined in turn using the PCB. In order to reduce the noise on the PCB readout and the effect of fluctuations in the value of T_{ES}, the PCB filter with a 3 second time constant was used.

4.8 Fitting Calibration Curves

4.8.1 Introduction

If a polynomial function ($y=f(x)$) is fitted using least squares, to a series of points (x_i, y_i, $i=1,n$) taken from a smooth curve, then the difference between the original values of the dependent variable and the values obtained using the fitted function ($y_i - f(x_i)$), varies in an oscillatory manner with respect to the independent variable (x). This is because the best fitting polynomial is the one which intersects the "true curve" as often as is permitted by the order of the polynomial. Increasing the order of the polynomial has the effect of decreasing both the amplitude and period of these oscillations.

If an accurate calibration of a germanium thermometer is performed, then the calibration points, (x_i, y_i, $i=1,n$) where $x_i=\log(R_i)$ and $y_i=\log(T_i)$, form just such a smooth curve. Any attempt to fit a polynomial function $y = \sum_{j=0}^{m} a_j x^j$ to these points results in the oscillations described above. If insufficient calibration points are used, then the scatter of the points about the fitted curve appears to be random. Although an increase in the order of the fitting polynomial, leads to a decrease in the amplitude of these oscillations, and improves the overall fit of the calibration curve to the calibration data; it has

little effect on the amplitude of the corresponding oscillations of the first derivative of the fitted curve.

When a calibration is transferred from one thermometer to another, the errors arising from the oscillations produced by the fitting procedures, accumulate leading to errors larger than the experimental error of the original measurement. The error associated with calibration transfer can be minimised by using a high order polynomial fit, to reduce the amplitude of the oscillations superimposed on the calibration curve by the fitting procedure.

The measurement of thermal conductivity, involves the measurement of a temperature difference, using two different thermometers with different calibration curves. Thus the fractional error associated with the measured values of thermal conductivity is given by:

$$\frac{\delta k}{k} = \frac{\delta T_2 + \delta T_1}{T_2 - T_1} \approx 10. \left(\frac{\delta T}{T}\right)$$

where δT_1 & δT_2 are the errors associated with the values of sample temperature T_1 & T_2 due to the oscillations of the fitted calibration curve. It can be seen that the fractional error associated with the measured values of temperature, must be very small in order to obtain a reasonable value for the fractional error associated with the conductivity values.

The measurement of heat capacity, which involves the measurement of a temperature difference using a single thermometer, will reflect the oscillations of the first derivative of the calibration curve y=f(x) since:

$$\frac{\Delta T}{T} \approx \log\left(1+\frac{\Delta T}{T}\right) \approx \left(\frac{dy}{dx}\right) \log\left(1+\frac{\Delta R}{R}\right)$$

where y=log(T), x=log(R), and ΔT is the change in temperature (T), which is associated with ΔR, the change in the resistance (R) of a thermometer. The use of a high order polynomial does not reduce

significantly the amplitude of the oscillations of the first derivative of the fitted curve, and so this method does not reduce the corresponding error associated with the measured values of heat capacity. In order to avoid these problems a fitting procedure developed by Godratt et Al (1977) has been used.

4.8.2 Fitting procedure of Godratt et Al

A low order polynomial $y = \sum_{j=0}^{m} a_j x^j$ (typically m=4) is fitted using least squares, to n calibration points (x_i, y_i, i=1,n) where $x_i = \log_{10}(R_i)$ and $y_i = \log_{10}(T_i)$. A ripple is taken to mean a half cycle oscillation arising from the fitting procedure. The use of a low order polynomial reduces the number of ripples, and therefore increases the number of points in any given ripple.

The computer program automatically sorts the calibration points into ripples, by examining the sign of each value of z in turn, where z is the difference between the values of temperature input to and output from the fitting procedure described above.

$$z_i = T_i - 10.0^{**}\left\{\sum_{j=0}^{m} a_j x_i^j\right\}$$

A ripple consists of consecutive points whose z values all have the same sign. If after a change of sign, a ripple contains an insufficient number of points, then all the points prior to the next change of sign are also included in the ripple. A polynomial with a maximum order of 4 is then fitted to each ripple in turn as follows: $z = \sum_{j=0}^{4} b_{jk} x^j$ where k is the number of the ripple. The ripple fitting polynomials are made to overlap by including points from adjacent ripples, to ensure a smooth interchange from one polynomial to the next (see section 4.9.2).

The full calibration curve is given by:

$$T = 10.0^{**}\left\{\sum_{j=0}^{m} a_j x^j\right\} + \sum_{j=0}^{4} b_{jk} x^j$$

where $x=\log_{10}(R)$ and k is the number of the ripple, whose range includes x. Godratt et Al have compared this method of fitting calibration curves with other methods, including cubic spline and smoothed spline methods,

and found it to be superior.

It is obvious that this fitting procedure can only be used if the calibration dataset has sufficient points, and the experimental scatter of these points about the "true curve" is sufficiently small. Since a typical ripple fit uses at least 25 fitting parameters, it can only be used with safety on datasets with more than 50 points. If the experimental scatter of the calibration points is significant, then the effect of both the high order polynomial fit and the ripple fitting procedure, is to incorporate the experimental errors into the calibration curve, giving rise to oscillations of both the calibration curve and its first derivative, which are larger than those associated with a low order polynomial fit. This constitutes overfitting of the calibration data. Thus while the ripple fitting procedure reduces the oscillations of the calibration curve in the case of high quality data, it increases these oscillations in the case of calibration data which is inaccurate or contains insufficient points.

When calculating experimental results using these calibration curves, the dataset input to the relevant computer program includes both the values of thermometer conductance generated by the experiment, and the coefficients of the calibration curve (a_j, j=0,m and b_{jK}, j=0,4; k=1,k_R). A subroutine then evaluates the temperature values which correspond to the input values of conductance.

4.9 Modifications to the Calibration procedure Arising From The Heat Capacity Measurements

After calculating the heat capacity C at temperature T, from the energy E supplied to the sample during a heat pulse, and the observed temperature rise ΔT; it was observed that the variation of log(C) with respect to log(T) exhibited scatter absent from the variation of log(E) with log(T).

$$\log(C) = \log(E) - \log(\Delta T)$$

$$\log\left(1+\frac{\Delta T}{T}\right) \approx \left(\frac{dy}{dx}\right) . \log\left(1+\frac{\Delta R}{R}\right)$$

where y=log(T), x=log(R) and $\left(\frac{\Delta R}{R}\right) \approx$ constant (see section 5.5).

It can be seen that the scatter of the heat capacity results arose from defects in the calibration curves of thermometers Ge1 & Ge3. The variation of $\log(\Delta T_i)$ with log(T) was plotted, where ΔT_i is the change in temperature corresponding to a 10% change in the conductance of the thermometer. These curves have been included (see figure 4.2). The observed distortion of the curves of $\log(\Delta T_i)$ against log(T) was found to have several distinct causes.

4.9.1 Bad Calibration Points

The most obvious cause, was the existence of a pair of bad calibration points, clearly visible on the calibration curves (see figure 4.1). An immediate improvement was effected by removing the bad points and refitting the calibration curves. A further improvement was achieved by recalibrating the thermometers. During the recalibration, after stabilising the temperature of the experimental section, the measurement of the conductance of each thermometer in turn, was performed six times. Previously these measurements had only been performed twice. As a result of increasing the number of measurements per calibration point, no bad points were found when curves were fitted to the calibration data. The scatter of the conductance values about each of the mean values of conductance could also be calculated.

The number of calibration points was also increased, so that bad points if they arose, could be discarded safely. Over the temperature range 0.05K to 2.0K, 100 calibration points were taken, equally spaced along the log(R) axis, in order to improve the accuracy of the fitting procedures. This increase in the number of calibration points and the number of measurements per calibration point was only possible after the installation of the overnight running system.

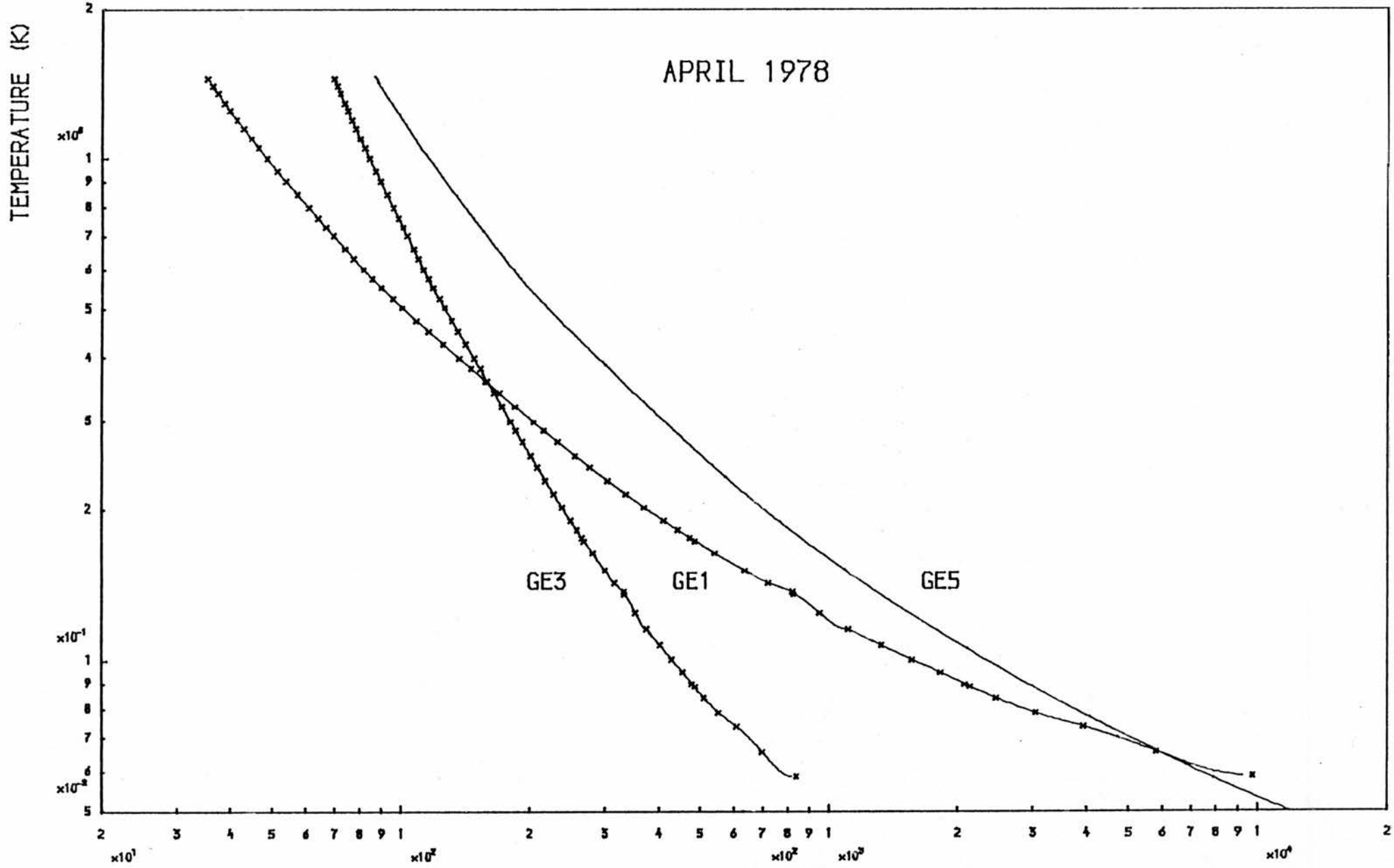

FIGURE 4.1 THE THERMOMETER CALIBRATION CURVES CURRENT IN APRIL 1978.

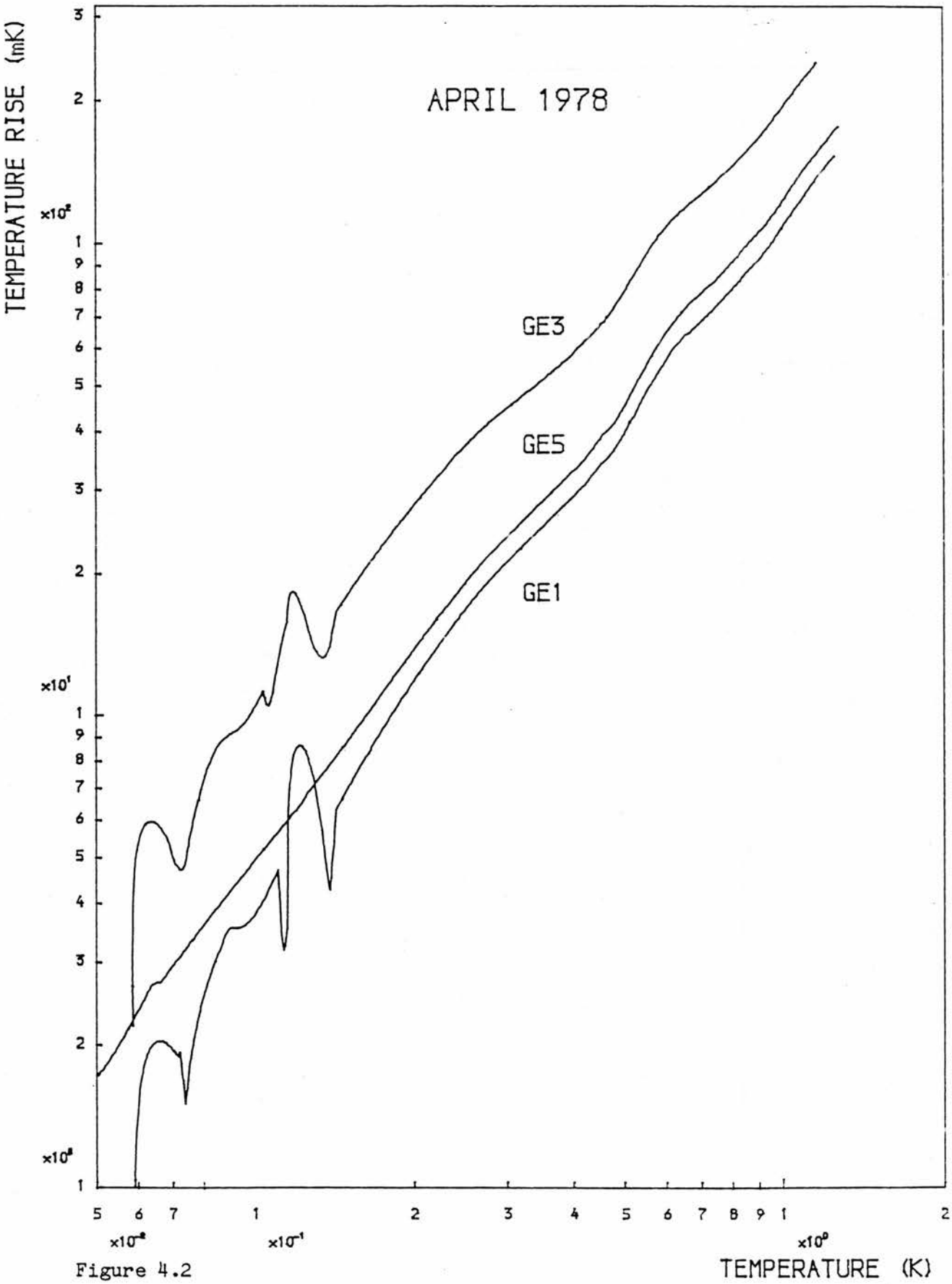

Figure 4.2

The variation of temperature rise with temperature, for the thermometer calibration curves current in April 1978. The temperature rise corresponds to a 10% change in thermometer conductance.

4.9.2 Ripple Interchange

Some of the bumps in the variation of $\log(\Delta T_1)$ with $\log(T)$ were found to coincide with the point at which the change over between two adjacent ripple fitting polynomials occurs. These bumps were eliminated by increasing the degree of overlap between adjacent ripple fitting polynomials. Previously one point from each of the adjacent ripples had been included in the points to be fitted by the ripple fitting polynomial. This overlap was increased, so that if consecutive ripples have n_i, n_j & n_k points respectively, then the jth ripple fitting polynomial is fitted to $n_j + \frac{1}{2}\min(n_i, n_j) + \frac{1}{2}\min(n_j, n_k)$ points. Consequently most of the calibration points are used in two ripple fitting procedures. The minimum number of points per ripple is five, and so the minimum number of points to which a ripple fitting polynomial is fitted is nine.

4.9.3 Primary Calibration

The oscillations seen on the curve of $\log(\Delta T_1)$ against $\log(T)$ at the high temperature end of the curve, derive from the calibration curve of the thermometer with the primary calibration (Ge5), against which both Ge1 & Ge3 were calibrated. This curve had been fitted by the manufacturers of the thermometer, Lake Shore Cryotronics Inc. It is clear that they committed the error described earlier, of using a high order polynomial to fit an insufficient quantity of data points. The effect of this proceeding is to generate a calibration curve which follows the calibration points too closely, incorporating the experimental errors in the calibration data into the curve, and generating oscillations in the first derivative of the calibration curve.

The manufacturers were persuaded in accordance with their original instructions, to recalibrate the thermometer and provide us with the calibration points rather than a calibration curve. They

supplied 31 experimental points over the temperature range 0.045K to 2.0K. The distribution of these points along the log(R) axis was uneven. The quality of this data, both in number of points and in accuracy, was such that the use of a ripple analysis or a high order polynomial would have led to overfitting. Consequently a simple low order polynomial was used to fit these data points.

$$\log(T) = \sum_{i=0}^{4} a_i \, (\log(R))^i$$

No additional oscillatory effects have been introduced by the transfer of this primary calibration to thermometers Ge1 & Ge3, because the quantity and quality of the secondary calibration data, permitted the use of the fitting procedure of Godratt et Al. Thus the only error due to calibration fitting procedures, arises from the oscillations of the primary calibration curve, which have been minimised by the use of a low order polynomial.

The success of these improvements to the calibration procedure and the fitting of the calibration curves, is shown by the current calibration curves and the corresponding curves of $\log(\Delta T_i)$ against log(T) for thermometers Ge1 & Ge3 (see figures 4.3 & 4.4). A dramatic decrease in the scatter of the heat capacity results occurred, when the new calibration curves were used to calculate the experimental values of heat capacity. Without these changes, the scatter in the experimental values of the heat capacity of the polyethylene samples, after the subtraction of the heat capacity of the addenda, would have been so large as to render the measurements virtually worthless.

4.10 Quality of the Secondary Calibrations

4.10.1 Random Errors (See table 4.1)

The success of the fitting procedures can be assessed using the following parameter:

$$\xi = \left\{ \left(\frac{1}{n}\right) \sum_{i=1}^{n} 10^4 \left(\frac{T_{FIT} - T_{EXP}}{T_{EXP}} \right)_i^2 \right\}^{\frac{1}{2}}$$

where (R_{EXP}, T_{FIT}) is a point on the calibration curve corresponding to

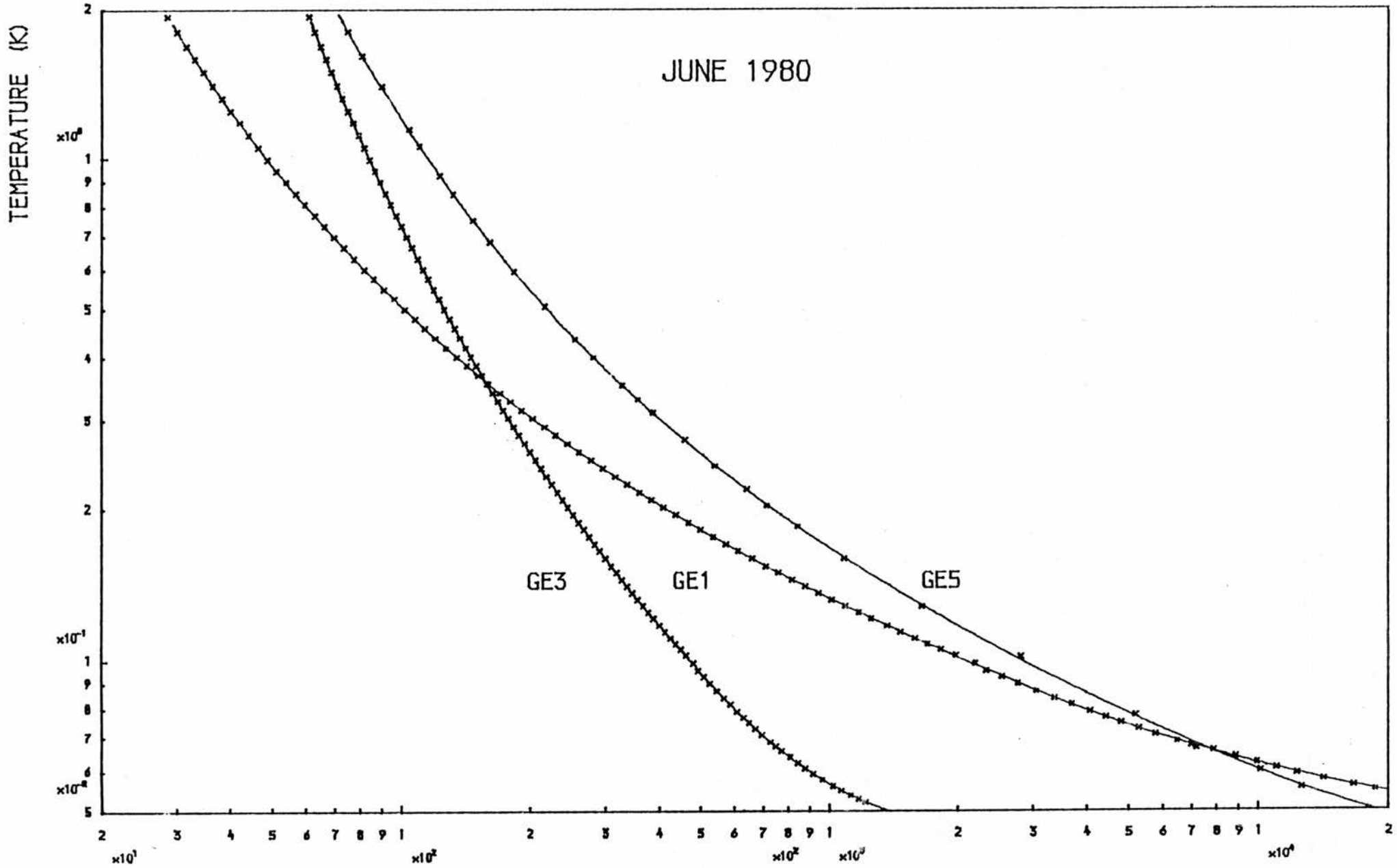

FIGURE 4.3 THE THERMOMETER CALIBRATION CURVES CURRENT IN JUNE 1980.

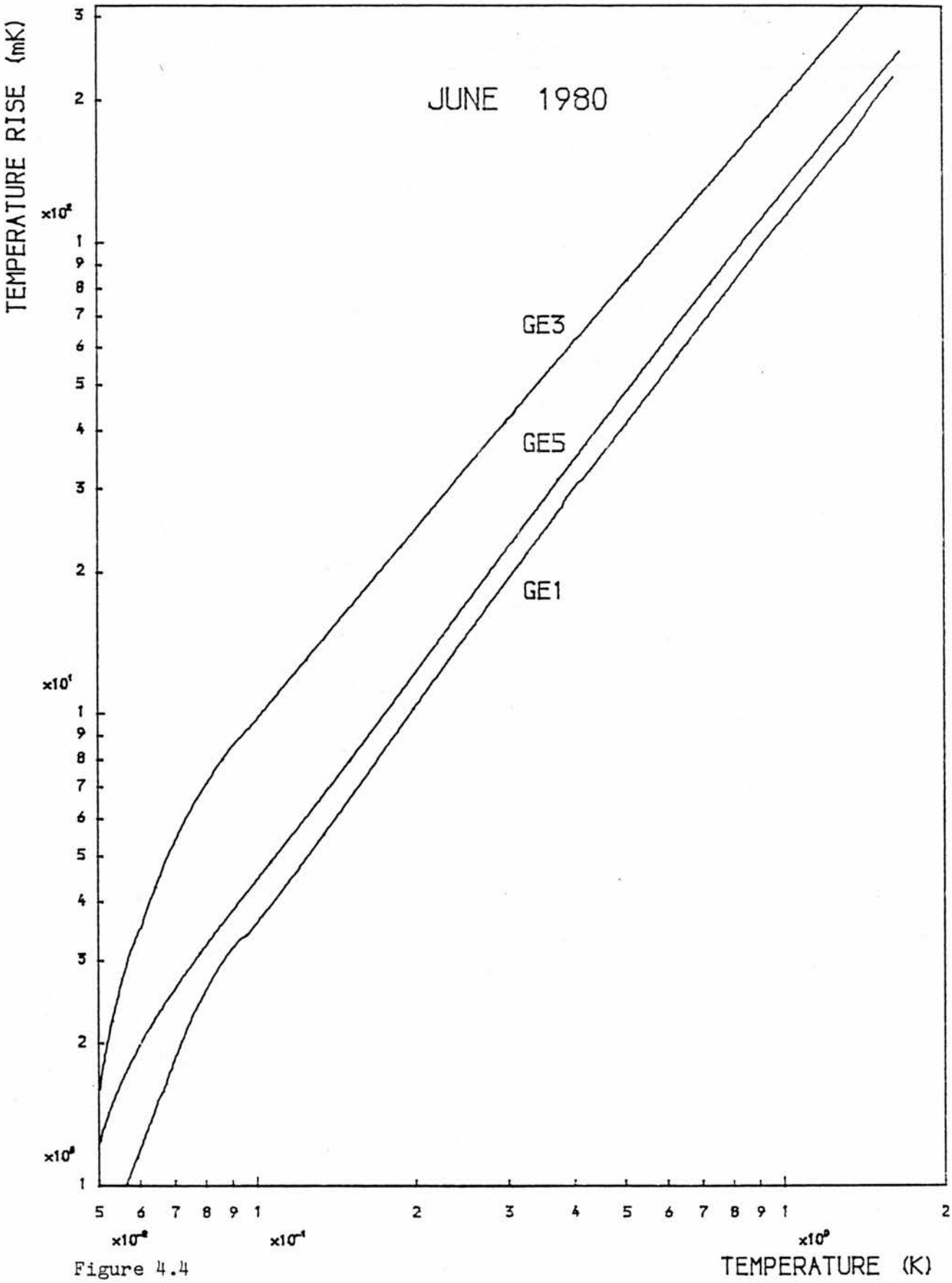

Figure 4.4

The variation of temperature rise with temperature, for the thermometer calibration curves current in June 1980. The temperature rise corresponds to a 10% change in thermometer conductance.

the experimental calibration point (R_{EXP}, T_{EXP}). Parameter ξ is the standard deviation of the percentage difference between the fitted and experimental temperature values. ξ_P is obtained using a polynomial fit of order m. ξ_R is obtained using a ripple fitting analysis and m is the order of the underlying polynomial fitted to all the calibration points. ξ_C is a similar parameter, which reflects the scatter, associated with the values of thermometer conductance, observed during the calibration experiment.

$$\xi_C = \left\{ \frac{1}{P} \sum_{i=1}^{n} \left[\frac{100}{T_i} \left(\frac{dT}{dG} \right)_{T_i} \right]^2 \sum_{j=1}^{l_i} (G_{ij} - \bar{G}_i)^2 \right\}^{\frac{1}{2}}$$

where G_{ij} is the jth measurement of conductance obtained during the determination of the ith calibration point, $\bar{G}_i = \frac{1}{l_i} \sum_{j=1}^{l_i} G_{ij}$; $P = \sum_{i=1}^{n} l_i$ and l_i is the number of measurements made during the determination of the ith calibration point.

It should be noted that the estimate of the error introduced by the ripple fitting procedure ξ_R, is dominated by the values of ΔT associated with 9 of the 100 calibration points. This is because the calibration was performed in two stages. The calibration over the temperature range required for the heat capacity experiments (0.1K to 2.0K) was extended to include the range 0.05K to 0.1K. A difference of 0.9mK occurred at the point of overlap (0.1K). If the values of ΔT, associated with these nine calibration points, (84mK to 107mK) are omitted from the calculation of ξ_R, then the value designated ξ_R^* is obtained. This provides a true reflection of the error associated with the fitting procedures, and is comparable with the value of ξ_C, which reflects the effect of the random variations of thermometer conductance during the calibration experiment.

TABLE 4.1

Thermometer	Ge1	Ge3	Ge5
n	100	100	31
m	4	4	4
ξ_P	0.63%	0.30%	0.60%
ξ_R	0.13%	0.095%	-
ξ_R^*	0.088%	0.032%	-
ξ_C	0.023%	0.030%	0.023% (n=100)

4.10.2 Consistent Errors (See table 4.2)

It is more difficult to detect the existence of consistent errors introduced by the calibration procedure; such as the error detected by performing the calibration in two stages, as described above. The most likely cause of a consistent error would be imperfect thermal contact between the thermometers and the experimental section. The effect of consistent errors on the thermometer calibration curves is most easily judged by considering the reproducibility of the calibration curves. The most obvious way of doing this is to compare the two sets of calibration data obtained during this research. The values of conductance of thermometers Ge5, Ge3 & Ge1, obtained during the first calibration (April 1978), which correspond to the same temperature value, have been used to calculate three temperature values T_5, T_3 & T_1, using the calibration curves obtained during the second calibration (June 1980). As before the parameter ξ provides a suitable measure of the resulting temperature differences over the whole temperature range.

$$\xi(T_3,T_5) = \left\{ \frac{1}{n} \sum_{i=1}^{n} 10^4 \left(\frac{T_3 - T_5}{T_5} \right)_i^2 \right\}^{\frac{1}{2}}$$

Parameters $\xi(T_1,T_5)$ and $\xi(T_3,T_1)$ have been defined in a similar way. The values of these parameters are given in table 4.2. These temperature differences include the effect of any consistent errors present in the

calibration data, and also any changes in the "true calibration curve" which have occurred over a two year period, due to repeated thermal cycling of the thermometers.

In order to compare the reproducibility of the data and curves generated by the secondary calibration procedure, with the reproducibility of the primary calibration data, obtained during the calibration of Ge5 against magnetic temperature by Lake Shore Cryotronics Inc, the parameter $\xi(T_5', T_5)$ has been calculated. T_5' and T_5 are temperature values, which correspond to the same value of conductance, on the original and current calibration curves of thermometer Ge5. $\xi(T_5', T_5)$ is dominated by the values of $(\Delta T/T)$ from the low temperature end of the calibration curve. This is not true of the other values of ξ, for which the individual values of $(\Delta T/T)$ are approximately independent of temperature, which was the reason for the choice of this parameter. It can be seen that $\xi(T_5', T_5)$ is much larger than the other values of ξ. It follows that $\xi(T_5', T_5)$ reflects the effect of the experimental errors present in the primary calibration data, rather than the effect of curve fitting or thermal cycling.

It should be noted that consistent errors produce shifts in the calibration curve rather than changes in its shape. Thus the effect of consistent errors on the gradient of the calibration curve, and hence on the measurements of heat capacity and thermal conductivity, is small compared with the effects of the oscillations introduced by a random error. A consistent error will of course give rise to an error in the temperature value, corresponding to the measured value of heat capacity or thermal conductivity.

The following conclusions can be drawn:

(1) The additional error incorporated into the calibration curves of Ge3 and Ge1, by the transfer of the calibration from Ge5 to these thermometers, is small compared with the error involved in the original

calibration of Ge5, performed by the manufacturers.

(2) The variation of $\log(\Delta T_1)$ with $\log(T)$ and the value of parameter ξ, can be used to strike a balance between overfitting and underfitting the calibration data.

TABLE 4.2

Parameter	value	n	temperature range
$\xi(T_3, T_5)$	0.57%	57	0.08K - 1.45K
$\xi(T_1, T_5)$	1.56%	57	0.08K - 1.45K
$\xi(T_3, T_1)$	1.23%	57	0.08K - 1.45K
$\xi(T_5', T_5)$	4.5%	74	0.08K - 1.5K
$\xi(T_5', T_5)$	7.1%	96	0.045K - 1.5K

CHAPTER V

THE EXPERIMENTAL MEASUREMENT OF HEAT CAPACITY

5.1 Introduction

The heat capacity of four polyethylene samples was measured using a heat pulse technique similar to that described by Scott et Al (1973) and by Lasjaunias et Al (1977). The sample was attached to the experimental section of the refrigerator using a nylon screw, which acted as a weak thermal link. A heat pulse was supplied to the sample, by passing a current through the sample heater for a short length of time. The sample temperature before, during and after the heat pulse was monitored by two GRT's, mounted on copper wires passing through the samples. The heat lost from the sample during the heating period, could be calculated from the observed variation of sample temperature with time during the cooling period. The heat capacity of the sample and its addenda could then be calculated from the observed temperature rise and the heat supplied to the sample, corrected for the heat lost during the heating period.

Measurements of the heat capacity of a nylon sample, with addenda identical to that used for the measurements of the heat capacity of the polyethylene samples, were made and used to deduce the heat capacity of the addenda. Thus the specific heat capacity of both the polyethylene samples and the nylon sample could be calculated. The remaining sections of this chapter describe in more detail, the experimental arrangement of the sample and its addenda, the experimental measurements, and some of the problems associated with the experiment.

5.2 The Polyethylene Samples

The specific heat capacity of 4 polyethylene samples, provided by the Leeds University Polymer Group, was measured over the temperature range 0.15K to 1.3K. These samples are designated SH0, SH1, SH2 & SH3.

Samples SH1, SH2 & SH3 are samples of extruded polyethylene, with extrusion ratios of 3.08, 3.85 & 4.4 respectively. Sample SH0 is a sample of isotropic polyethylene.

The samples were in the form of cylindrical rods, 1.0 cm in diameter and 6.5 cm long. At one end of the sample, a recess had been cut to form a neck, around which a 1000Ω sample heater had been wound using 46 SWG manganin wire. This sample heater was unsuitable for low temperature heat capacity measurements, because of its position and large heat capacity, and so it was removed. The exposed neck had a diameter of typically 0.55 cm, and a length of 1.0 cm, and was about 0.3 cm from one end of the sample. At the other end of samples SH1 & SH3, a hole had been drilled and tapped to take a 6BA screw, which provided the thermal link through which the sample was cooled. Samples SH0 & SH2 originally had a similar threaded hole, but in order to improve thermal contact of the samples to the cooling system, during the measurement of thermal conductivity below 1.5K, this hole had been drilled out leaving a plain hole, 0.5 cm in diameter and 0.6 cm deep, in the base of these samples (see section 7.2). All 4 samples had two holes drilled along parallel diameters positioned 2.0 cm and 3.5 cm from the base of the sample. The purpose of these holes was to allow the copper wires, on which the thermometers measuring the sample temperature were mounted, to pass through the sample (see section 5.3.4).

5.3 The Experimental Arrangement of the Sample and its Addenda

5.3.1 The Experimental Section of the Refrigerator

This consisted of two copper sections attached to each other using non superconducting solder. The first was a half cylinder of copper, 14.0 cm long, with a diameter of 1.8 cm, it will be referred to as the tail. The second section was a copper block 3.8 cm x 2.1 cm x 1.4 cm referred to as the specimen block (see figure 5.1). A copper rod 4 cm long with a diameter of 0.75 cm, provided the

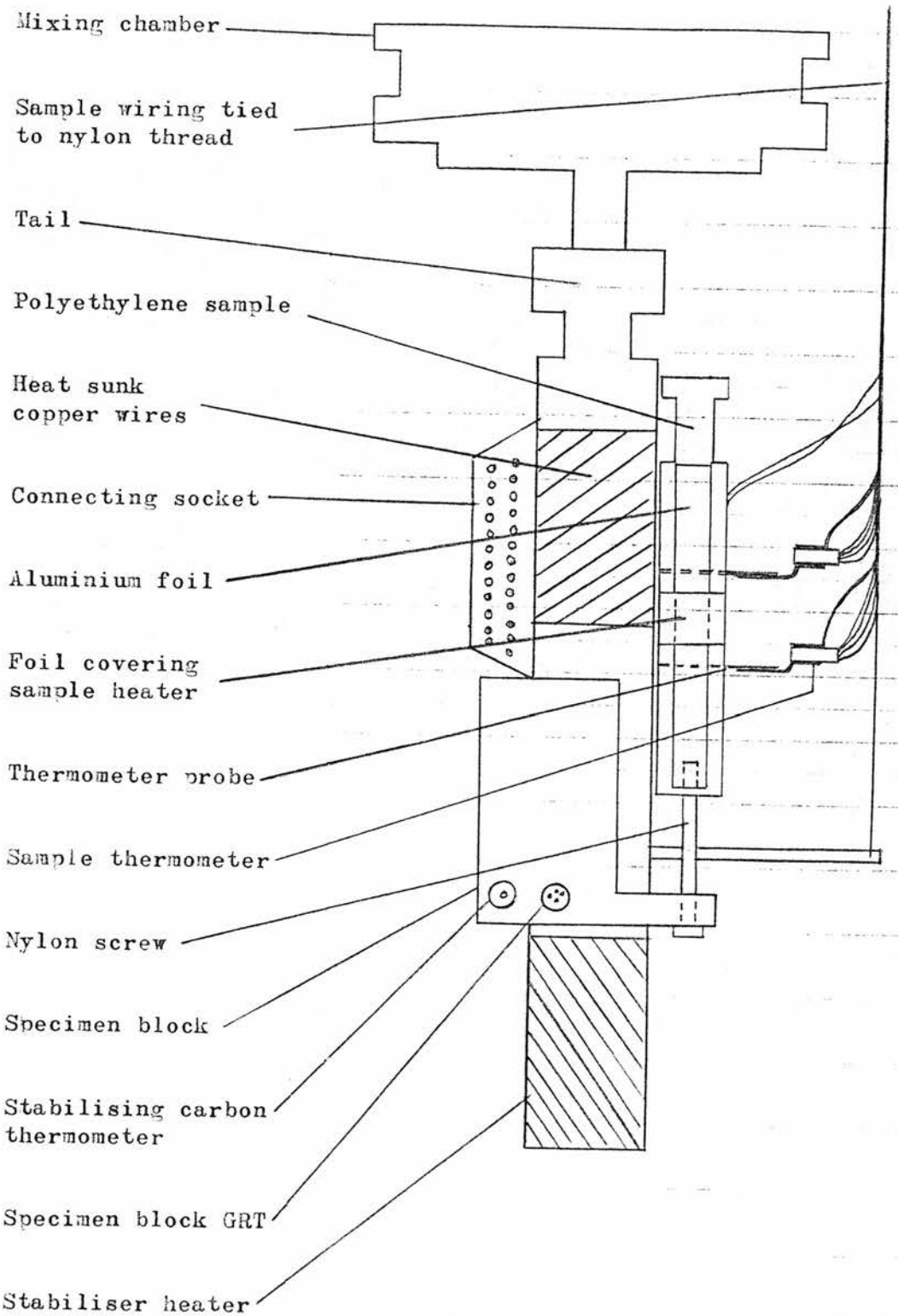

Figure 5.1

The experimental arrangement used to measure the heat capacity of the polyethylene samples.

thermal link between the experimental section of the refrigerator and the mixing chamber. One end of this rod was positioned inside the mixing chamber, and the rod formed an integral part of the bottom plate of the mixing chamber. The other end of this rod screwed into a threaded hole (0BA) in the top of the tail. The thermal contact between this rod and the experimental section was improved by greasing the screw thread using Apiezon grease, and since no difficulty in cooling the experimental section has been experienced, it appears to be adequate.

The GRT (Ge5), used to monitor the temperature of the experimental section, is partially embedded in Woods metal, inside a hole in the specimen block. The carbon thermometer used to stabilise temperature (see section 4.6) is mounted in a hole in the specimen block, and the stabiliser heater is wrapped around one end of the tail. 32 SWG enamelled copper wires, were attached to the other end of the tail using GE varnish, in order to heat sink the leads of the thermometer Ge5, the stabilising thermometer & the stabiliser heater, to the experimental section. In order to obtain a good thermal link, the section of each wire in contact with the tail was 25 cm long.

5.3.2 The Thermal Link Between Sample and Experimental Section

A 6BA nylon screw 2.5 cm long, passed through a suitable threaded hole in the copper shelf 1.5 cm x 1.4 cm x 0.5 cm, which forms part of the specimen block. The other end was screwed into a threaded hole about 0.6 cm deep, in the sample. The screw supports the sample. Thermal contact between the screw and both the sample and the specimen block, was improved by greasing the relevant threads using Apiezon grease, and by ensuring that both of the screw connections were as tight as possible.

In order to support samples SH0 & SH2 using a 6BA screw, a nylon fitting was made which could be inserted into the hole drilled in these samples (see section 5.2). The dimensions of the fitting were slightly

larger than the dimensions of the hole, and so the fitting had to be forced into the hole, the tight fit ensuring good thermal contact. The fitting was drilled and tapped to receive a 6BA screw. The same fitting was used with both samples. The heat capacity of this fitting was determined from the measured specific heat capacity of nylon, and had to be included in the heat capacity of the addenda, when the specific heat capacity of these samples was calculated.

The length of the screw between the specimen block and the sample was about 1.5 cm. The thermal resistance between the sample and the experimental section is determined by the thermal conductivity of nylon, and the length and cross-sectional area of the screw. It was chosen so that the time constant, with which the rise in sample temperature produced by the heat pulse decays, was reasonable over the temperature range of the heat capacity measurements.

5.3.3 The Sample Heater

The sample heater consisted of a piece of 48 SWG eureka wire 32.6 cm long with a resistance of about 116Ω below 1K. Eureka wire was used, because a suitable resistance can be obtained using a relatively short piece of wire, and the change in the resistance of the heater over the temperature range of the experiment (0.15K to 1.3K) is negligible. Eureka is not entirely suitable, because of its relatively large specific heat capacity which goes through a minimum at 0.3K and then increases as temperature decreases (Ho, O Neal & Phillips 1963). The wire was insulated by a layer of enamel and a layer of double silk. The same heater was used for all six samples and by the end of the experiments, the quality of the insulation was beginning to deteriorate.

Aluminium foils were used to minimise temperature gradients and to ensure that the heat was supplied uniformly along the length of the sample. Two pieces of aluminium foil 5.0 cm x 0.6 cm x 20 μm were attached to the surface of the sample using a thin layer of Apiezon

grease. The two pieces of foil were arranged parallel to each other along the length of the sample, and separated by a diameter of the sample, which was perpendicular to the thermometer probes (see section 5.3.4). The heater wire was then wound around the central section of the sample, approximately midway between the two thermometer probes. A third piece of aluminium foil 3.9 cm x 0.85 cm x 20 μm covered with a thin layer of Apiezon grease, was then wound around the sample in such a way as to completely cover the sample heater. Five pieces of nylon thread (diameter 0.17 mm) were tied around the sample and held the foils, heater and heater leads in position.

The heater leads were two 50 cm lengths of 0.002" diameter, lead covered manganin wire. This wire is superconducting at low temperature, so that the electrical resistance of the heater leads is negligible. Each heater lead was connected at the mixing chamber socket, to two leads of the refrigerator wiring, so that a four terminal measurement of the resistance of the sample heater and its leads could be made using the PCB. Since both of the soldered connections between the heater and the heater leads were underneath the aluminium foil, one of the connections had to be covered by a tiny piece of PVC insulating tape, to prevent the foils from short circuiting the heater.

5.3.4 The Sample Thermometers

The sample temperature was monitored by two GRT's (Ge1 & Ge3), mounted on copper wires passing through the sample along parallel diameters 1.5 cm apart. These wires were 2.0 cm long and were made by removing the insulation from 28 SWG copper wire (diameter 0.376 mm). They will be referred to as the thermometer probes. They were coated with apiezon grease and inserted with difficulty into holes drilled through the sample with a No 79 drill bit (diameter 0.38 mm). When the sample cooled, because of the relatively large coefficient of thermal expansion of polyethylene, it contracted onto the thermometer probes,

improving thermal contact between the probes and the sample.

For reasons discussed in section 4.3, it was necessary to provide a thermal link between the sample and both the case and the leads of the GRT. This was achieved by taking a piece of 28 SWG copper wire about 8 cm long without any insulation, and wrapping the middle section of the wire around the case of the GRT. This wire spiral was attached with great care to the case of the thermometer using Woods metal. It will be referred to as the thermometer support wire. One of the thermometer current leads, which had been shortened to a length of about 3 cm, was soldered to one of the ends of the thermometer support wire. The other end of the thermometer support wire was attached using Woods metal to the thermometer probe. Thus a thermal link between the sample, the thermometer case and the germanium crystal was established.

It was intended to use the same thermometer probes for all the samples, so that the heat capacity of the sample addenda remained constant. This proved to be impractical, as the insertion of the wires into the samples led to work hardening, and one of the wires snapped, leaving a short section of wire inside SHO which could not be removed. Another hole had to be drilled through the sample, and new probes used, whose combined length was reduced by the length of the wire remaining inside the sample. Thereafter new probes of the same length as the original wires, were used for each sample. It should be noted that with the exception of the thermometer probes, the same addenda was used for all the samples. In particular it was only necessary to attach the thermometer support wire to the thermometer case once, so that the amount of Woods metal remained constant.

The thermometer leads were connected to the connecting socket below the mixing chamber, by 44 SWG, enamelled, double silk covered, eureka wires about 50 cm long and twisted in pairs. Eureka wires were chosen for their high thermal resistance, in order to minimise the heat

flow between the sample and its surroundings via the thermometer leads, and so minimise any temperature difference between the sample and the thermometers. This choice was not entirely satisfactory because of the large heat capacity of these leads at low temperatures. The effect of this heat capacity is discussed in more detail in section 6.7.

It was also important that the thermometer leads and heater leads did not touch any part of the system, particularly the radiation shield suspended from the first step heat exchanger and the wall of the IVC. More than one method of hanging the thermometer and heater leads was used during the heat capacity measurements. Initially the wiring was suspended by means of six trapezes, made of nylon line (diameter 0.55 mm) and attached to the mixing chamber. This method was abandoned in favour of a simpler method, made possible by the increase in the diameter of the IVC from 4" to 6". The bundle of 8 thermometer leads and 2 heater leads was attached to two taut parallel nylon threads. These threads had a diameter of 0.17 mm and were attached at one end to the experimental section and at the other end to the first step heat exchanger. The bundle of wires was loosely tied to the central section of these threads, passing up one thread and down the other, so as to form a U shape.

5.4 The Nylon Sample

The heat capacity of the addenda, used in the measurements performed on the polyethylene samples, was determined by measuring the heat capacity of a nylon sample and the addenda, and then repeating the measurement after the mass of the sample had been reduced by approximately half. Nylon was used, because it was the only readily available material, whose specific heat capacity and thermal conductivity was similar to that of the polyethylene samples.

The sample was a cylinder, of diameter 0.95 cm and 7.0 cm long. A 6BA hole was drilled and tapped in the base of the sample. The holes for the thermometer probes were drilled 1.5 cm and 3.0 cm from the base of the sample. The length of the sample and the non symmetrical positioning of the thermometers, was necessary to permit the heat capacity measurements to be repeated after the sample had been cut into two pieces. The shortened sample was 3.8 cm long.

The foils were attached to the original nylon sample as follows: one foil extended from the heater to the top of the sample, while the second foil extended from the heater to the base of the sample, and the third foil covered the heater, which was placed above the upper sample thermometer, midway along the length of the sample. This non standard arrangement was necessary, because of the length of this sample and the absence of a neck.

5.5 The Experimental Procedure

The temperature of the experimental section was stabilised in the manner described in section 4.6, for sufficient time to allow the sample temperature to come to equilibrium (between 15 and 30 minutes). A heat pulse was then supplied to the sample, and the temperature rise and its subsequent decay monitored using thermometer Ge3. After the sample had returned to equilibrium again, a second smaller heat pulse was supplied to the sample, and the sample temperature was monitored using thermometer Ge1. The temperature of the experimental section was then raised, and a second pair of heat capacity measurements made. The change in equilibrium sample temperature between readings, was approximately equal to the sample temperature rise produced by the heat pulses.

The heat pulse was supplied to the sample using the arrangement of instruments shown in figure 5.2. The switch timer closed a relay, for a preset length of time (usually 10 seconds) allowing a current to flow through the sample heater and a standard resistor. The length of the

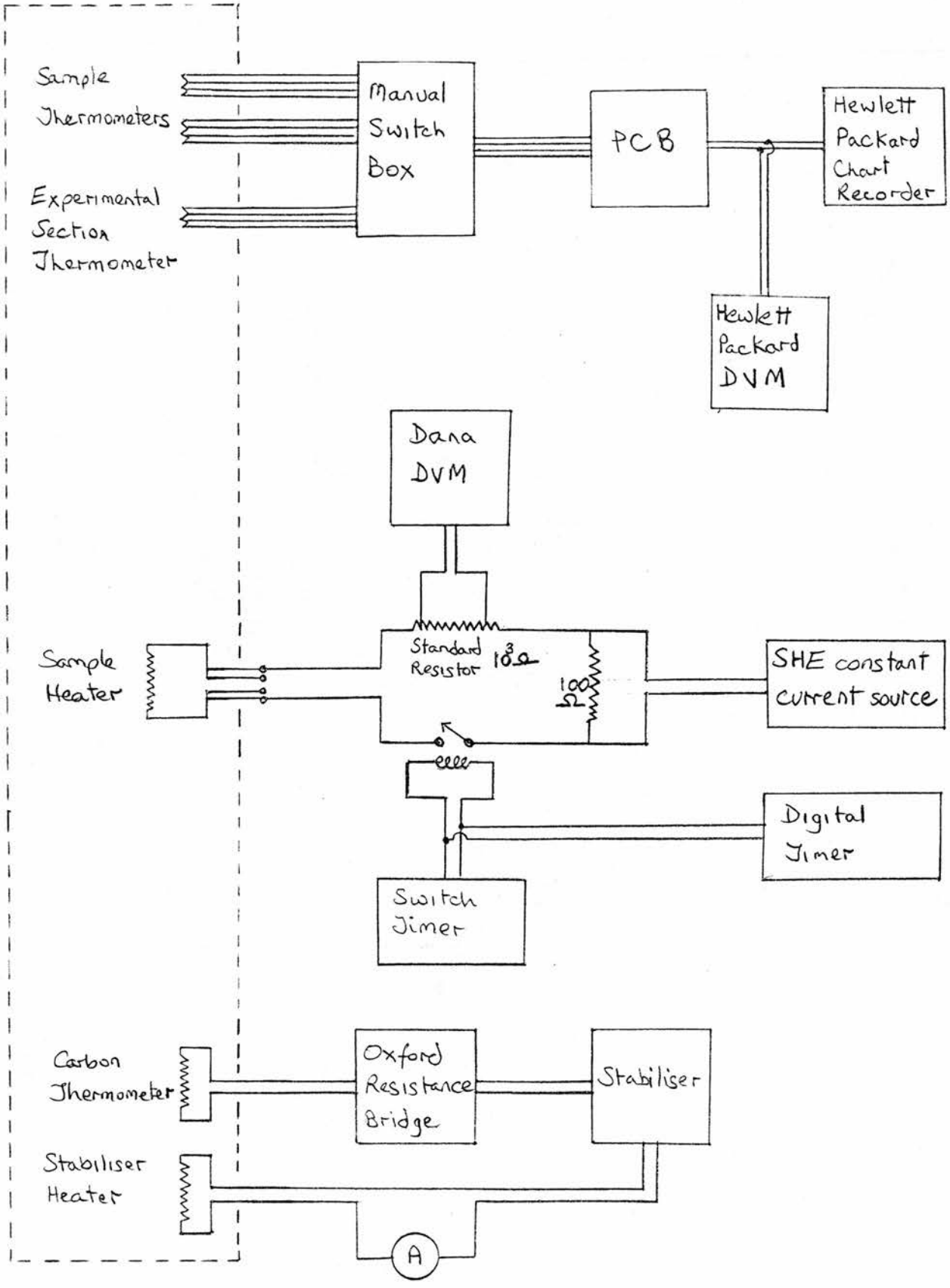

Figure 5.2

The arrangement of the instruments used to measure the heat capacity of the polyethylene samples.

heating period was measured using a digital timer, triggered by the change in voltage across the coil which opened and closed the relay. It was considered sufficient to measure the length of the heat pulse to an accuracy of ± 1 ms. The delay between the change in voltage which triggered the timer, and the closing and opening of the relay was 0.1 ms & 0.2 ms respectively. The 100Ω resistor in parallel with the sample heater and standard resistor, ensured that when the relay closed, the fractional change in the power supplied by the constant current power supply was negligible; so that the shape of the pulse was as close to a step function as possible. The sample heater current was measured using a Dana DVM with a $5\frac{1}{2}$ digit readout, and a minimum full scale reading of 0.12 volts, connected across a 1000Ω standard resistor. Using these instruments a current of 4 μA, the minimum current value used, could be measured to an accuracy of 0.17%.

The sample heater could be disconnected from the sample heater circuit and connected to the PCB, by simply removing a DIN plug from one socket and inserting it into another. Measurements of the resistance of the sample heater were made using the PCB, in between the heat capacity measurements. The average value of the sample heater resistance was used to calculate the energy supplied to the sample during a heat pulse. The size of the heat pulse could be calculated to a nominal accuracy of 0.3%. This contribution to the experimental error is negligible, compared with other errors involved in the heat capacity measurements.

A record of the variation of the analogue output voltage of the PCB with time, during each heat capacity measurement, was obtained using a Hewlett Packard chart recorder. This output voltage (V) is nominally related to the measured values of thermometer conductance (G), by the expression $V = 100 \left(\frac{G - G_{SET}}{G_{SET}} \right)$ where $-12 \leqslant V \leqslant +12$ volts.

Prior to the application of the heat pulse, G_{SET} is adjusted by means of a ten turn potentiometer, until the PCB analogue output voltage is zero,

the value of G_{SET} is then read off from the PCB display. The maximum percentage change in the thermometer conductance which can be recorded in this manner is 12%. For this reason the energy supplied to the sample is adjusted, by adjusting the output of the constant current supply, so as to produce a temperature rise equivalent to a 10% increase in thermometer conductance, and a peak 10 cm high on the plotter output. The thermometer conductance was monitored using the PCB and chart recorder, until its value had returned to within 0.5% of its equilibrium value. This took 4 minutes at 0.2K, and 13 minutes at 1.3K.

In order to process the data, a smooth pencil line was drawn through the noise on the PCB output voltage/time curves; and the coordinates of about 40 points were read off from each curve. This set of points consists of the points which coincide with the start and end of the heating period, and points taken from the curve obtained during the cooling period. These coordinates and the value of G_{SET} were input to the computer, which converted the PCB output voltages into conductance values, and then converted these conductance values into temperature values using the thermometer calibration curves. This sample temperature/time curve was used to calculate the heat capacity of the sample and its addenda (see section 6.1).

5.6 Minimum Sample Temperature

The lowest temperature to which the sample could be cooled, depends on the size of the thermal resistance between the sample and the experimental section, and the extraneous heat input to the sample. When the experiment was first set up, the minimum sample temperature was 220mK. It was realised that the pumps used to evacuate the IVC, were causing the sample mounted on the experimental section to vibrate, giving rise to a large heat input to the sample. The IVC was isolated and the pumping system shut down with the result that the sample cooled to 110mK. This was considered to be a reasonable value for the minimum

sample temperature.

The cryostat and its frame are supported on mountings, which partially isolate it from the vibrations of the building. The only remaining source of vibration within the laboratory, was the rotary pump used to circulate the mixture. This pump was mounted on springs and isolated mechanically from the cryostat by lengths of flexible plastic tubing. Thus a further reduction in the heat input to the sample due to vibration would be difficult to achieve.

When the measurement of the heat capacity of the nylon sample was attempted, it was found that the sample could not be cooled below 210mK. A calculation to determine the expected rate of change of sample temperature with time after the application of a heat pulse, based on the dimensions and thermal conductivity of the nylon screw was performed, and the results compared with observed values of this parameter. The purpose of this calculation was to establish whether the observed value of minimum sample temperature was the result of: (1) a substantial thermal resistance between the screw and either the sample or the experimental section; or (2) an increase in the heat input to the sample. When the system is at equilibrium, the extraneous heat input ($\dot{q}_E$) to the sample is given by:

$$\dot{q}_E = \frac{A}{L} \int_{T_o}^{T_1} k(T)dT \qquad 5.1$$

where A is the cross-sectional area of the nylon screw,

L is the length of the screw,

T_o is the temperature of the experimental section,

T_1 is the equilibrium temperature of the sample and

k(T) is the thermal conductivity of nylon.

After the application of a heat pulse to the sample, the rate of change of sample temperature (T) with time (t) is given by:

$$-C\left(\frac{dT}{dt}\right) = \frac{A}{L} \int_{T_o}^{T_1+\Delta T} k(T)dT - \dot{q}_E = \frac{A}{L} \int_{T_1}^{T_1+\Delta T} k(T)dT$$

where C is the heat capacity of the sample and its addenda at temperature ($T_1 + \Delta T$) and ΔT is the sample temperature rise. The integral was evaluated using an expression for k(T), obtained by fitting a curve to the experimental measurements of the thermal conductivity of nylon made by Scott et Al (1973). Reasonable agreement between the calculated and observed values of the rate of change of sample temperature with time was found, showing that the observed rate of cooling was consistent with the thermal resistance of the nylon screw. Equation 5.1 was used to estimate the extraneous heat input to the sample.

The radiation shield attached to the warmest step heat exchanger, was too short to enclose the sample, and the clearance between the shield and the step heat exchangers was too small to permit the sample leads to be hung inside the shield. Consequently the sample and its wiring were exposed to radiation from the wall of the IVC at a temperature of 4.2K. The radiation shield was modified so that it enclosed both the sample and its leads. Following this modification, the heat input to the nylon sample was reduced from 0.055 erg/s to 0.021 erg/s, and the minimum sample temperature dropped to 0.13K, which was considered adequate.

When the mixing chamber temperature reaches its lowest value, the temperature of the radiation shield is about 0.2K. If this shield enclosed the sample completely, then the heat input to the sample due to radiation would be negligible, however some radiation from the IVC wall will leak through small gaps in the shield and reach the sample. The heat input to the sample due to conduction by helium atoms left within the IVC, is also reduced as a result of the adsorption of these atoms by the shield.

The difference in the extraneous heat input to the polyethylene and nylon samples can be explained using the results of Anderson et Al (1971), who measured the emissivity of various surfaces at low temperatures. They found that at 0.2K, the emissivity of copper is 8×10^{-4}, while the emissivity of stainless steel is 0.07. The change in the extraneous heat input to the samples, coincided with the replacement of the copper can, which enclosed the IVC, by a stainless steel can. Thus the emissivity of the wall enclosing the samples increased by a factor of 90, leading to an increase in the heat input to the sample due to radiation.

It was noted that the extraneous heat input observed during the thermal conductivity experiment, was less than that observed during the heat capacity experiment, using the same radiation shields. The sample is more rigidly held in the thermal conductivity experiment than in the heat capacity experiment, as the sample is mounted on a copper stud instead of a nylon screw. Thus it seems likely that the component of the extraneous heat input due to vibration, has been reduced.

CHAPTER VI

THE ANALYSIS OF THE HEAT CAPACITY DATA

6.1 The Correction for the Heat Loss during the Heating Period

From the data acquired during an experimental measurement, the energy generated within the sample heater during the heating period, is easily calculated. The variation of PCB output voltage with time, is converted into the variation of sample temperature with time, in the manner described earlier (see section 5.5); and can be used to calculate the heat capacity of the sample and its addenda, corrected for the heat loss during the heating period, using the following method devised by Collan et Al (1970).

During the heating period, the energy Q absorbed by the sample is given by:

$$dQ = C(T).dT = (P - \dot{q}(t)).dt$$

$$Q = \int_{T_o}^{T_f} C(T).dT = P.\Delta t - \int_{o}^{\Delta t} \dot{q}(t).dt$$

where C(T) is the heat capacity of the sample and its addenda,

P is the power generated within the sample heater,

$\dot{q}(t)$ is the rate of heat loss from the sample,

T_o is the sample temperature before the start of the heating period,

T_f is the sample temperature at the end of the heating period and

Δt is the length of the heating period.

This equation can be rearranged in such a way as to replace the integration with respect to time (t), by an integration with respect to temperature (T).

$$Q = \int_{T_o}^{T_f} C(T).dT = P.\Delta t - \int_{T_o}^{T_f} \frac{\dot{q}(T).C(T)}{P - \dot{q}(T)} \, dT$$

The rate of heat loss from the sample ($\dot{q}(T)$) is a function of sample temperature only, and this function is the same for both the heating and cooling periods, provided that the following assumptions are valid:

(1) The temperature of the experimental section of the refrigerator remains constant throughout the measurement.

(2) The extraneous heat input to the sample remains constant throughout the measurement.

(3) The time taken to establish thermal equilibrium within the sample, is negligible with respect to the length of the heating period, and the time constant of the cooling period. The validity of this assumption is discussed in section 6.6.

Thus the function $\dot{q}(T)$ can be determined from the variation of sample temperature with time during the cooling period since

$$\dot{q}(T) = -C(T)\left(\frac{dT}{dt}\right)_{CP} \quad .$$

The functional form of the temperature dependence of the heat capacity of the sample and its addenda is unknown, and so it is assumed that this parameter is independent of temperature over the temperature range of the measurement, so that:

$$C(\bar{T}).(T_f - T_o) = P.\Delta t - \int_{T_o}^{T_f} \frac{-C(\bar{T})^2.\left(\frac{dT}{dt}\right)_{CP}.dT}{\left(P + C(\bar{T})\left(\frac{dT}{dt}\right)_{CP}\right)} \qquad 6.1$$

where $\bar{T} = \frac{1}{2}(T_o + T_f)$.

The gradient of the sample temperature/time curve during the cooling period $\left(\frac{dT}{dt}\right)_{CP}$ can be obtained as a function of sample temperature (T) as follows: The points (t_i, T_i, i=1,n), taken from the sample temperature/time curve observed during the cooling period, are fitted using a least squares procedure, by a curve of the form:

$$T(t) = T_o + \exp\left\{\sum_{j=1}^{m} a_j t^{j-1}\right\} \qquad \text{where } m \leqslant 4 \ .$$

The values of time (t_i) are measured relative to the end of the heating

period, so that the value of the sample temperature at the end of the heating period T_f is given by: $T_f = T_o + \exp(a_1)$. The derivative of the fitted curve is evaluated, and a series of points $(x_i, y_i, i=1,n)$ are obtained, where $x_i = T(t_i) - T_o$ and $y_i = \left[\frac{d}{dt}(T(t))\right]_{t=t_i}$. These points are then fitted using a least squares procedure, by a curve of the form: $y = \sum_{j=1}^{m} b_j x^j$, $m \leqslant 4$. This curve can be used to determine the value of $\left(\frac{dT}{dt}\right)_{cP}$ corresponding to any value of temperature T; $T_o \leqslant T \leqslant T_f$.

Assuming initially that the heat lost from the sample during the heating period is negligible, a first estimate of the heat capacity can be made: $C_1(\overline{T}) = \left(\frac{P.\Delta t}{T_f - T_o}\right)$. This value of the heat capacity can then be used in conjunction with the expression for $\left(\frac{dT}{dt}\right)_{cP}$ obtained earlier, to evaluate the RHS of equation 6.1; obtaining an improved estimate of the heat capacity $C_2(\overline{T})$, which can itself be used to evaluate the RHS of equation 6.1. This iterative procedure converges rapidly, the third iteration producing a change of less than 0.3% in the calculated value of the heat capacity of the sample and its addenda. The percentage of the heat supplied to the sample, which is lost during the heating period, decreases from typically 8% at 0.15K to about 2% at 1.5K.

The most obvious source of error in this calculation of the heat capacity is in fact the determination of the values of T_o and T_f. The error δT_o in the determination of T_o, which arises from the noise on the PCB analogue output, is typically 1% or more of the temperature rise $(T_f - T_o)$. An uncertainty of one second in the position of the point, on the fitted sample temperature time curve, which corresponds to the end of the heating period, gives rise to an error δT_f in the value of T_f, which is typically 1.5% of the temperature rise. The speed of the chart recorder (0.69 mm/s) makes such an uncertainty likely.

The other serious error in this analysis of the heat capacity data, arises from the change in the extraneous heat input to the sample, which occurs during a measurement as a result of the way in which the thermometer leads absorb heat from the sample (see section 6.7).

The calculated value of the heat capacity of the sample and its addenda $C(\overline{T})$, is assumed to correspond to the mean value of temperature during the measurement $\overline{T} = \frac{1}{2}(T_o+T_f)$. The error implicit in this assumption, has been estimated by fitting a curve to the variation of the heat capacity of the sample and its addenda with temperature, and then using this curve to evaluate numerically the integral in the following expression for the error:

$$\%\text{Error} = 100 \left\{ \int_{T_o}^{T_f} C(T)dT - C\left(\frac{T_o+T_f}{2}\right).(T_f-T_o) \right\} \Big/ \left\{ \int_{T_o}^{T_f} C(T)dT \right\}$$

It was found that at low temperatures this error is negligible increasing to a maximum value of 0.8% at 1.5K.

The heat capacity of the sample and its addenda, corrected for the heat loss during the heating period, can be calculated using an alternative procedure devised by Keesom & Kok (1932). The results obtained using this method were found to be very similar to the results obtained using the method of Collan et Al. The method of Collan et Al was preferred, as the derivation of this method makes fewer assumptions than the derivation of the method of Keesom & Kok.

6.2 Correction of Error Introduced by Use of PCB Analogue Output Voltage

After plotting, the calculated values of the heat capacity of the sample and its addenda against temperature, it was noticed that a divergence of up to 15%, existed between the results of measurements taken using thermometers Ge1 and Ge3, at temperatures below 0.19K. It was also noticed that at 0.19K, the conductance of thermometer Ge1 was 2.0 mMho, at which value it is necessary to change the scale of the PCB.

These observations led to a systematic check of the relationship between the PCB analogue output voltage V_o and the reading G displayed by the PCB. A comparison between the observed output voltage V_o, and the value of voltage V_c, calculated using the relationship $V_c = 100 \left(\frac{G - G_{SET}}{G_{SET}}\right)$ specified by the manufacturers, revealed a consistent error, the magnitude of which is a function of G_{SET}:

$$\xi = \left(\frac{V_c - V_o}{V_o}\right) = \left(\frac{0.0105\ G_{MAX}}{G_{SET}}\right)$$

where G_{MAX} is the maximum value of conductance which can be measured on the relevant scale of the PCB. Thus the relationship between the observed analogue output voltage and the PCB reading is determined empirically to be:

$$G = G_{SET}\left(1 + \frac{V_o}{100}\left(1 + 0.0105\ \frac{G_{MAX}}{G_{SET}}\right)\right)$$

The heat capacity results were recalculated using the corrected relationship. The observed divergence between measurements made using different thermometers disappeared. A similar divergence at temperatures exceeding 0.9K also disappeared, confirming the validity of the correction.

6.3 Calculation of the Addenda Heat Capacity

The addenda heat capacity includes the heat capacity of the sample heater, the aluminium foils, the germanium resistance thermometers and the copper wires which provide the thermal link between the GRT's and the sample. It also includes the effective heat capacity of the thermometer and heater leads (see section 6.7); as well as smaller contributions due to nylon threads, grease, solder and Woods metal. The addenda heat capacity $C_A(T)$, can be deduced from the measurements of the heat capacity of the nylon sample and its addenda, described in section 5.4.

$$C_K(T) = C_A(T) + m_K \cdot c_N(T) \quad ; \quad k=1,2 \quad ; \quad (m_1/m_2)=1.874$$

where $C_K(T)$ is the combined heat capacity of a nylon sample of mass m_K

and the addenda; and $c_N(T)$ is the specific heat capacity of nylon.

$$C_A(T) = \left(\frac{m_2 . C_1(T) - m_1 . C_2(T)}{m_2 - m_1} \right) \qquad 6.2$$

The functional form of $C_K(T)$ is not known, as the temperature dependence of the specific heat capacities of the sample and the individual components of the addenda is too dissimilar. Consequently a simple low order polynomial was fitted using least squares to the experimentally obtained points (x_i, y_i, i=1,n) where $x_i = \log(T_i)$ and $y_i = \log(C_{K_i})$; obtaining two curves of the form:

$$\log(C_K) = \sum_{j=0}^{m} a_{jK} (\log T)^j \quad , \quad k=1,2.$$

It was found that an adequate fit to the experimental data was obtained using m=2. These two curves in conjunction with equation 6.2 can be used to determine the heat capacity of the addenda at any value of temperature. Figure 6.1 shows the experimental values of the combined heat capacity of sample and addenda for both nylon samples, and the curves fitted to this data.

6.4 Functional Form of the Specific Heat Capacity of Polyethylene

For each individual measurement of the combined heat capacity of a polyethylene sample and its addenda, the corresponding value of addenda heat capacity was calculated and used to obtain the value for the specific heat capacity of polyethylene $c_P(T)$. In order to determine the relationship between specific heat and temperature, a series of curves were fitted to the experimental data. These curves (ten in all) had the following form:

$a.x + b.y = 1$ where $x_i = \left(\frac{T_i^m}{C_i} \right)$ and $y_i = \left(\frac{T_i^\ell}{C_i} \right)$; $1 \leqslant m < \ell \leqslant 5$; i=1,n

and were fitted by minimising $\sum_{i=1}^{n} (a.x_i + b.y_i - 1)^2$.

The variables x & y were chosen so as to give equal weight to the points over the whole temperature range. It was found that an adequate fit to the data could only be obtained using m=1 and ℓ=3, showing that the experimental data was best fitted by a curve of the form $c = aT + bT^3$.

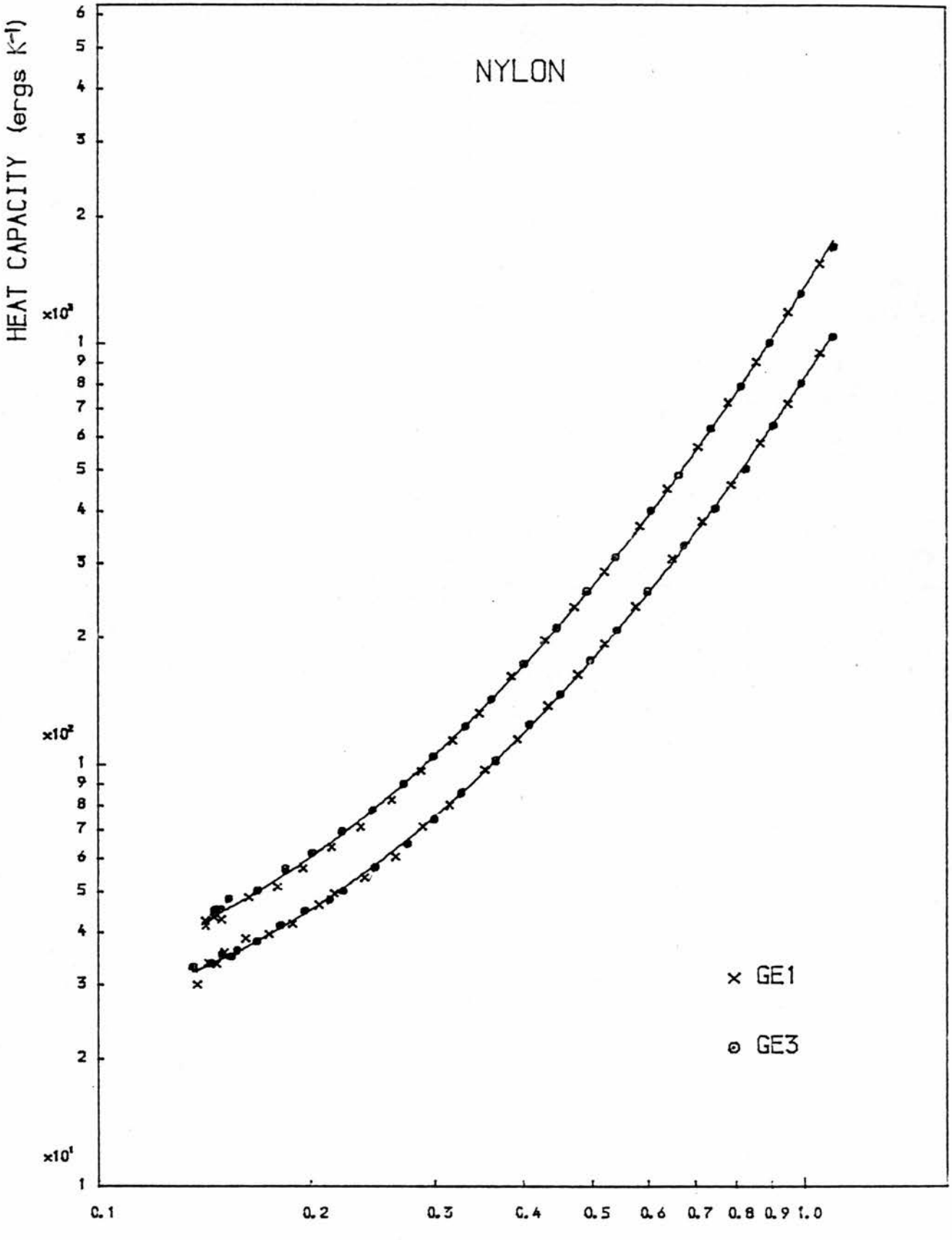

Figure 6.1

Experimental values of the heat capacity of the nylon sample and the addenda, before and after the sample was cut into two pieces. The fitted curves are of the form $\log(C)=a+bx+cx^2$ where $x=\log(T)$.

Figures 6.2 to 6.6 show the experimental values of specific heat capacity of the four polyethylene samples and also the nylon sample, with the curves fitted to the experimental data. For the purposes of comparison figure 6.7 shows the fitted curves for all four polyethylene samples and the experimental points for SH0 & SH3. Table 6.1 gives the coefficients a & b for each of the fitted curves. It also includes an estimate of the standard error of the regression coefficients, based on the scatter of the experimental points about the fitted curve.

It should be noted that an effect of subtracting the addenda heat capacity C_A, from the combined heat capacity of the sample and its addenda ($C_T = C_A + m.c_p$), to obtain the specific heat capacity c_p, is that the fractional error associated with the value of c_p, is a factor ($C_T/m.c_p$) larger than the corresponding error associated with the value of C_T. Thus for SH0:

$$\left\{\frac{1}{n}\sum_{i=1}^{n}\xi_i^2\right\}^{\frac{1}{2}} = 6.5\% \quad \text{where} \quad \xi_i = 100\ m\left(\frac{c_{pi} - a.T_i - b.T_i^3}{m c_{pi}}\right) \quad \text{and}$$

$$\left\{\frac{1}{n}\sum_{i=1}^{n}\eta_i^2\right\}^{\frac{1}{2}} = 2.1\% \quad \text{where} \quad \eta_i = 100\ m\left(\frac{c_{pi} - a.T_i - b.T_i^3}{m c_{pi} + C_{Ai}}\right) .$$

Values for $\bar{\xi}$ and $\bar{\eta}$ for the other samples are given in table 6.2. Thus the differences between the experimental and fitted values of specific heat capacity, correspond to errors in the experimental values of the heat capacity of the sample and its addenda, which can easily be explained in terms of the errors associated with the determination of the sample temperature rise (see sections 6.1 and 6.8). It can be concluded therefore that $c = aT + bT^3$, provides an adequate description of the experimental measurements of the specific heat capacity of the polyethylene and nylon samples.

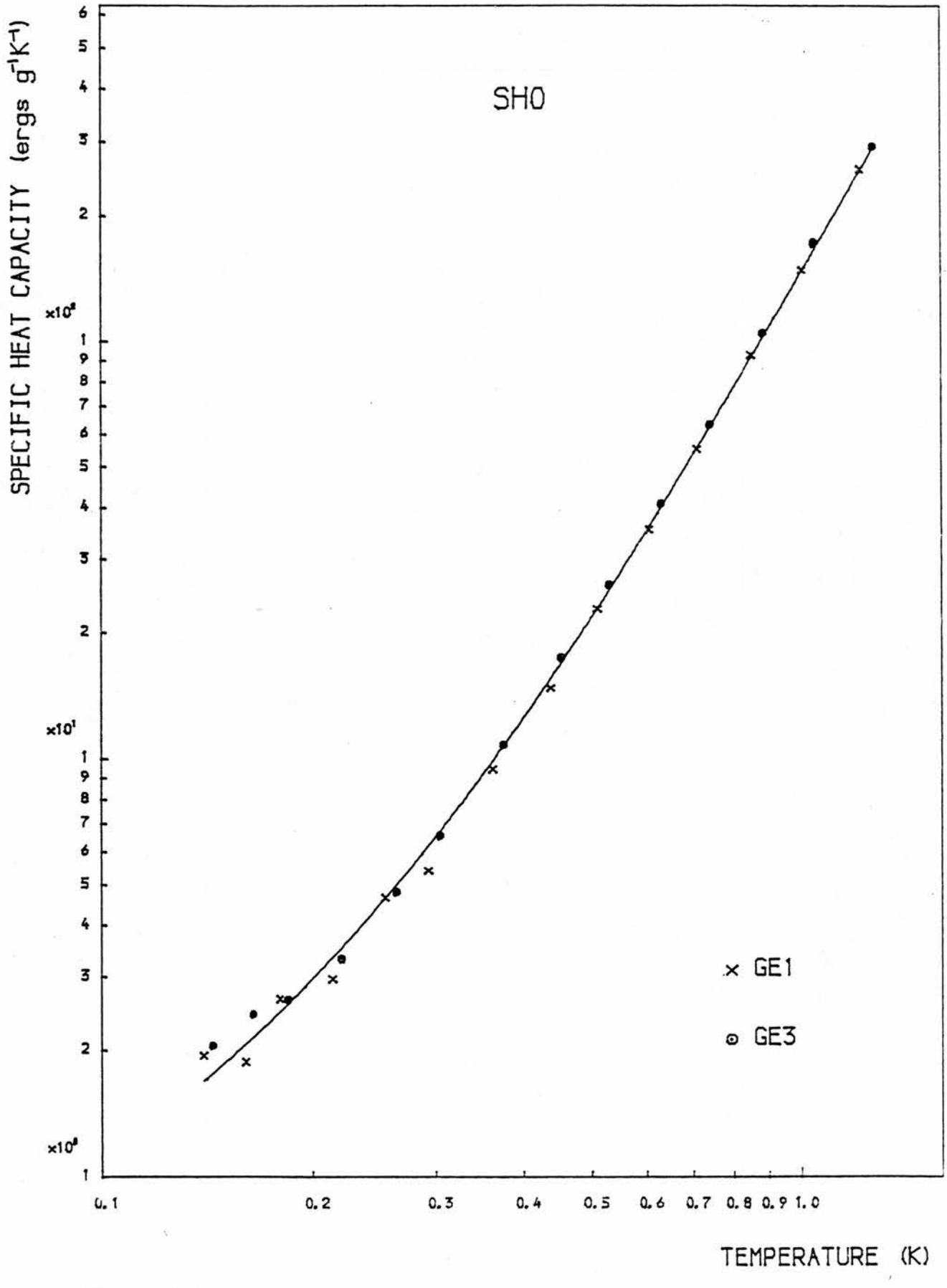

Figure 6.2

Experimental values of the specific heat capacity of the polyethylene sample SH0, fitted by a curve of the form $c = aT + bT^3$.

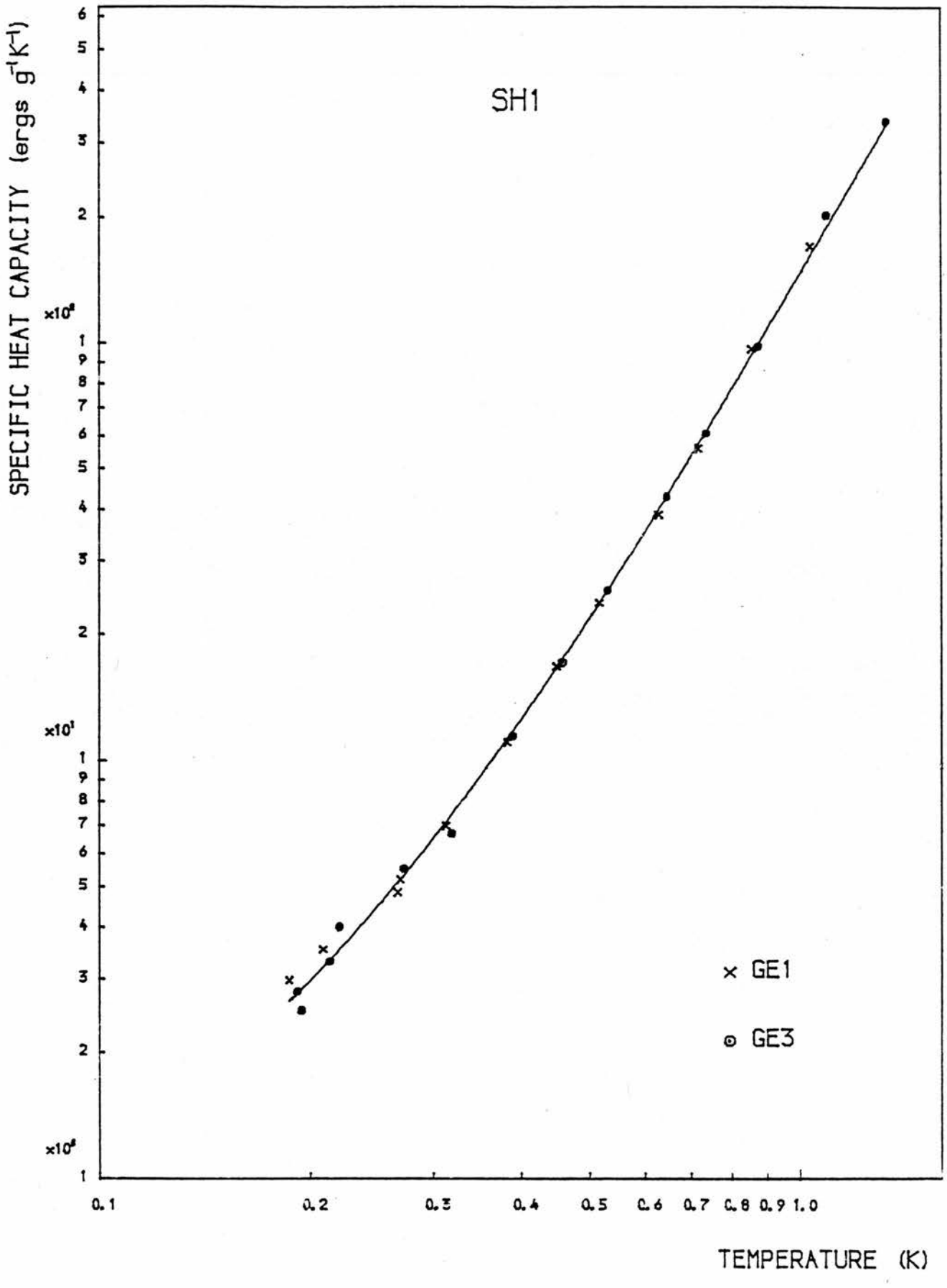

Figure 6.3

Experimental values of the specific heat capacity of the polyethylene sample SH1, fitted by a curve of the form $c = aT + bT^3$.

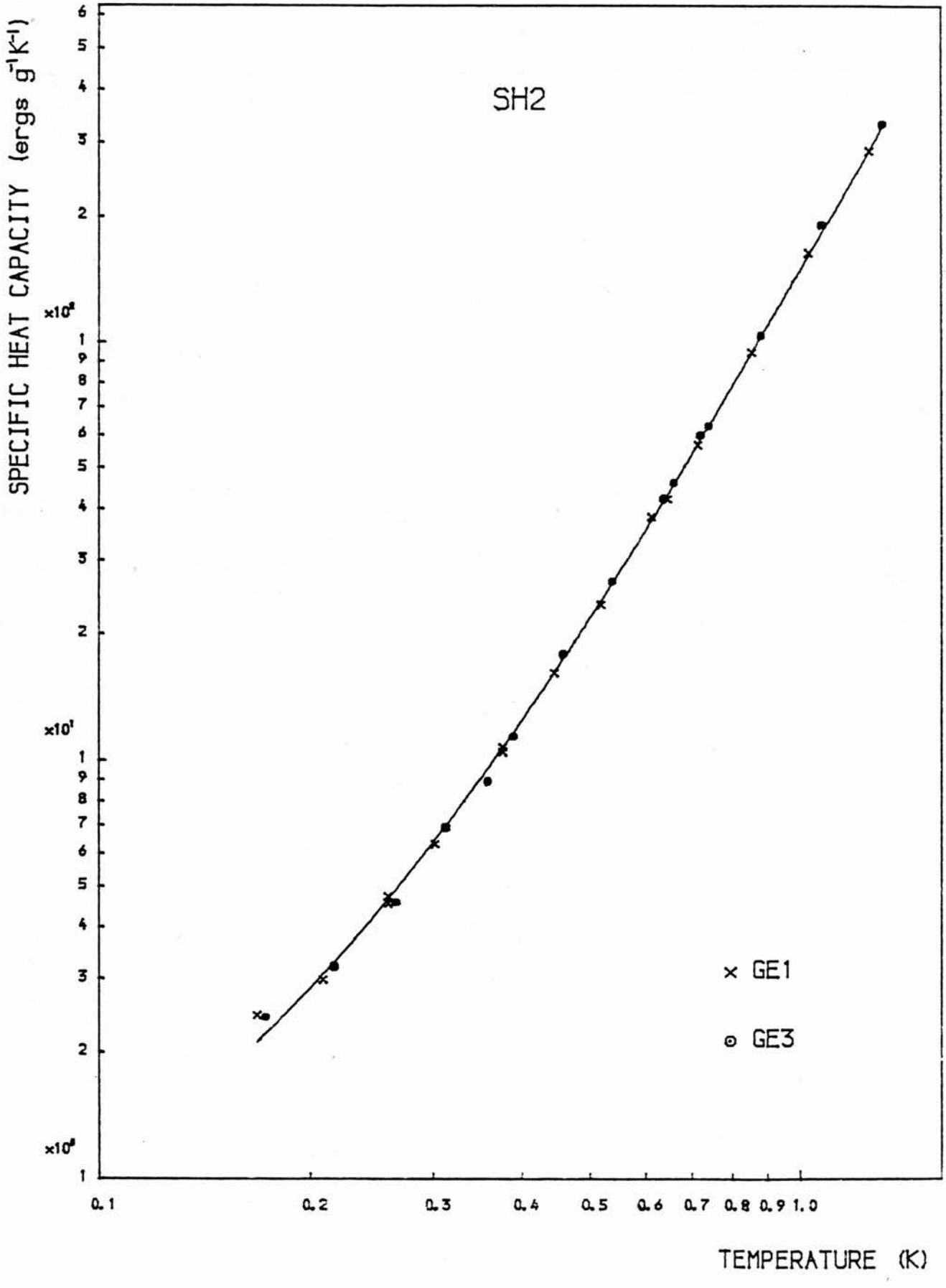

Figure 6.4

Experimental values of the specific heat capacity of the polyethylene sample SH2, fitted by a curve of the form $c = aT + bT^3$.

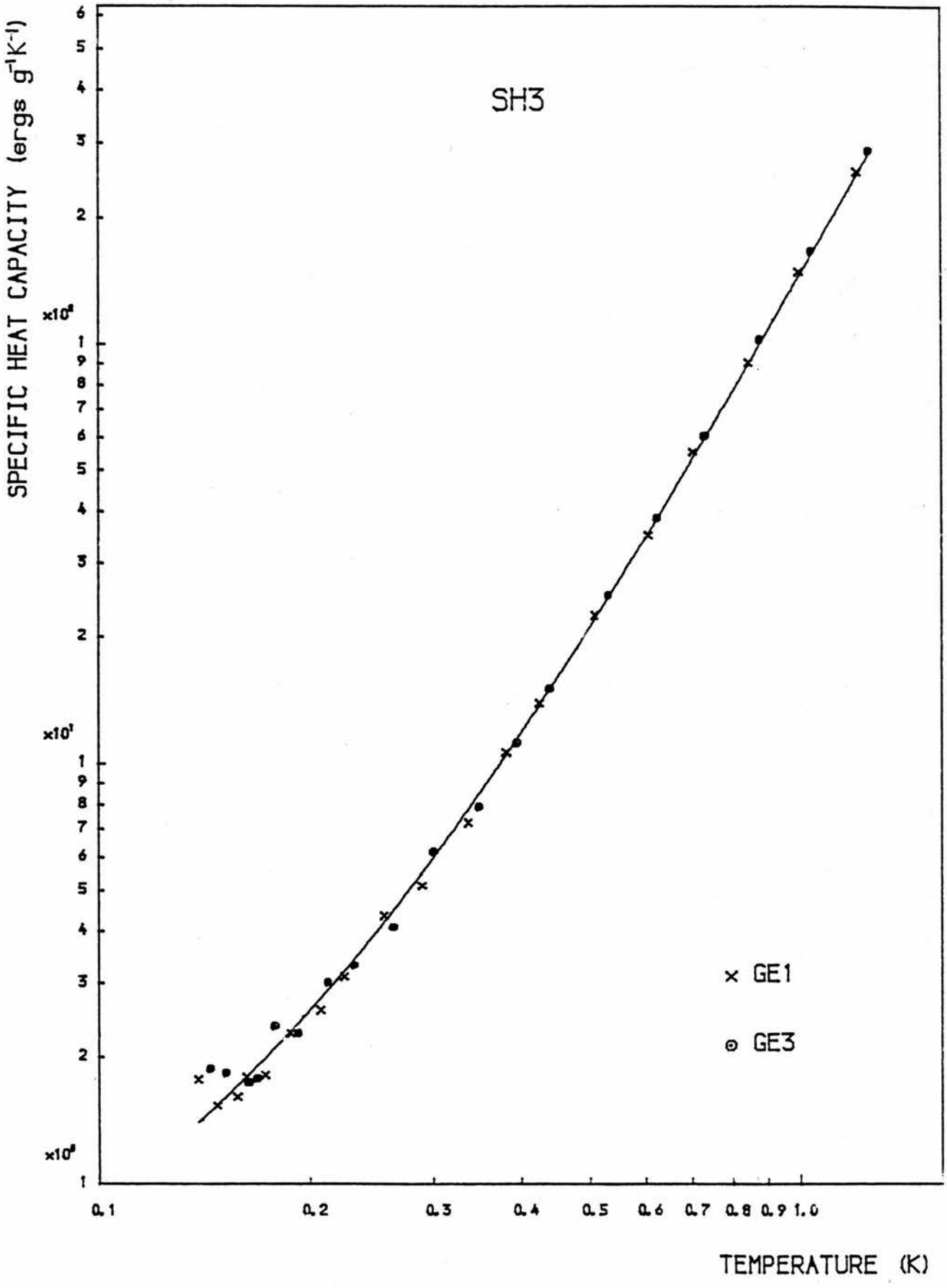

Figure 6.5

Experimental values of the specific heat capacity of the polyethylene sample SH3, fitted by a curve of the form $c = aT + bT^3$.

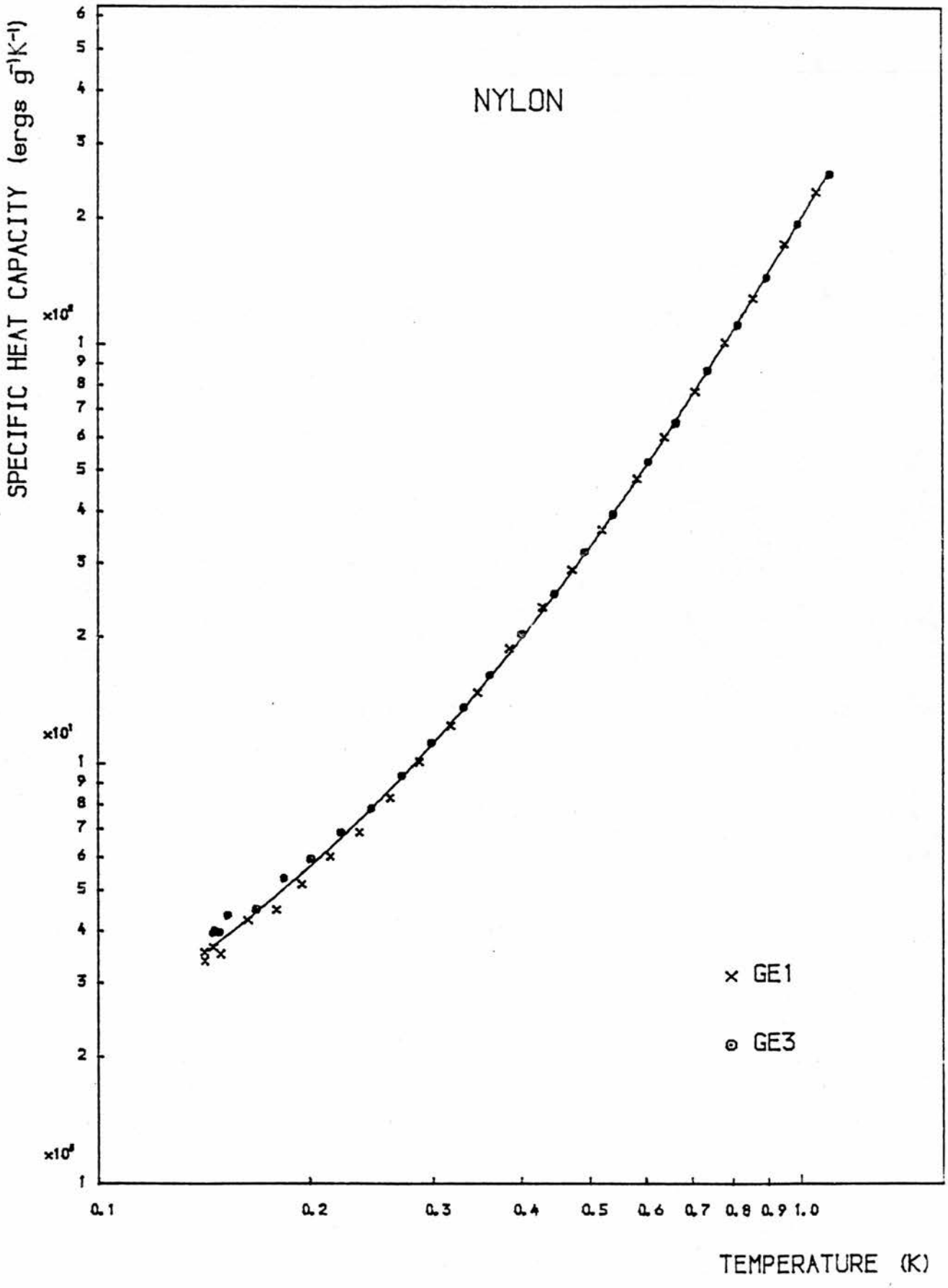

Figure 6.6

Experimental values of the specific heat capacity of the nylon sample, fitted by a curve of the form $c = aT + bT^3$.

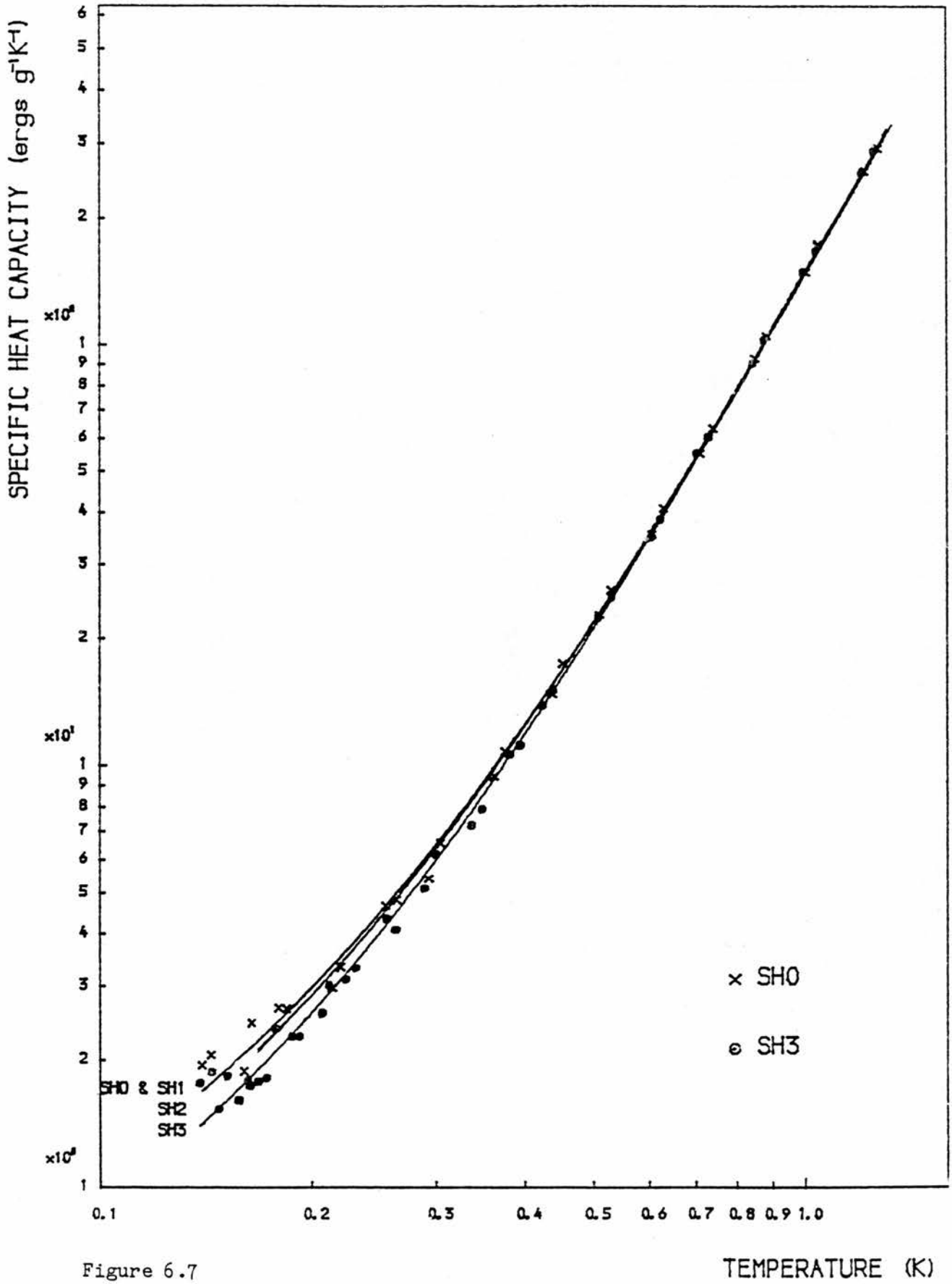

Figure 6.7

Specific heat capacity as a function of temperature for the four polyethylene samples, with the experimental points for samples SH0 & SH3.

TABLE 6.1

	a	b	$\left(\frac{100\,\Delta a}{a}\right)$	$\left(\frac{100\,\Delta b}{b}\right)$
	erg $g^{-1} K^{-2}$	erg $g^{-1} K^{-4}$		
SH0	9.44	136.1	3.6%	2.2%
SH1	9.41	136.8	3.8%	2.1%
SH2	8.67	140.0	2.7%	1.2%
SH3	7.40	139.1	3.3%	2.2%
Nylon	21.3	176.3	1.1%	1.1%

TABLE 6.2

	$\overline{\xi}$	$\overline{\eta}$
SH0	6.5%	2.1%
SH1	5.6%	2.3%
SH2	3.9%	1.5%
SH3	6.9%	2.0%
Nylon	3.7%	1.9%

6.5 A Computer Model of Heat Flow within the Sample during A Pulse Measurement

This model was set up in order to estimate the length of the time interval, at the end of the heating period, during which the temperature gradients present within the sample during the heating period, are replaced by those present during the cooling period. The model also estimated the size of these temperature gradients, and the consequent error associated with the measured values of heat capacity.

The model is constructed by representing the sample and its addenda by a series of "lumps" centred on nodal points. The lumps have a heat capacity C_i and the thermal resistance between neighbouring lumps

designated by i & j is R_{ij}. The heat conduction equation:

$k.\nabla^2 T + \dot{q} = \mathcal{C}.c\left(\frac{dT}{dt}\right)$ is replaced by a finite difference equation:

$$\sum_j \left(\frac{T_j - T_i}{R_{ij}}\right) + \dot{q}_i = \frac{C_i(T_i' - T_i)}{\delta t}$$

where T_i & T_j are the temperatures of nodes i & j at time t, and T_i' is the temperature of node i at some later time $t+\delta t$; $\dot{q}_i$ is the rate at which heat is generated within node i. The sum is taken over the nearest neighbours of node i. This equation can be used to calculate the temperature of any node within the sample at a time $t+\delta t$, provided the temperature of every node at time t is known. Therefore by starting from the initial temperature distribution within the sample, the temperature distribution at some later time can be calculated by simply evaluating the finite difference equation for every point in the sample, and repeating this procedure for the required number of time increments. The size of the time increment is limited by the condition:

$$\delta t \ll \left(\sum_j \frac{1}{R_{ij} C_i}\right)^{-1} .$$

If this condition is not satisfied, then the iterative procedure becomes unstable, resulting in wild oscillations of node temperatures. If the model is to work satisfactorily, care has to be taken when setting the values of R_{ij}, $\dot{q}_i$ & C_i for each node.

The equilibrium temperature distribution within the system, can be determined using the equation:

$$T_i'\left\{\sum_j \frac{1}{R_{ij}}\right\} = \dot{q}_i + \sum_j \frac{T_j}{R_{ij}}$$

to calculate the temperature T_i' at each node, starting from an arbitrary temperature distribution, and repeating the procedure until the changes in temperature values are negligible. Thus the heat flow within any system can be modelled, the accuracy of the model being limited only by the amount of computer time available, and the assumption that the values of C_i, R_{ij} & $\dot{q}_i$ are independent of

temperature. In a three dimensional system decreasing the separation of the nodes by a factor of 2, increases the required computer time by a factor of 32. Any symmetry possessed by the system can be used to reduce the calculation time, by reducing the number of nodes whose temperature has to be evaluated. A complete description of the setting up of this numerical model for the heat flow within a conducting solid is given by Chapman (1974).

The polyethylene samples were represented by 400 nodes, with additional nodes to represent the thermometers, heater and foils mounted on the sample. In order to model the temperature changes within the sample over a period of 15 seconds, using a time increment of 20 ms, about 150 seconds of CPU time were required.

Included in the model was the presence of the neck, and the thermal resistance of the nylon screw linking the sample to the experimental section of the refrigerator. The only heat loss from the sample was assumed to be via the screw. The heat capacity of the polyethylene nodes was calculated using the results given in this thesis, and the thermal resistance between these nodes was calculated using the results obtained by Rogers (1980).

The thermal conductivity of aluminium foil was taken from the results of Sharma (1967). Below 1.18K aluminium is superconducting, and its thermal conductivity decreases rapidly with decreasing temperature. At temperatures above 0.3K, the thermal conductivity of aluminium is sufficiently high to justify the assumption that the temperature gradients within the foils are negligible. Consequently the foils can be represented by a single node, linked by thermal resistances, to those polyethylene nodes whose surface is covered by foil. Below 0.3K this assumption is no longer valid, and so the presence of the foils was modelled by adjusting the heat capacity of a polyethylene node, whose surface is covered by foil, to include the heat capacity of the foil.

The thermal resistance between two such adjacent nodes, was adjusted to include the resistance between the nodes via the foil, in parallel with the existing resistance between the nodes due to the polyethylene. It was not possible to represent the foils by separate nodes, as the thermal resistance of these nodes is small enough to force a small time increment, such that the required computer time is prohibitively long. The thermal resistance of the grease (including the Kapitza resistance) between the foils and the sample, was calculated using the results of Anderson and Peterson (1970), but in general the contribution of this resistance to the calculated values of R_{ij} was negligible.

The heat capacity of the heater was calculated using the results of Ho, O Neal & Phillips (1963). In the high temperature model ($T > 0.3K$), the heat capacity of the heater was included in the heat capacity of the node representing the foils. In the low temperature model, the heat capacity of the heater is assumed to be distributed equally between those polyethylene nodes, around whose surface the heater wire is wrapped. During the heating period, the energy delivered by the heater is assumed to be equally apportioned between those nodes, whose heat capacity contains a contribution due to the heater.

The heat capacity of the nodes representing the thermometers, was calculated by assuming that the combined heat capacity of the two thermometers and their leads, equalled the heat capacity of the addenda measured experimentally, less the calculated heat capacity of the foils and heater. Whenever it was impossible to represent the experimental set up exactly, the representation of the system by the model was deliberately pessimistic, so that the results obtained using the model provide an upper limit to the errors arising due to the presence of temperature gradients.

6.6 Results Obtained Using the Computer Model

In view of the approximate nature of the model and the physical data, together with the simplifying assumptions used in the construction of the model, not much weight can be placed on the actual numerical results. The trends of these results however will be valid and are reported in this section.

The parameters which dominate the results, are the diffusivities of aluminium and polyethylene. The former decreases rapidly, while the latter increases with decreasing temperature. At 0.15K, the diffusivity of aluminium is comparable to that of polyethylene, so that temperature gradients within the foil and the sample relax at similar rates. At 0.15K, significant temperature gradients exist along the length of the sample during the cooling period, and the model predicts that one thermometer will underestimate the temperature rise while the other overestimates it, with a difference of about 4% between the temperature rise measured by the different thermometers. The experimental results do not exhibit any systematic differences between those obtained using different thermometers, suggesting that the error introduced by the temperature gradients is smaller than that predicted by the model, and is smaller than the random errors arising from other sources. These temperature gradients could be reduced if copper or silver foils were used in future experiments.

At the high temperature end of the measurements ($T \sim 1.25K$) the thermal diffusivities of aluminium and polyethylene are such, that the temperature gradients along a radius of the sample, are larger than those along the length of the sample. These gradients give rise to a consistent error in the temperature rise measured by both thermometers of about 0.4%. This is negligible when compared with the other errors associated with the results.

The percentage difference between the temperature rise of each node, and the mean sample temperature rise was calculated at one second intervals. It was found that the values obtained 1 second after the end of the heating period, do not change significantly thereafter. The mean sample temperature rise is taken to be $\overline{\Delta T} = \left\{ \frac{\sum_i C_i \Delta T_i}{\sum_i C_i} \right\}$. Thus the temperature gradients present within the sample during the heating period, are replaced by the temperature gradients present during the cooling period, within a very short period of time. This time interval is comparable to the response time of the PCB, which monitors the sample temperature, and is therefore negligible.

The model was also used to determine the effect on the experimental results, of an extraneous heat input to the sample. It was found that provided the extraneous heat input remained constant throughout the experiment, it did not affect the values of temperature rise recorded by the thermometers.

6.7 A Computer Model of the Thermometer Leads

The thermal resistance of these leads is high, so that the thermal link provided by these leads between the experimental section and the sample is negligible. However because of the large heat capacity of these leads, a significant proportion of the energy supplied to the sample during the heating period is absorbed by the wiring. A numerical heat flow model similar to that described in section 6.5, was set up to estimate the effect of the wiring on the experimental results. The sample itself was represented in this model by a single node, connected to the experimental section by a thermal resistance, which represents the nylon screw. This representation is reasonable, because temperature gradients within the sample, relax much faster than temperature gradients within the wiring. Values for the specific heat capacity of constantan were taken from the results of Ho, O Neal & Phillips (1963), and values for the thermal conductivity were obtained by extrapolating

the results of Berman (1951).

The accuracy of the results obtained using this model, is limited by the assumption that the thermal resistances and heat capacities are independent of temperature, since significant temperature gradients exist within the wiring, due to the temperature difference between the sample and the experimental section. Also in the case of those experiments, where the wiring was not shielded from the radiation from the wall of the IVC, radiative transfer of heat to the wiring will render these gradients more severe.

Using the model, the following results were obtained. During the sample heating period, the energy absorbed by the wiring is proportional to the temperature rise, and the constant of proportionality is a function of temperature only. Thus the wiring appears to have an effective heat capacity, which will be included in the addenda heat capacity, and is typically about 5% of the total heat capacity of the sample and its addenda at 0.15K. However because the time taken by the wiring to reach a state of equilibrium, is much longer than the sample heating period, the wiring continues to absorb heat from the sample after the end of the heating period. After a further period of time has elapsed, the length of which is a function of the heat capacity of the sample and its addenda, the thermal resistance of the nylon screw and temperature, the wiring also starts to cool and the heat flow from the sample to the wiring is reversed. It is obvious therefore that the assumption that: the rate of heat loss from the sample is a function of temperature, which is the same for both the sample heating and cooling periods, is not valid. Thus an error in the calculation of the heat lost from the sample during the heating period, which is based on this assumption, arises. The situation is complicated because the size of the error is a function of the heat capacity of the sample and its addenda and also the thermal resistance of the nylon screw.

In order to estimate the effect of this error, on the experimentally obtained results for the specific heat capacity of polyethylene, it was necessary to use the model to calculate the variation of sample temperature with time for three different samples (designated N1, N2 & P), with heat capacities corresponding to those of the two nylon samples and a polyethylene sample. These three sample temperature/time curves were then used to calculate first the addenda heat capacity and then the specific heat capacity of polyethylene, using the method of Collan et Al to correct for the heat lost during the heating period.

It was found that the error associated with the values of specific heat capacity, arising from the behaviour of the wiring, was most important at low temperatures, typically 5% at 0.15K dropping to below 1.5% at 0.4K. It was also found that if the thermal resistance between the polyethylene sample and the experimental section, was 20% larger or smaller than that for the nylon samples, then the error in the specific heat capacity of polyethylene became 10% or zero respectively at 0.15K. The behaviour of the wiring therefore gives rise to a possible explanation for the observed divergence between the experimental results for SH3, and those for SH0, SH1 & SH2 at low temperatures. This possibility is supported by the observation that a calculation of the thermal resistance between the sample and the experimental section, based on the observed time constants of the variation of sample temperature with time, shows that this resistance is 25% smaller for SH3 than for the other three polyethylene samples.

The model also shows that the presence of temperature gradients within the wiring, provided that the system including the wiring is in a state of equilibrium prior to the measurement, does not affect the way in which energy is absorbed and released by the wiring, and so does not affect the experimental results. This particular inference from the

model is severely qualified by the assumptions made by the model.

In the light of this discussion, it is apparent that an improvement to these experimental measurements of specific heat capacity could be achieved, if the energy absorbed by the wiring could be reduced. This could be done by either using a material whose thermal resistivity is similar to that of constantan, but with a specific heat capacity which is much smaller than that of constantan; or alternatively by reducing the cross-sectional area of the wires used.

The model described above can also be used to estimate the error, associated with experimental values for specific heat capacity, derived from values of heat capacity obtained by simply dividing the supplied energy by the observed temperature rise. This procedure simply ignores the effect of the heat lost during the heating period. If the thermal resistance between samples N1, N2 & P, and the experimental section is either constant or varies only slightly (less than 5%), then at low temperatures the error which results from ignoring the heat loss during the heating period is less than that which results from using the method of Collan et Al to correct for this heat loss. This is because under these circumstances, both the heat loss via the screw and the heat absorbed by the wiring during the heating period, are proportional to the temperature rise of the sample, and the constants of proportionality are the same for all three samples, and so behave like an additional contribution to the addenda heat capacity, and are therefore eliminated by the calculation procedure. If there are significant changes in the thermal resistance of the screw from sample to sample, or the effect of the wiring is reduced in the manner described above, then the method of Collan et Al gives the more accurate results.

As temperature increases the effect of the wiring decreases, and the accuracy of the method of Collan et Al improves. In the case of a calculation which ignores the heat lost during the heating period, the

errors arising from variations in the thermal resistance of the screw from sample to sample, will remain significant as temperature increases.

In the present case, significant variations in the thermal resistance between the experimental section and the samples occurred, and so the results obtained using the correction for the heat loss during the heating period will be more accurate than those obtained with no such correction.

6.8 Experimental Errors Associated with the Specific Heat Capacity Measurements

These errors have already been described in earlier sections, and it only remains to list the most important sources of error. The principal sources of random error are: (1) the experimental error associated with the measurement of the sample temperature rise, which is due to the noise on the PCB output voltage/time curves; (2) fluctuations in the extraneous heat input to the sample during a measurement; (3) the temperature gradients which exist within the sample at low temperature, during both the heating and cooling periods. The scatter of the experimental points about the fitted curves represents the combined effect of these errors.

It should be noted that the random errors involved in the measurements of the heat capacity of the nylon samples, used to calculate the addenda heat capacity, have been smoothed out by the fitting procedures used, and so these errors have been replaced by a consistent error in the calculated values of the addenda heat capacity, which should however be much smaller than the original random errors.

The other important sources of consistent errors are: (1) the error associated with the calibration of the primary thermometer Ge5; (2) the absorption and release of energy by the wiring during the measurement; (3) any inadvertent changes in the addenda heat capacity. Each of these possible errors increases with decreasing temperature. The

error associated with the calibration of Ge5 will be the same for each of the samples, and the uncertainty in the observed values of temperature is estimated to reach about 5% at 0.15K. This estimate is based on the observed differences between the two calibration curves provided by Lake Shore (see section 4.10.2).

This discussion of errors in this and preceding sections is of necessity qualitative, however it is safe to draw the following conclusions. Firstly the observed scatter of the experimental points is consistent with the size of the random errors associated with the measurements. Secondly the combined effect of the scatter of the experimental points with possible consistent errors, renders the differences between the results obtained for the different samples insignificant.

CHAPTER VII

THE EXPERIMENTAL MEASUREMENT OF THERMAL CONDUCTIVITY

7.1 Introduction

The thermal conductivity of the polyethylene samples SH0, SH2 & SH3 was measured over the temperature range 0.08K to 1.8K using a steady state method. One end of the sample was attached to the experimental section of the refrigerator, which was held at a constant temperature by the stabiliser. The temperature gradient, which arises because of the extraneous heat input to the sample, was measured using two GRT's which were mounted on copper wires inserted in holes drilled through the samples. A known steady heat input was then applied to the other end of the sample by passing an electrical current through a heater. The resulting increased temperature gradient was measured using the GRT's. The conductivity of the sample could then be determined from the observed temperature gradient and the net heat input to the sample, which includes the extraneous heat input. The remaining sections of this chapter describe in more detail the experimental measurement of thermal conductivity and the analysis of the data derived from the experiment.

7.2 The Experimental Arrangement

The arrangement of the experimental section of the refrigerator, was identical to that described earlier for the heat capacity experiment (see section 5.3.1). This includes the arrangement of the carbon thermometer and the heater used to stabilise the temperature of the experimental section (T_{ES}) and the GRT (Ge5) used to monitor T_{ES} (see sections 4.6 & 5.3.1).

The sample arrangement is shown in figure 7.1. In order to minimise the thermal resistance between the sample and the experimental section of the refrigerator, a copper stud was inserted into a hole in the base of the sample and the stud was attached to the shelf of the

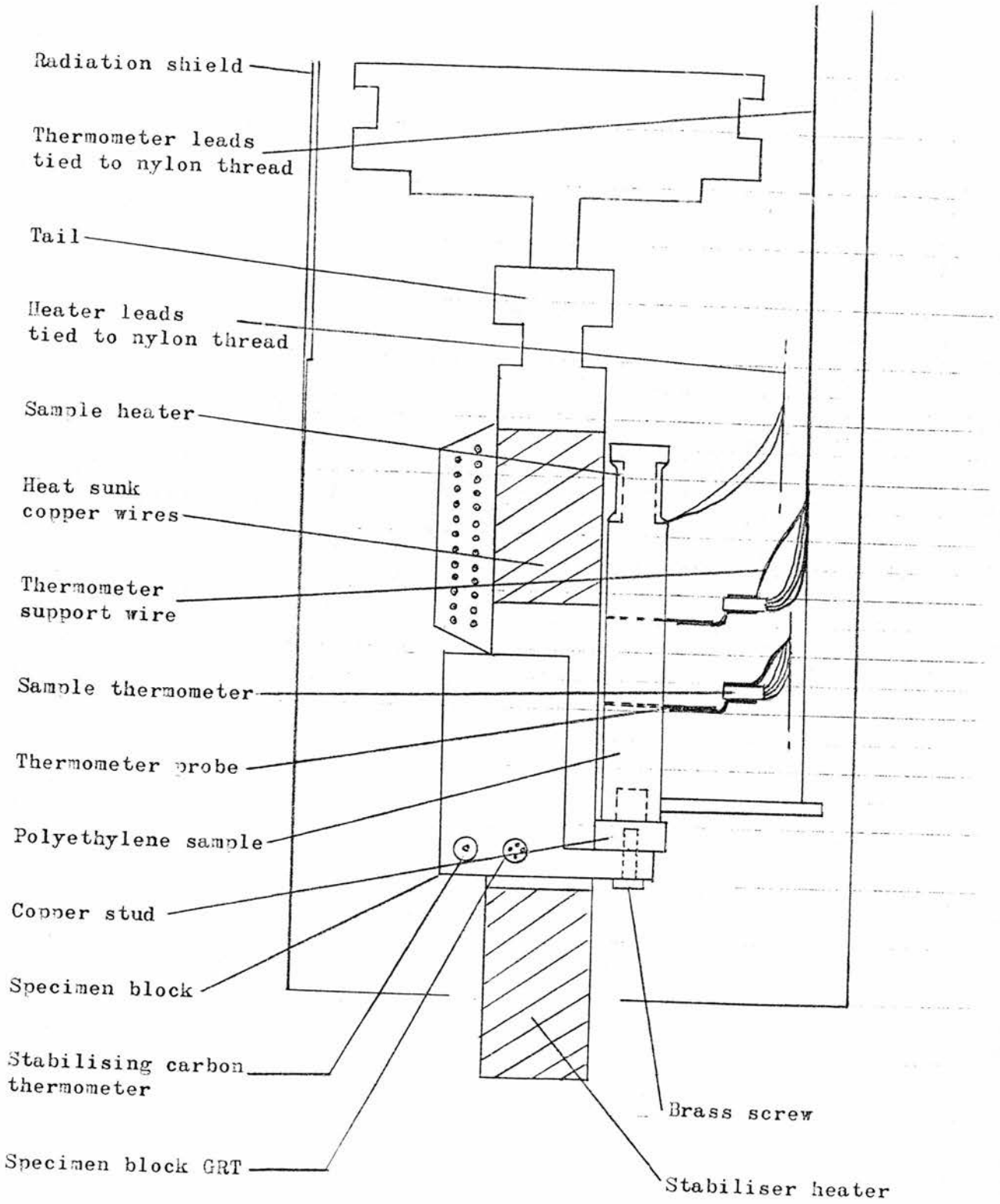

Figure 7.1

The experimental arrangement used to measure the thermal conductivity of the polyethylene samples.

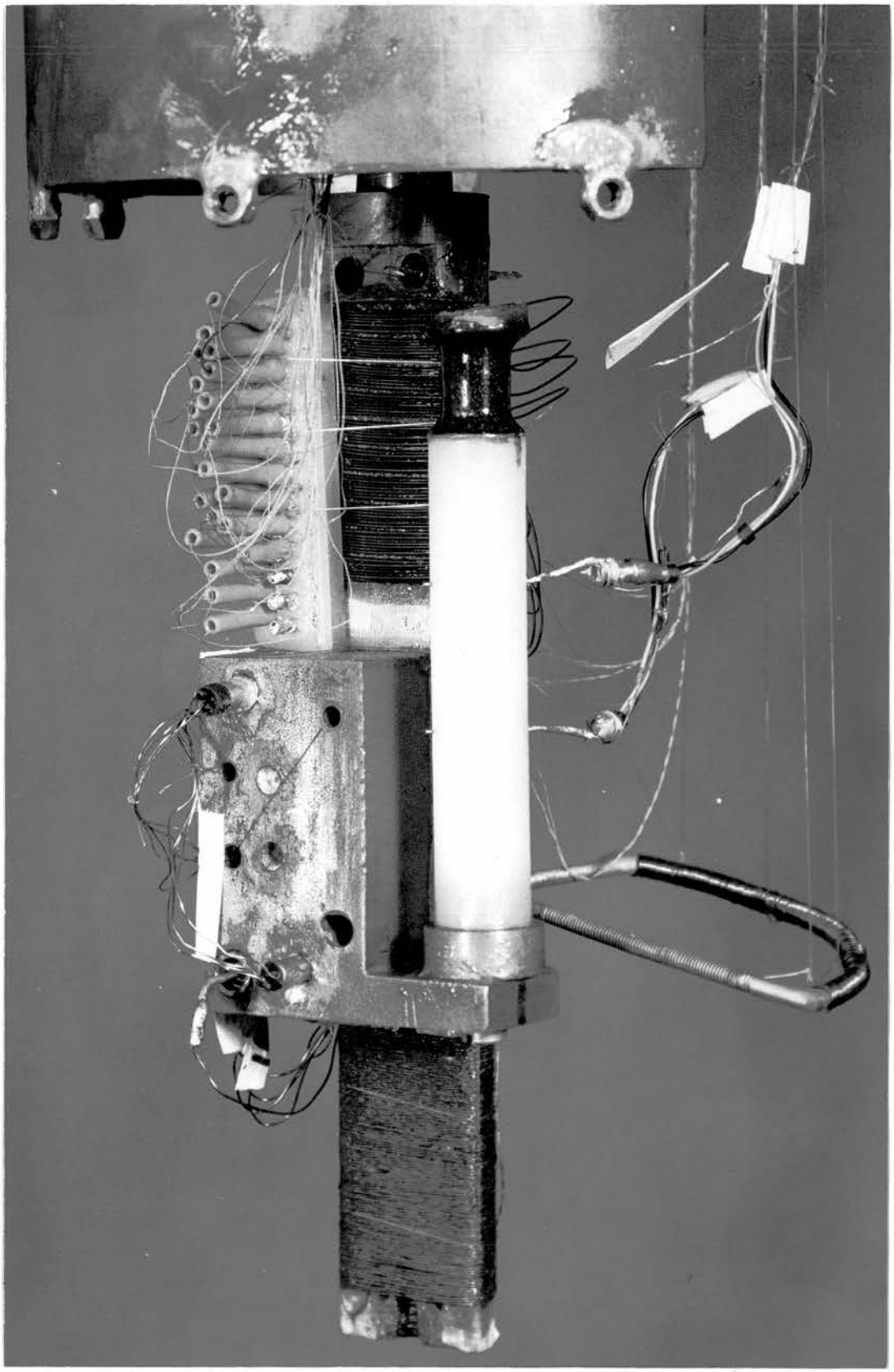

Plate 3

The experimental arrangement used to measure the thermal conductivity of the polyethylene samples.

experimental section using a 6BA screw. In the case of sample SH3, the required hole in the base of the sample had to be made by drilling out the 6BA threaded hole used to attach the sample to the nylon screw in the heat capacity experiment. This had already been done for samples SH0 & SH2 (see section 5.2). The stud was 0.5 cm long and had a diameter of 0.5 cm so that the area of good contact between the sample and the stud was 0.8 cm^2. The surfaces of the stud in contact with both the sample & the shelf were greased using apiezon grease. The fit between the sample and the stud was a tight one at room temperature, and as the sample cooled it contracted onto the stud improving the thermal contact between the sample and the stud.

The method used to attach the GRT's (Ge1 & Ge3) to the sample was identical to that used during the heat capacity measurements (see section 5.3.4). For each sample the separation of the thermometer probes was measured using a travelling microscope and the sample diameter was measured using a micrometer screw gauge.

The sample heater was initially formed by winding 8m of 46 SWG manganin wire around the neck of sample SH3. It had a resistance of 1200Ω and consisted of 6 layers of wire, which were impregnated with GE varnish. However this heater was found to be unsuitable because of its large heat capacity and its effect on the time constant of the experiment (see section 7.4). It was replaced by an 1100Ω heater which was wound using 200 cm of 48 SWG wire, made from an alloy consisting of 92% platinum and 8% tungsten. It consisted of a single layer of wire. In addition to the layer of GE varnish between the sample and the wire, a thick layer of GE varnish was applied to the surface of the heater in order to establish a good thermal link between the wire and the sample. In order to avoid the formation of large vapour bubbles within the GE varnish, which might impair the thermal link, this layer consisted of 10 separate layers formed by the daily application of GE varnish mixed with

an equal amount of toluene. In this way, the diameter of the vapour bubbles was limited to the thickness of the individual layers.

The thermometer and heater leads, each 50 cm long, were tied to 4 taut parallel nylon threads, in order to ensure that these leads were thermally isolated except for the connections at each end of the leads. These nylon threads had a diameter of 0.17 mm and were attached at one end to the warmest step heat exchanger and at the other end to the experimental section. The threads were positioned so as to be equidistant from the refrigerator heat exchangers and the enclosing radiation shield, which were separated by a gap of 2.0 cm. The leads were loosely tied to the central section of these nylon threads, passing up one thread and down another to form a U shape. The leads were divided into three bundles, one connected to each of the thermometers and one connected to the sample heater. These bundles were isolated from each other, over that half of their length which was closer to the sample, by attaching them to separate nylon threads. Over the second half of their length, the bundles were combined and attached to the remaining nylon thread. The heat input to the sample due to the conduction of heat along these nylon threads, was estimated to be 8×10^{-4} erg/s (T_{ES} =0.05K), which is small compared with the observed values of the extraneous heat input to the sample.

In order to limit the heat input to the sample due to radiation, the sample and its wiring was enclosed by a radiation shield attached to the warmest step heat exchanger (see section 5.6).

7.3 Heat Flow within the Thermometer and Heater Leads

44 SWG eureka wires were used to connect the thermometers to the connecting socket below the mixing chamber. These wires were 50 cm long and twisted in pairs, and were identical to those used in the heat capacity measurements (see section 5.3.4). The heat lost from the sample through these leads, is less than 0.25% of the heat input via the sample

heater.

In the absence of any such deliberate heat input, a small extraneous heat input to the sample flows through the thermometer leads, from the warmest step heat exchanger via the nylon threads which support the wiring. This heat current flows through the thermal resistance between the thermometer and the sample and gives rise to an error in the recorded value of sample temperature. This thermal resistance is only significant at the very lowest temperatures, when the boundary resistances between dissimilar materials become important. Using the results obtained by Anderson & Peterson (1970) an estimate of this resistance was made. This calculation suggests that the heat flow through this resistance at 0.05K, will give rise to an error in the conductivity measured at 0.08K of less than 2%. Furthermore the errors associated with the temperatures recorded by the upper & lower sample thermometers will tend to cancel each other. At these very low temperatures, the heat flow within the thermometer leads is reduced, when the sample heater current is switched on; while at higher temperatures the heat flow is reversed.

The sample heater was connected to the connecting socket by 2 lead covered manganin leads, with a diameter of 0.002" and 50 cm long. At the connecting socket, each heater lead was connected to 2 leads of the refrigerator wiring, in order to permit a 4 terminal measurement of the heater resistance. These lead covered manganin leads are superconducting below 7.2K, so that no thermal energy is released by the electrical current flowing through these leads. At temperatures above 1.0K, the thermal resistance of these leads is small due to the relatively large thermal conductivity of superconducting lead. In order to prevent a significant loss of heat through these leads, a short section of resistance wire of the same type as that used to wind the heater, is included between the sample and the lead covered manganin

lead. The optimum length of this section of wire, has to be chosen so as to achieve a compromise between: the thermal resistance of the wire which limits the heat lost from the heater, and the electrical resistance of the wire which gives rise to heating within the heater leads.

In order to do this, a computer model was set up, which modelled the steady state heat flow within the sample, the heater leads and the thermometer leads. The sample and its wiring is represented by a series of nodes linked by resistances, and as the model is time independent, the heat capacity of the nodes is irrelevant. The model requires relatively few nodes, as only those nodes in which heat is generated need be included, in addition to the nodes at which the wiring connects with the sample. The thermal conductivity data required by this model was taken from the following sources: constantan - Berman (1951), lead - Olsen & Renton (1952), manganin - Zavaritskii & Zeldovich (1956), platinum tungsten alloy - Buhl & Giauque (1965).

The maximum value with respect to temperature, of the experimental error due to heat loss through the heater leads, was calculated for several lengths of resistance wire, and that length was selected, for which this value was smallest. It was found that a variation, by a factor of 2 or 4, in the conductivity values used by the model, did not lead to a significant variation in the length of the wire associated with the minimum experimental error, although the value of that experimental error did vary between 1% & 2%. Thus the results obtained using this model do not depend critically on the accuracy of the conductivity data, which is uncertain. It was found that the optimum lengths were 3.0 cm for 46 SWG manganin wire and 1.5 cm for 48 SWG platinum tungsten wire. These lengths do not include the section of resistance wire which was tinned with superconducting solder and used to connect the resistance wire to the lead covered manganin leads.

7.4 The Sample Time Constant

During the experimental measurement of thermal conductivity at temperatures below 0.2K, it was found that a deliberate change in the heat input to the sample, caused the temperatures recorded by the sample thermometers to drift for long periods of time. It was assumed that the sample temperatures had reached their equilibrium values, when the steady drift was replaced by random fluctuations in the observed temperature values. The time taken to reach this "equilibrium" was typically 1 hour at 0.12K and 2 hours at 0.08K. A time dependent computer model was set up in order to investigate the reason for these long time constants.

This model used an implicit formulation of the finite difference equation rather than the explicit formulation described in section 6.5. This formulation defines the temperature change $(T_i' - T_i)$ of node i during a time interval $(t' - t)$ in terms of the temperatures T_j' of neighbouring nodes at time t' as follows:

$$\frac{C_i}{(t'-t)}(T_i'-T_i) = q_i + \sum_j \frac{T_j'-T_i'}{R_{ij}}$$

Thus for a system of n nodes, the temperatures of the nodes at time t', can only be determined by solving n simultaneous equations, using an iterative calculation. The advantage of this formulation is that the length of the time interval $(t' - t)$ is arbitrary, so that long time intervals can be used in conjunction with closely spaced nodes. Thus the implicit formulation is used to investigate temperature changes over relatively long periods of time, for which the number of iterations required to solve n simultaneous equations, is less than the number of time increments (δt), required by the explicit formulation to cover the time interval $(t' - t)$.

The model used 150 nodes to represent the sample wiring, so that each node represented a section 1 cm long. The heat capacity of the sample was divided between the 3 nodes which represented the sample

heater and the 2 thermometers. The model used thermal conductivity data which was identical to that used by the model described in section 7.3. The heat capacity data was taken from the following sources: constantan & manganin - Ho, O Neal & Phillips (1963), platinum tungsten alloy - Ho & Phillips (1965).

It was found that the large heat capacity of the manganin sample heater controlled the time constant of the experiment, and that the time taken to achieve a temperature gradient within 2% of the equilibrium value, could be reduced by a factor of 80 at 0.1K by replacing the 46 SWG manganin heater with a 48 SWG platinum tungsten heater. It was also found that if the thermometer leads were replaced by leads with a lower heat capacity, then a further small reduction in the time constant of the experiment could be achieved.

As a result of these predictions, the manganin heater was replaced by a platinum tungsten heater (see section 7.2), and the measurements of the thermal conductivity of the sample (SH3) were repeated. The thermometer leads were not changed. Following this alteration, the sample temperatures responded quickly to any change in the heat input to the sample, so that the time taken to reach equilibrium was reduced to reasonable values. At very low temperatures (T~0.05K), in the absence of a deliberate heat input to the sample, the random fluctuations in the sample temperature increased. This increase is a consequence of the reduction in the time constant of the sample, which allows the sample temperature to follow changes in the extraneous heat input more closely (see section 7.6).

The measurements of the conductivity of the remaining samples (SH0 & SH2) were made using platinum tungsten heaters.

7.5 The Experimental Procedure

The instrumentation used to measure thermal conductivity is shown in figure 7.2. The temperature of the experimental section (T_{ES})

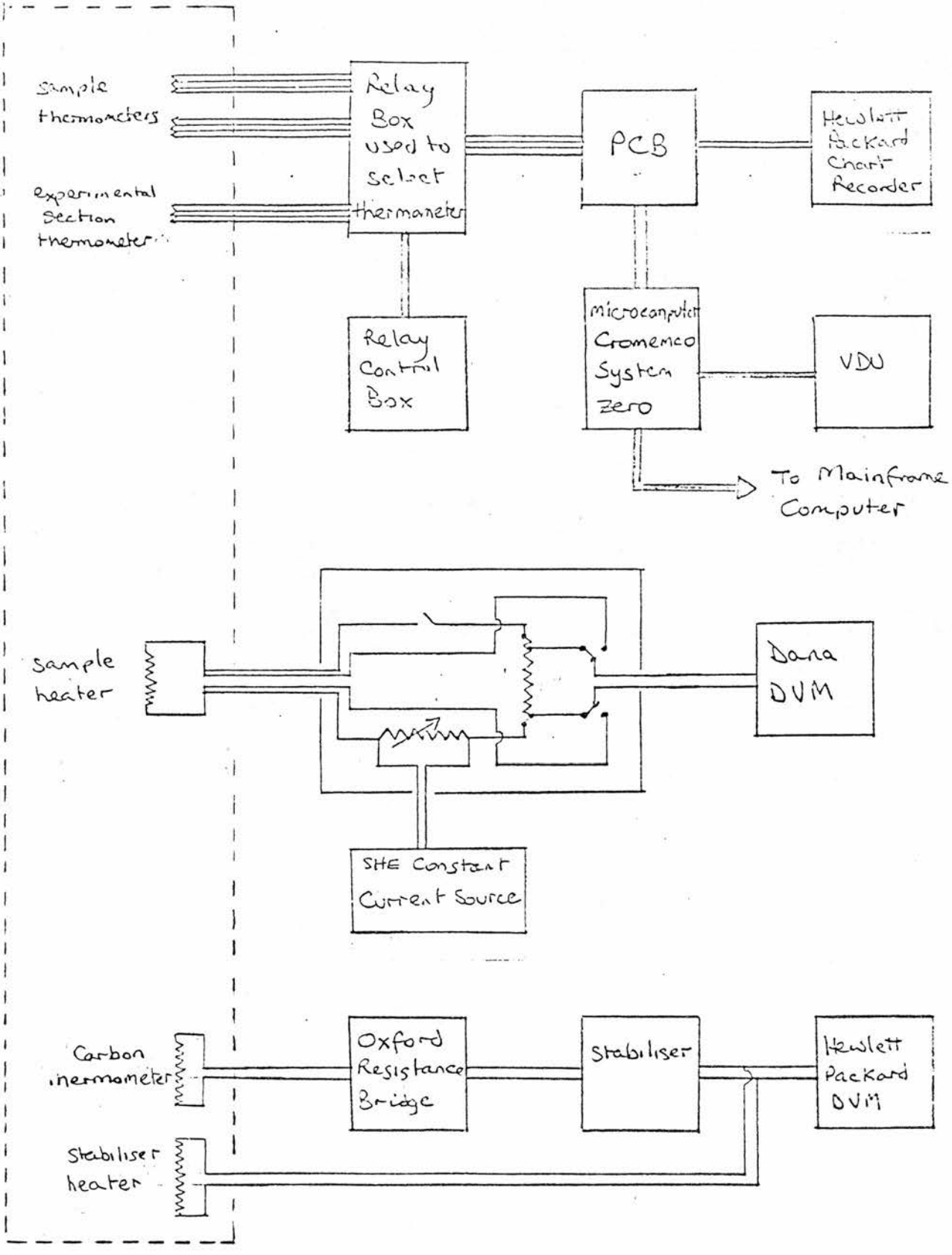

Figure 7.2

The arrangement of the instruments used to measure the thermal conductivity of the polyethylene samples.

is held at a chosen value by the stabiliser (see section 4.6). The sample thermometers (Ge1 & Ge3) and the experimental section thermometer (Ge5) are monitored using the PCB. Any drift or fluctuation in the sample temperature, appears on the record of the PCB analogue output voltage, which is made by the chart recorder connected to the PCB. Once steady values of sample temperature are observed, then the conductance of each thermometer is determined and noted. The noise on the PCB digital display can be reduced by selecting the filter with a time constant of 10 seconds. Alternatively, the microcomputer can be linked to the digital output of the PCB, and used to take a large number of readings, which can be averaged to eliminate the effect of this noise. This method can only be used at temperatures above 0.25K (see section 7.6).

A current, whose value is predetermined, is then passed through the sample heater, and the sample thermometers are monitored until the observed values of sample temperature are steady. The conductance of each thermometer is then determined and noted. The voltage across the sample heater, and the voltage across a standard resistor ($10^4\Omega$) in series with the sample heater, are then measured using the Dana DVM. A further conductivity measurement is then made by increasing the sample heater current, waiting till the sample temperature values are steady, and then noting the values of thermometer conductance and the values of voltage as before.

In this manner, several measurements of the conductivity are made without changing the temperature of the experimental section, such that the observed values of sample temperature difference lie within the following range: $0.18 < \frac{\Delta T}{T} = 2\left(\frac{T_2 - T_1}{T_2 + T_1}\right) < 0.25$. A lower limit for the values of temperature difference, is required in order to limit the size of the fractional error associated with the temperature difference. The upper limit is discussed in section 7.7. In order to obtain

conductivity measurements at the very lowest temperatures, temperature differences which are smaller than this minimum value, have to be used in conjunction with the lowest possible value for T_{ES}, which is the lowest temperature value on the primary thermometer calibration curve.

The current, which was passed through the sample heater, varied between 1.2μA and 85μA over the temperature range of the experiment, and the associated heat input varied between 0.015 erg/s and 80 erg/s. The sample heater current varied by less than 0.12% during a conductivity measurement. The experimental error, associated with the measurement of the smallest values of the electrical heating power, was 0.5%.

An immediate computer analysis of the experimental data was performed during the experiment. The values of thermometer conductance obtained using the microcomputer, were transferred directly to the mainframe computer and the rest of the experimental data was input by hand at the VDU. Using the mainframe computer, the observed values of thermometer conductance were converted into temperature values, and used in conjunction with the values of voltage, to calculate the heat input to the sample (including the extraneous heat input), and the thermal conductivity of the sample. Thus the significance of a change in the values of thermometer conductance, observed with either a zero or a non zero value of sample heater current, can be established immediately by calculating the fractional change in the thermal conductivity value, resulting from the observed change in sample temperature.

Using the computer, the values of T_{ES} and of sample heater current, which were required to obtain particular values of the mean sample temperature T and of the fractional temperature difference ($\Delta T/T$), could be calculated by extrapolating the conductivity curve obtained already. These predictions were accurate provided that the range of the extrapolation was small.

7.6 The Extraneous Heat Input

Following the reduction in the time constant of the experiment (see section 7.4), the sample thermometers responded more quickly to changes in the extraneous heat input. Thus it became possible to associate possible causes with observed changes in the extraneous heat input.

External fields cause electrical currents to flow within the thermometer circuitry, giving rise to thermometer self heating. These fields may be associated with equipment operating at either mains frequencies or radio frequencies. The consequent increase in the temperature recorded by the thermometer, depends on the rate at which energy is released within the thermometer, the thermal resistance between the thermometer and its heat sink, and the heat capacity of this heat sink.

Carbon thermometers are particularly sensitive to r.f. fields. The stabiliser responds to self heating within the carbon thermometer, by reducing the heat input to the experimental section, in order to compensate for the change in the resistance of this thermometer. Consequently the temperatures recorded by the GRT's mounted on the sample and experimental section decrease. Thus the intermittent operation of radio transmitting devices in the vicinity of the laboratory, severely disturbs the equilibrium of the sample and the experimental section at low temperatures.

At low temperatures, it was found that connecting the microcomputer to the PCB altered the temperature values recorded by both the GRT's and the stabilising thermometer. It was also found that if the microcomputer and the VDU were disconnected from the PCB, but remained close to the cryostat, then the effect was reduced but not eliminated. At 0.1K, the operation of the computer within the laboratory, caused the temperature recorded by the most sensitive thermometer (Ge5) to increase

by 4%. A direct connection between the computer and the PCB affected thermometer Ge5 at temperatures below 0.5K. However Ge5, which is used to set the temperature of the experimental section and to check that it remains steady, need only be read occasionally. The other thermometers were less sensitive and the computer could be connected to the PCB without altering the temperature values recorded by these thermometers, provided that these values exceeded 0.25K. At temperatures below 0.25K, the experimental data was input by hand to the mainframe computer, using a VDU in another room.

The fluctuations in temperature which were observed at very low temperatures, were found to be less during the evening and at the weekend than during normal working hours. It was assumed that equipment operating in adjacent laboratories gave rise to this effect. In order to minimise these effects, the instrumentation and its associated leads were screened as carefully as possible, particular care being taken to avoid earth loops and holes in the screening. The relays, which are used to select the thermometer connected to the PCB, are contained in a box close to the cryostat, and are remotely controlled; so that the 12 leads which link the cryostat to this box are as short as possible. The instruments were connected to the mains power supply via a filter, in order to remove any high frequency signals which might be present. Conductivity measurements at temperatures below 0.15K were made during the weekend.

When the Dana DVM was connected across the sample heater, it was observed that the temperatures recorded by the sample thermometers increased. Upon investigation it was found that a small low frequency (44Hz) voltage appeared across a resistor connected to the input terminals of the Dana DVM. Consequently the DVM was connected across the standard resistor, and it was not connected across the sample heater until after the values of sample temperature had been obtained. However

when the switch was closed, which allowed the DC current to flow through the sample heater, it also allowed the AC current generated by the DVM to flow through the heater, giving rise to a 2.5% error in the value obtained for the electrical heat input at the very lowest temperatures. The effect of this error on the experimental conductivity values is similar for each sample, and rapidly becomes negligible as temperature increases.

It was observed that at 0.05K, the conductance of the upper sample thermometer (Ge1), rose by about 3% during the period immediately after the PCB was switched to this thermometer, even though the minimum value of sensor excitation voltage (10 μV) was used. The observed change in the conductance of Ge1 is equivalent to a 0.5% temperature rise, and leads to a 1.5% change in the value obtained for the thermal conductivity. Consequently the conductance of this thermometer was obtained within a few seconds of switching to this thermometer, using the 0.3 second time constant. This effect was not observed for the lower sample thermometer (Ge3).

The sample temperatures were often observed to rise as a result of mechanical vibrations. For this reason, care was taken to avoid touching the cryostat and its supporting frame during the measurements. In particular, liquid helium was not transferred into the cryostat until after the measurements of that day were complete. A nitrogen transferring device which operated at a preset time, was used to transfer liquid nitrogen into the cryostat, 2 hours before the start of the working day.

7.7 The Analysis of the Thermal Conductivity Data

For 1 dimensional steady state heat flow, the thermal conductivity (k) is defined by:

$$\dot{Q} = -k.A \left(\frac{dT}{dx}\right) \qquad 7.1$$

where $\dot{Q}$ is the rate at which energy crosses an area A, which is normal

to the direction of the heat flow, and (dT/dx) is the temperature gradient within the sample. An approximate form of this equation is used to calculate the experimentally obtained values of thermal conductivity:

$$\dot{Q} = \frac{k.A.(T_2-T_1)}{L_1} \qquad 7.2$$

where $\dot{Q}$ = the rate of heat flow parallel to the sample axis,

A = the cross-sectional area of the sample,

L_1 = the separation of the sample thermometers,

T_1 & T_2 = the temperature values recorded by the sample thermometers. Thus assuming that the thermal current ($\dot{Q}$) equals the rate at which heat is generated within the sample heater (resistance R) by an electrical current (i), the thermal conductivity of the sample is given by: $k = \frac{i^2.R.L_1}{A(T_2-T_1)}$. Each conductivity value (k) is associated with the mean sample temperature observed during the conductivity measurement ($T = \frac{1}{2}(T_1+T_2)$). It was found that a linear relationship existed between the variables log(k) and log(T) so that: log(k) = log(a) + n.log(T) and $k=a.T^n$. Two or three such lines were required to represent the conductivity curves obtained for the polyethylene samples, over the entire temperature range 0.08K to 1.8K. The experimental points were divided into 2 or 3 groups, and a line was fitted to each group of points using a least squares method. The positions of the divisions between these groups, were varied until the grouping was found, which gave rise to the best fit between the experimental data and the fitted lines.

Using the equation for the conductivity of the sample obtained in this manner, the extraneous heat input to the sample ($\dot{Q}_X$) can be calculated as follows:

$$\dot{Q}_X = a\left(\frac{T_{1X}+T_{2X}}{2}\right)^n \left(\frac{A}{L_1}\right)(T_{2X}-T_{1X}) \qquad 7.3$$

where T_{1X} & T_{2X} are the temperature values recorded by the sample thermometers in the absence of a deliberate heat input, and the

conductivity of the sample at temperature $T_X = \frac{1}{2}(T_{1X}+T_{2X})$ is given by the equation $k=a.T^n$. Using this result, the total heat input to the sample during the conductivity measurement can be determined, and used to calculate a more accurate conductivity value:

$$k = \frac{(\dot{Q}_X + i^2R).L_1}{A(T_2-T_1)} \qquad 7.4$$

Thus an iterative procedure for the calculation of the conductivity values has been established, which converges extremely rapidly. At the lowest temperatures, the extraneous heat input typically equals 20% of the total heat input to the sample. This proportion decreases rapidly as temperature increases, so that the effect of the extraneous heat input on the conductivity values obtained at temperatures above 0.3K is negligible.

This analysis makes the following assumptions:

(1) The net heat input to the sample equals the thermal current flowing through the section of the sample between the two thermometers. This assumption is valid if heat is lost from the sample, only at the connection between the sample and the experimental section. The error which arises from the heat lost through the sample wiring has already been discussed in section 7.3.

(2) The extraneous heat input to the sample is the same during the measurements of both the extraneous heat input and the conductivity. It is impossible to assess the validity of this assumption, as it depends on the relative size of each of the several heat inputs which combine to form the extraneous heat input, and on the changes in these heat inputs as a result of the changes in sample temperature. It seems likely that the heat inputs due to vibration, conduction by helium atoms, and radiation leaking through the radiation shield, will not change significantly.

(3) It is assumed that equation 7.1 which is exact, can be replaced by equation 7.2 which is approximate. Equation 7.1 can be transformed as

follows:

$$\dot{Q} = \left(\frac{A}{L_1}\right)\int_{T_1}^{T_2} k(T).dT = \left(\frac{A}{L_1}\right)\int_{T-\frac{\Delta T}{2}}^{T+\frac{\Delta T}{2}} a.T^n.dT$$

$$= \left(\frac{A}{L_1}\right)\left(\frac{a}{n+1}\right)\left[\left(T+\frac{\Delta T}{2}\right)^{n+1} - \left(T-\frac{\Delta T}{2}\right)^{n+1}\right]$$

The terms within the square brackets can be expanded using the binomial expansion. The fractional error associated with the approximation made by equation 7.2 can then be shown to be equal to: $\frac{n(n-1)}{24}\left(\frac{\Delta T}{T}\right)^2$. For the conductivity curves obtained for the polyethylene samples $n<2$, and during the experimental measurements ($\Delta T/T$) < 0.25 (see section 7.5), so that the error introduced by this assumption is less than 0.5%.

The conductivity values obtained for samples SH0, SH2 & SH3 are shown in figure 7.3. The lines which were fitted to these conductivity values are also shown in figure 7.3. The parameters a & n which can be used to reproduce these lines, are given in table 7.1, and provide an adequate description of the experimental data. The values of parameter a are quoted in cgs units so that the values of conductivity ($k=a.T^n$) are obtained in erg $s^{-1}cm^{-1}K^{-1}$. Table 7.1 also includes values of the parameter ξ , which is a measure of the scatter of the experimentally obtained conductivity values about the fitted lines, and is defined as follows:

$$\xi = 100\left\{\frac{1}{m}\sum_{i=1}^{m}\left(\frac{k_i - a.T_i^n}{a.T_i^n}\right)^2\right\}^{\frac{1}{2}}.$$

TABLE 7.1

	SH0	SH2	SH3
a_1	73.2	535.7	609.7
n_1	1.116	1.634	1.805
a_2	105.4	222.2	219.4
n_2	1.481	1.070	1.142
a_3	124.2	221.0	216.7
n_3	1.885	1.187	1.238
ξ	1.22%	1.18%	1.71%

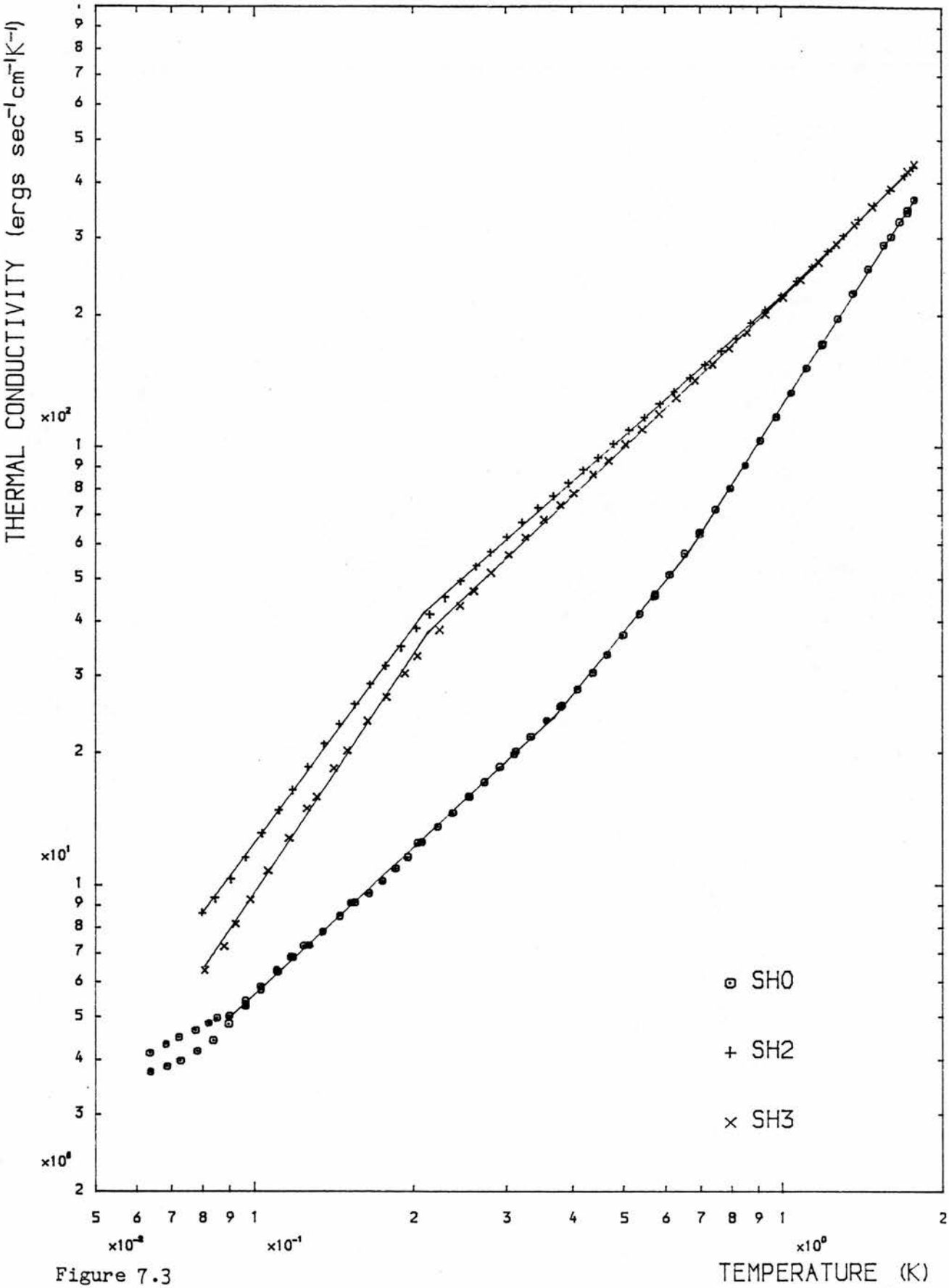

Figure 7.3

The experimental values of thermal conductivity obtained for the polyethylene samples. The curves fitted to the experimental data, each consist of 3 lines of the form $k = aT^n$.

7.8 Experimental Errors Associated with the Thermal Conductivity Measurements

It is difficult to assess quantitatively the experimental error associated with measured values of conductivity for several reasons:
(1) The error associated with a conductivity value, depends critically on whether or not an experimental error affects the temperature values recorded by the sample thermometers equally. Thus a 2% error in the temperature recorded by one thermometer, could lead to a 10% error in the conductivity value; whereas an identical 2% error in the temperature values recorded by both sample thermometers, leads only to a 2% error in the temperature value associated with the conductivity value.
(2) It is impossible to determine the size of some experimental errors; such as the error arising from the existence of a thermal resistance of unknown size, between the sample and the thermometer.
(3) A calculation of the error arising from the heat loss down the thermometer and heater leads, depends critically on the accuracy of the values assumed for the conductivity of the materials used to make these leads; and many of these values are obtained by extrapolating conductivity curves obtained at higher temperatures.
(4) The quality of the primary thermometer calibration is unknown (see section 4.10.2).

Thus it seems unwise to attempt a calculation of the experimental error associated with the conductivity measurements. However a consideration of the reproducibility and consistency of the experimental observations can be used to assess the quality of the experimental data.

In order to assess the possible effect of the experimental error, associated with the accepted primary calibration curve for thermometer Ge5, it was replaced by the curve originally supplied by the manufacturers with this thermometer (see section 4.9.3). The secondary

calibration data was not changed. The conductivity calculations were redone using the modified calibration curves, and the conductivity curves obtained are shown in figure 7.4. It was found that these changes led to an 18% change in the conductivity values obtained at 0.08K.

7.8.1 Sample SH0

The first set of conductivity values obtained for sample SH0, reveals a change in the slope of the conductivity curve at about 0.09K. As this change in slope is close to the low temperature limit of the measurements, it was not certain whether this change in slope really existed, or whether it was the result of experimental error.

Consequently the sample thermometers were interchanged so that the upper sample thermometer became the lower sample thermometer and vice versa; and the measurements of the conductivity of sample SH0 over the entire temperature range were repeated. The results obtained before and after the thermometers were interchanged are shown in figure 7.3. The results obtained below 0.09K after the interchange, differed from those obtained prior to the interchange. At temperatures above 0.09K, the effect of interchanging the thermometers, on the conductivity values obtained, was negligible.

An experimental error, which leads to a change in the conductivity values as a result of interchanging the thermometers, can arise from one of two sources. Firstly an error in the calibration of one of the thermometers, which leads to an increase in the observed temperature gradient (ΔT), will lead to a decrease in ΔT after thermometer interchange. Secondly a significant thermal resistance between one of the thermometers and the sample, due to a poor connection between the thermometer probe and the thermometer support wire, may have been either introduced or removed, when the thermometers were interchanged and the connection in question was remade. A poor contact effectively increases the thermal resistance at a boundary, by

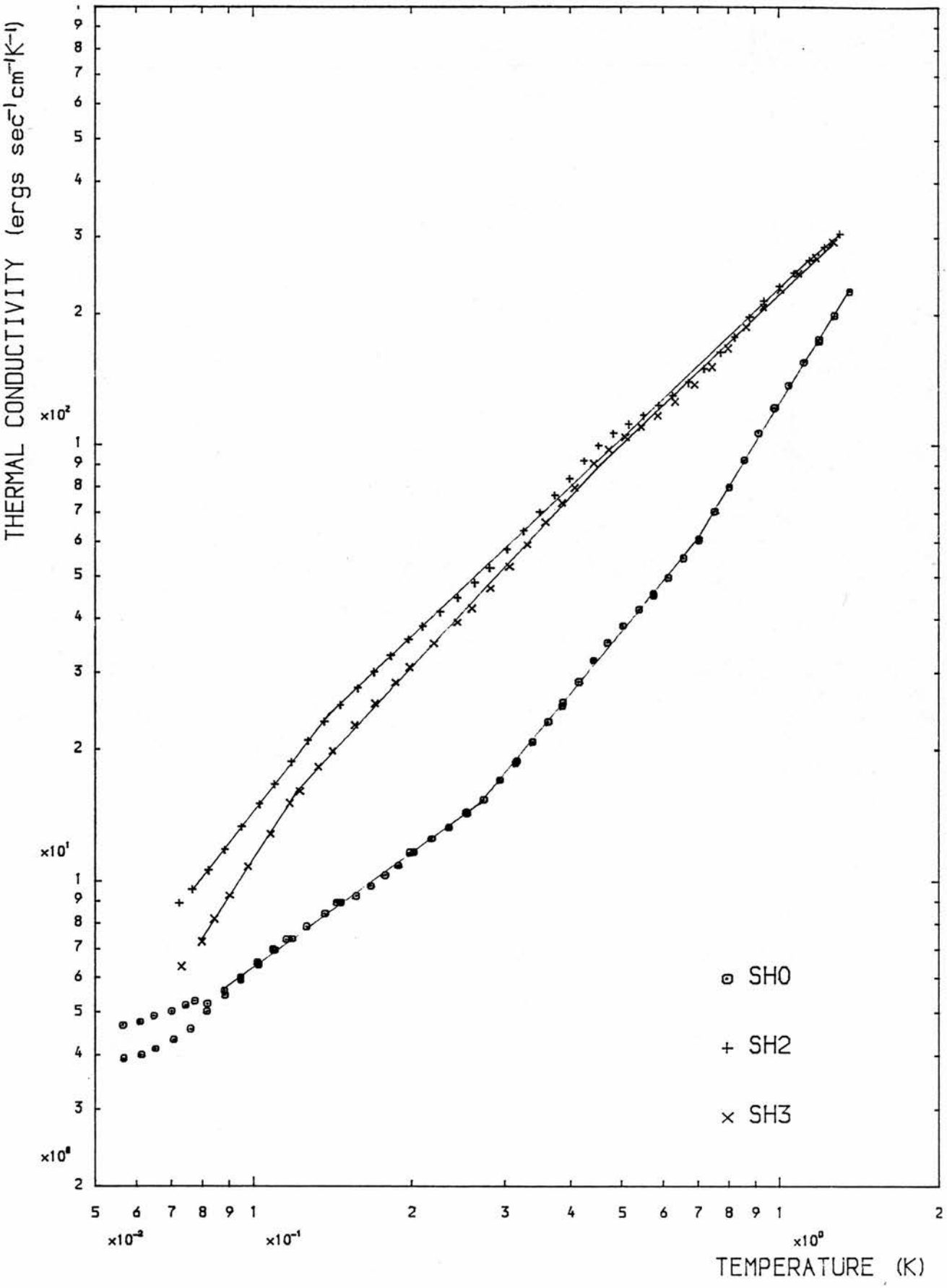

Figure 7.4

The experimental values of thermal conductivity obtained using the modified thermometer calibration curves described in the text.

decreasing the area across which the heat can flow. However the thermal resistance between dissimilar materials, decreases rapidly as temperature increases (Anderson & Peterson 1970); so that the effect of the resistance may only be significant at very low temperatures.

It was found that the values of extraneous heat input obtained using the second dataset, are less than those obtained using the first dataset, and are unrealistically low. In contrast the deviation of the conductivity values, from the extrapolation of the conductivity curve observed above 0.09K, is greater for the first dataset than for the second dataset. This suggests that a combination of errors is required to explain the observations. However, it is safe to conclude that there is a significant experimental error, associated with the conductivity values obtained for sample SH0 below 0.09K. Consequently these values have been excluded from both the least squares calculation and the theoretical calculation, which are used to fit curves to the experimental conductivity values.

7.8.2 Samples SH2 & SH3

The experimentally obtained conductivity curves for samples SH2 & SH3 are indistinguishable at temperatures above 1.0K; but at lower temperatures the curves diverge as temperature decreases (see figure 7.3). At 0.1K, the conductivities of samples SH2 & SH3 differ by about 25%. It is necessary to consider the experimental errors which may be associated with these measurements, in order to determine whether this apparent divergence of the conductivity curves is real, or whether it arises from experimental error.

It is clear that the observed divergence can not be the result of a thermometer calibration error, since such an error would affect the measurements of the conductivity of both samples equally. It is also clear that no calibration error exists, which significantly affects the temperature differences recorded by the sample thermometers, over the

temperature range 0.1K to 2.0K; since such an error would have led to a divergence between the results obtained before and after, the thermometers on sample SH0 were interchanged.

Two distinct sets of results have been obtained for sample SH3. The first set of results was obtained using a manganin heater, while the second set was obtained using a platinum tungsten heater (see section 7.4). Above 0.2K, these sets of results are indistinguishable; while below 0.2K the two sets of results diverge, giving rise to a 12% difference in the conductivity values at 0.1K. This difference must be attributed to changes in the experimental set up; the most important of which is the reduction in the heat capacity of the sample heater, which radically reduces the time constant of the experiment, making it easier to determine when the sample temperatures have reached their equilibrium values.

During each of the measurements of the extraneous heat input to the sample SH2, it was found that the lower sample thermometer (Ge3) registered a slightly higher temperature than the upper sample thermometer (Ge1); while both sample thermometers registered a significantly higher temperature than the experimental section thermometer (Ge5). The most likely explanation of these observations is that the temperature recorded by the lower sample thermometer is too high, due to the presence of a significant thermal resistance between the thermometer and the sample. Examination of the thermometer support wire attached to the case of the lower sample thermometer, revealed that the section of the wire which is attached using Woods metal to the thermometer probe, was poorly tinned. This observation could explain an increase in the thermal resistance between this thermometer and the sample.

When the sample heater current is switched on, the sample temperatures rise, leading to a reduction in the heat current flowing through the thermometer leads to the sample, and also to a possible reduction in the thermal resistance between the thermometer and the sample. Thus the temperature difference, which exists between the sample and the lower sample thermometer during the conductivity measurement (δT_1), will be less than that which exists during the extraneous heat input measurement (δT_{1X}), so that $0 < \delta T_1 < \delta T_{1X}$. Starting from equations 7.3 & 7.4 it can be shown that:

$$\left(\frac{\delta k}{K}\right) = \frac{1}{(T_2 - T_1)} \left\{ \delta T_1 - \left(\frac{T_{2X} + T_{1X}}{T_2 + T_1}\right)^n . \delta T_{1X} \right\}$$

where δk is the error associated with the conductivity value (k) due to the errors δT_1 and δT_{1X}. Thus this type of experimental error can give rise to either a net increase or a net decrease in the values obtained for the conductivity, depending on the relative sizes of δT_1 and δT_{1X}.

In order to eliminate the effect of this error, which is associated with the temperature values recorded by the lower sample thermometer (Ge3), during the measurement of the conductivity of sample SH2; the temperature values T_2 & T_S recorded by the upper sample thermometer (Ge1) and the experimental section thermometer (Ge5) respectively, were used to recalculate the experimental values of both the extraneous heat input to the sample and the conductivity of the sample, for both of the samples, SH2 & SH3.

The error associated with the approximation required to obtain equation 7.4, is significant for the relatively large values of ($\Delta T/T$), which arise in this calculation (see section 7.7). In order to avoid this error, the conductivity values were calculated using the following iterative procedure. A curve consisting of three lines of the form $k = a.T^n$, was fitted to the conductivity values obtained using the following equation, which is approximate: $k\left(\frac{T_2 + T_S}{2}\right) = \frac{(\dot{Q}_X + i^2R).L_2}{A(T_2 - T_S)}$.

An improved estimate of each of the conductivity values can then be obtained using: $k\left(\frac{T_2+T_S}{2}\right) = \alpha.\left(\frac{T_2+T_S}{2}\right)^n$, where the value of the coefficient α is obtained by solving the following equation for each conductivity value.

$$(\dot{Q}_x + i^2R) = \left(\frac{A}{L_2}\right)\int_{T_S}^{T_2} (\alpha T^n)dT \qquad 7.5$$

A new set of lines of the form $k=a.T^n$, are then fitted to these improved conductivity values, so that new values of the parameter n are obtained, which can then be used to evaluate a further set of conductivity values using equation 7.5. This iterative procedure converges rapidly. The thermometer separation (L_2) cannot be determined by direct measurement, because of the shape of the copper stud on which the sample is mounted. Instead the value of L_2 is determined using the following equation:

$$\left(\frac{1}{L_2}\right)\int_{T_{SM}}^{T_{2M}} k(T).dT = \left(\frac{1}{L_1}\right)\int_{T_{1M}}^{T_{2M}} k(T).dT$$

where T_{2M} , T_{1M} & T_{SM} are the temperature values associated with that measurement which was performed at the highest temperature; and k(T) is the conductivity curve obtained using the temperature values recorded by the sample thermometers Ge1 & Ge3.

The conductivity values obtained in this manner for samples SH2 & SH3, using the temperature values recorded by the upper sample thermometer (Ge1) and the experimental section thermometer (Ge5) are shown in figure 7.5.

If the thermal resistance at the boundary between the sample and the copper stud (on which it is mounted) is significant, then the temperature recorded by the experimental section thermometer (Ge5) is less than the temperature at the base of the sample. Thus an extra experimental error may be introduced into the conductivity calculation, by using the temperature values recorded by thermometer Ge5. However the conductivity values obtained for sample SH3 using thermometers Ge1 & Ge5, differ from those obtained using thermometers Ge1 & Ge3 by less than 3%, showing that it is reasonable to neglect this error.

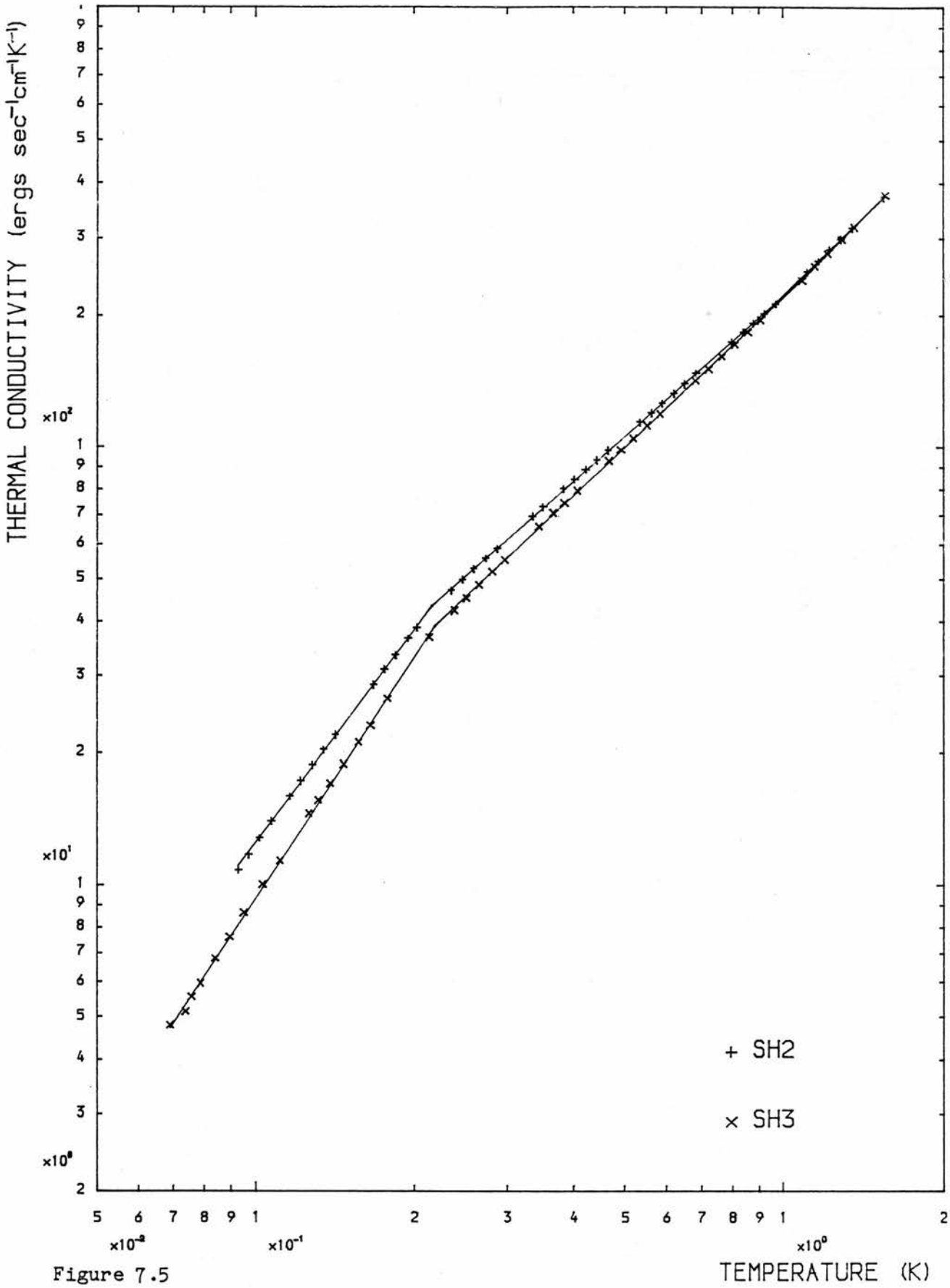

Figure 7.5

The experimental values of thermal conductivity obtained using the temperature values recorded by the upper sample thermometer (Ge1) and the experimental section thermometer (Ge5).

The effects of replacing the temperature values recorded by thermometers Ge1 & Ge3, by those recorded by thermometers Ge1 & Ge5 were as follows:

(1) The changes in the values obtained for the extraneous heat input for sample SH3 were negligible.

(2) The original negative values of the extraneous heat input obtained for sample SH2, were replaced by positive values comparable to those obtained for sample SH3, leading to a 22% increase in the total heat input to the sample at the lowest temperature.

(3) The changes in the values obtained for the conductivity of both of the samples (SH2 & SH3), were found to be negligible.

Thus it can be concluded that:

(1) An experimental error, which is significant at low temperatures, is associated with the temperature values recorded by thermometer Ge3, during the measurement of both the extraneous heat input and the conductivity of sample SH2.

(2) The errors associated with these measurements, are combined by the conductivity calculation, in such a way that they cancel each other out. This result is fortuitous.

Thus the divergence of the conductivity curves obtained for samples SH2 & SH3 is not the result of any known experimental error.

CHAPTER VIII

APPLICATION OF THEORY TO THE EXPERIMENTAL RESULTS

8.1 Specific Heat Capacity

It can be shown that the specific heat capacity of a phonon system with a Debye density of states, for a single polarization p is given by:

$$c_p(T) = \left(\frac{K_B^4}{2\pi^2\hbar^3}\right)\left(\frac{T^3}{v_p^3 \rho}\right)\int_0^{x_p} \frac{x^4 e^x}{(e^x-1)^2}\,dx \qquad 8.1$$

where v_p is the velocity of a phonon of polarization p. The Debye temperature (θ_{Dp}) associated with polarization p is defined by:

$x_p = \frac{\theta_{Dp}}{T} = \frac{\hbar\, v_p\, q_D}{K_B T}$, where q_D is the cut-off wave number introduced by the Debye theory. The total specific heat capacity can then be obtained by adding the heat capacities associated with the two transverse polarizations and the single longitudinal polarization.

$$c(T) = 2.c_T(T) + c_L(T) \qquad 8.2$$

Burgess & Greig (1975) measured the specific heat capacity of an isotropic polyethylene sample over the temperature range 10K to 100K. They obtained a curve using equations 8.1 and 8.2 which fitted their experimental results reasonably well. The values of the parameters used to obtain this curve are as follows:

the transverse velocity of sound $v_T = 2 \times 10^5$ cm/sec,

the longitudinal velocity of sound $v_L = 4 \times 10^5$ cm/sec,

the Debye cut-off wave number $q_D = 10^8$ cm^{-1} ,

the density $\rho = 0.935$ g cm^{-3} .

Thus the values of Debye temperature for the transverse and longitudinal polarizations are 153K and 305K respectively. Consequently for low values of temperature (T < 2K), the value of the upper limit of the integral in equation 8.1 ($x_p = \theta_{Dp}/T$) is relatively large ($x_L > x_T > 76$); so that x_p can be replaced by infinity without altering the value of the integral. Substituting the appropriate values for the

various parameters into equations 8.1 & 8.2, it can be shown that the specific heat capacity obtained using the Debye theory, for polyethylene at low temperature is: $c_D T^3 = 116\ T^3$ erg g^{-1} K^{-1} .

The values of the specific heat capacity of the polyethylene samples, which have been obtained experimentally at low temperatures, can be represented by the equation $c(T) = aT + bT^3$, where $a \approx 9$ erg g^{-1} K^{-2} and $b \approx 138$ erg g^{-1} K^{-4} (see section 6.4 and table 6.1). Stephens (1973) has shown that for a wide variety of amorphous materials, including glasses and polymers, the variation of the specific heat capacity with temperature can be represented by the equation $c(T) = \alpha T + \beta c_D T^3$, where $7 < \alpha < 50$ erg g^{-1} K^{-2}, $1.2 < \beta < 3.0$ and $c_D T^3$ is the specific heat capacity obtained using the Debye theory. Thus the difference between the experimentally observed values of heat capacity and the values predicted using the Debye theory $[aT+(b-c_D)T^3]$, can be attributed to the heat capacity of the amorphous regions within the semi-crystalline polyethylene samples.

The presence of the localised tunnelling states, proposed by Anderson et Al (1972) and by Phillips (1972), can be used to explain the aT component of the excess heat capacity; since the heat capacity per unit volume associated with these states is $\frac{\pi^2}{6} K_B^2 n_o T$, where $n_o d\varepsilon$ equals the number of tunnelling states per unit volume with an energy difference between ε and $\varepsilon + d\varepsilon$. Alternatively following the suggestion of Zaitlin & Anderson (1975b), it would be possible to explain the entire excess heat capacity $[aT+(b-c_D)T^3]$, if the density of tunnelling states was assumed to be $n(\varepsilon)d\varepsilon = (n_o + n_2\varepsilon^2)d\varepsilon$.

8.2 An Introduction to the Application of Theory to the Thermal Conductivity Results

The work described in this thesis, has shown that the specific heat capacity of a semi-crystalline polymer, is not significantly altered by extrusion. The linear component of the heat capacity has been

associated with the existence of localised tunnelling states within the amorphous regions of the polymer (see section 8.1). Thus it must be concluded that the density of these tunnelling states is not affected by extrusion, since the associated heat capacity is unaffected by extrusion. Consequently it is not possible to explain the change in the low temperature thermal conductivity of the polyethylene samples, which occurs as a result of extrusion, in terms of the scattering of phonons by localised tunnelling states.

The experimental results cannot be explained using the structure scattering theory developed by Walton (1974) for reasons discussed in section 8.6. Consequently the more sophisticated structure scattering theory developed by Morgan & Smith (1974) has been used to explain the thermal conductivity data.

8.3 The Phonon Mean Free Path

The expression for the mean free path of a phonon within a semi-crystalline polymer, which was used by Burgess & Greig (1975) (see equation 2.4, section 2.7.2), was extended by Rogers (1980) to include an extra term, which was originally proposed by Morgan & Smith (1974) to describe the effect of long range order within the amorphous regions (see equation 2.3, section 2.5). Thus the mean free path ($L_p(q)$) of a phonon of wave number q and polarization p, travelling at velocity v_p within a material with a fractional crystallinity X, is given by:

$$\frac{1}{L_p(q)} = \frac{1-X}{v_p t_p(q, a_s, \Delta_S^2)} + \frac{1-X}{v_p t_p(q, a_L, \Delta_L^2)} + \frac{X}{v_p t_p(q, a_c, \Delta_c^2)} + \frac{1}{L_B} + \frac{X}{L_u(q)} \qquad 8.3$$

The first three terms in equation 8.3 represent the effects of structure scattering. The correlation length a_S is related to the dimensions of the structural units of which the amorphous material is composed; while the correlation length a_L is associated with long range fluctuations in the properties of disordered materials. Due to the arrangement of amorphous and crystalline regions within a semi-crystalline polymer, additional fluctuations in the properties of

the material occur, which give rise to the correlation length a_c, which is therefore related to the dimensions of the crystalline regions within the sample.

Morgan & Smith (1974) used correlation lengths a_S & a_L to explain the conductivity curves observed for purely amorphous materials, over the temperature range 0.1K to 10K. Morgan & Smith also suggested that the correlation length a_c ($a_c \sim 100$ Å) could be used to explain the change in the slope of the conductivity of polyethylene at 0.8K, which was observed by Scott et Al (1973). Burgess & Greig (1975) used correlation lengths a_c & a_S to explain the conductivity curves observed for polyethylene over the temperature range 3K to 100K. Rogers (1980) used correlation lengths a_L,a_c & a_S to explain the conductivity curves observed for polyethylene over a larger temperature range 0.15K to 100K; and showed that the differences in the conductivity of extruded and non extruded polyethylene samples, which were observed below 2K, could be explained using different values of the correlation length a_c.

The fourth term in equation 8.3 takes into account the scattering of the phonons at the boundaries of the sample. This scattering process limits the mean free path of those long wavelength phonons which are not scattered by any other process; and would therefore give rise to an infinite value for the conductivity, if this term was not included.

The existence of tunnelling states has been used to explain the low temperature heat capacity of polyethylene. In order to obtain an explanation of the thermal conductivity of polyethylene, which is consistent with this explanation of the heat capacity; it is necessary to include a term in the expression for the phonon mean free path, which represents the effect of phonon scattering by these tunnelling states. The effect of this term, on the values obtained for the phonon mean free path, is very similar to the effect of the structure scattering term

associated with correlation length a_L (see section 8.6). The existence of this correlation length is difficult to justify in terms of the structure of a semi-crystalline polymer; and the only independent experimental evidence for the existence of the long range fluctuations in the properties of these polymers, which are associated with correlation length a_L, is provided by the light scattering experiments cited by Morgan & Smith (1974). Consequently the term in equation 8.3 associated with correlation length a_L has been replaced by a term associated with phonon scattering by tunnelling states. Thus the phonon mean free path is given by:

$$\frac{1}{L_p(q)} = \frac{1-X}{v_p t_p(q, a_S, \Delta_S^2)} + \frac{X}{v_p t_p(q, a_c, \Delta_c^2)} + \frac{1-X}{L_{TS}(q,T)} + \frac{1}{L_B} + \frac{X}{L_U(q)} \qquad 8.4$$

where $\frac{1}{L_{TS}(q,T)} = \left(\frac{\pi \alpha_{TS} q}{\rho v_p^2}\right) \tanh\left(\frac{\hbar v_p q}{2 k_B T}\right)$, and ρ is the density of the material. In terms of the parameters defined by Jackle (1972) $\alpha_{TS} = B^2 \bar{P}$, where B is a deformation potential parameter; and $P(\varepsilon,\lambda)\, d\varepsilon\, d\lambda = \bar{P}\, d\varepsilon\, d\lambda$ is the number of two level systems per unit volume, which can be described by parameters which lie within the ranges ε to $\varepsilon+d\varepsilon$ and λ to $\lambda+d\lambda$. Parameter λ is determined by the height and width of the potential barrier separating the two equilibrium positions of the atom (or group of atoms); and ε is the energy difference between the ground states which correspond to these equilibrium positions. Parameter $\bar{P}$ should not be confused with parameter n_o which was introduced in section 8.1; $n_o d\varepsilon$ is defined to be the number of tunnelling states per unit volume with an energy difference in the range ε to $\varepsilon+d\varepsilon$ and a potential barrier which permits phonon assisted tunnelling. Parameter α_{TS} will be treated as an adjustable fitting parameter; and it will be assumed that the value of α_{TS} is the same for both longitudinal and transverse polarizations.

Morgan & Smith (1974) evaluated the phonon relaxation time $t_p(q,a,\Delta^2)$, for a phonon of wave number q and polarization p, scattered within a material characterised by a correlation length (a) and the parameter Δ^2, in terms of the following function:

$$F_p(q.a) = \left(\frac{t_p(q,a,\Delta^2).\Delta^2.v_L}{a.v_N}\right) x10^{12} \text{ seconds/Angstrom} \quad 8.5$$

where v_L is the longitudinal velocity of sound and v_N is a normalising velocity (v_N=4x10^5 cm/sec). They evaluated this function for both types of polarization, and obtained curves which will be referred to as the Morgan Smith universal relaxation (MSUR) curves. In order to calculate the conductivity, it is necessary to integrate an expression involving the phonon mean free path ($L_p(q)$) with respect to wave number (q). This integration has to be performed numerically, so that it is necessary to evaluate equation 8.4 for a large number of different values of wave number. In order to facilitate the evaluation of the relaxation times $t_p(q,a,\Delta^2)$, a least squares fitting procedure was used to obtain a simple mathematical representation of the MSUR curves in terms of the variables y=log(F_p(q.a)) and x=log(q.a). The central section of the curve was represented by a low order polynomial, while each end of the curve was represented by a straight line.

If equation 8.4 is evaluated using a value of wave number for which a certain scattering process does not occur, then the value of the relevant term in this equation is negligible when compared with the other terms. Consequently this equation can be used over an unlimited range of wave number.

The final term in equation 8.4 represents the effect on the phonon mean free path of Umklapp processes, which may occur within the crystalline regions of the polymer at high temperature. The mean free path due to Umklapp scattering ($L_u(q)$) was obtained using the expression used by Burgess & Greig (1975):

$$L_u(q) = \frac{A}{q^2}.\exp\left(\frac{\theta_D}{2T}\right) \quad 8.6$$

where $A = 2.3 \times 10^8 \ cm^{-1}$.

For phonons propagating within the crystalline regions of an extruded polymer, parallel to the extrusion direction and therefore parallel to the chain axes, the value of the Debye temperature is large ($\Theta_{D//} \sim 1300K$), for reasons discussed in section 2.7.2. Consequently the value of the final term in equation 8.4 is negligible for the extruded polyethylene samples SH2 & SH3. However for phonons propagating normal to the chain axes, the value of Debye temperature is much lower ($\Theta_{D\perp} = 153K$); so that the effects of Umklapp processes are significant at high temperatures for the isotropic polyethylene sample SH0.

Equation 8.6 was originally obtained by Klemens (1951) and is valid for $T < \Theta_D/6$. However the effects of Umklapp scattering on the calculated conductivity values are only significant for $T > 30K$ or $T > \Theta_D/5$; thus the validity of this calculation must be regarded as doubtful. The value of parameter A is obtained using another result derived by Klemens (1958), of the form:

$$L_u = B.\exp\left(\frac{\Theta_D}{\alpha T}\right) \qquad 8.7$$

where α is a numerical constant whose value depends on the detailed structure of the material. Equation 8.7 is valid for phonons of frequency w and wave number q such that $\hbar w \approx K_B T << K_B \Theta_D$ or $q << q_D$. The value of parameter A, is then obtained by assuming an arbitrary value for parameter α and equating the results obtained by equations 8.6 & 8.7 for $q = q_D$. Thus the parameter A can only be regarded as an adjustable fitting parameter.

8.4 Calculation of the Theoretical Thermal Conductivity Curve

Using the relaxation time method to solve the Boltzmann equation, and the assumptions of the Debye theory, it can be shown that the thermal conductivity per polarization p is given by:

$$k_p(T) = \left(\frac{K_B^4}{6\pi^2 \hbar^3}\right)\left(\frac{T^3}{v_p^2}\right)\int_0^{x_p} L_p(x).\left\{\frac{x^4 e^x}{(e^x-1)^2}\right\}dx \qquad 8.8$$

where $L_p(x)$ is the mean free path of a phonon of polarization p and wave

number q travelling at a velocity v_p, and $x = \frac{\hbar v_p q}{k_B T}$. The Debye temperature (θ_{Dp}) associated with polarization p is defined by:

$x_p = \frac{\theta_{Dp}}{T} = \frac{\hbar v_p q_D}{k_B T}$, where q_D is the cut-off wave number introduced by the Debye theory. Taking into account the two transverse polarizations and the single longitudinal polarization, the total thermal conductivity is given by:

$$k(T) = 2\, k_T(T) + k_L(T) \qquad 8.9$$

The assumption that the heat current is carried by phonons with acoustic velocities and a Debye density of states, within a material whose low temperature heat capacity exceeds the value obtained using the Debye theory, is justified by the results obtained by Pohl et Al (1973) and Zaitlin & Anderson (1975a), which are discussed in section 2.6.

The values of the parameters required by the conductivity calculation, which are appropriate to the polyethylene samples are given below:

fractional crystallinity $X = 0.6$,

minimum sample dimension $L_B = 1.0$ cm,

transverse velocity of sound $v_T = 2.0 \times 10^5$ cm/sec,

longitudinal velocity of sound $v_L = 4.0 \times 10^5$ cm/sec,

Debye cut-off wave number $q_D = 10^8$ cm^{-1} .

The fractional crystallinity was determined from the sample density ($\rho = 0.935$ g cm^{-3}) (see section 2.7.1). The values of phonon velocity and Debye cut-off wave number, are those which were used by Burgess and Greig, to fit the values of specific heat capacity obtained for the polyethylene samples at high temperature (see section 8.1). Athougies et Al (1972) have shown that in many polymers the longitudinal velocity of sound is twice the transverse velocity of sound. The value chosen for the cut-off wave number has no effect on the conductivity calculation for low values of temperature, for which the value of $x_p = \theta_{Dp}/T$ is large. It has also been assumed that the phonon velocity is constant and

therefore independent of wave number.

The integral which appears in equation 8.8 has to be evaluated numerically. This calculation was performed on the computer using a subroutine written by the Nottingham Algorithm group (NAG), which calculates the value of an integral to a specified accuracy (set at 0.2%), using an automatic adaptive procedure and Gauss 30 point and Kronrod 61 point integration rules.

8.5 The Fitting of the Theoretical Curve to the Experimental Results

The values of the correlation lengths, parameters Δ^2, and parameter α_{TS} were selected in such a way as to obtain feasible values, which gave rise to a good fit between the experimentally observed conductivity values and the conductivity curve calculated using equations 8.4, 8.5, 8.6, 8.8 and 8.9. The fitting procedure used was as follows:

A conductivity curve was evaluated using a trial set of parameters over the full range of temperature 0.08K to 100K. A series of curves was then evaluated using sets of parameters, which were obtained from the trial set by varying the value of one of the parameters by a fixed factor above and below the trial value. This process was repeated for each parameter in turn, giving rise to typically 40 curves, in addition to the curve obtained with the trial set of parameters. These curves were used as input data to a program, which estimated the change in the calculated conductivity values resulting from a change in the trial set of parameters, by interpolating between the supplied curves. This program incorporated a NAG subroutine, which varied the parameter values until a minimum value of the function

$\sum_i \left\{ \log(k_{exp}(T_i)) - \log(k_{CAL}(T_i)) \right\}^2$ was found; where $k_{CAL}(T_i)$ is a calculated conductivity value obtained using the current set of parameters, and $k_{exp}(T_i)$ is an experimentally obtained conductivity value. In this way a new set of parameters was obtained, which gave rise

to an improved fit between the theoretical curve and the experimental data.

This procedure could be iterated, in that the selected set of parameters could be used to obtain a fresh set of curves, which could then be used to select a new set of parameters. It was possible to vary the temperature range over which the fitting procedure operated, and to select the parameters which were to be allowed to vary. It was found that parameter α_{TS} affected only the low temperature conductivity values, and that parameters a_S and Δ_S^2 affected only the high temperature conductivity values.

It was found that a reasonable fit between the theoretical curves and the experimental data could be obtained using the parameter values given in table 8.1. The theoretical curves obtained using these parameter values are shown in figures 8.1 & 8.2, with the experimental data obtained for the polyethylene samples. The conductivity values obtained by Burgess & Greig (1975) over the temperature range 3K to 100K are also shown.

TABLE 8.1

		SH0	SH2	SH3
a_S	(Å)	5.0	5.0	5.0
Δ_S^2		0.210	0.210	0.210
a_C	(Å)	272	81.5	71.0
Δ_C^2		0.130	0.130	0.130
α_{TS}	(erg cm^{-3})	1.38×10^8	1.35×10^8	1.93×10^8

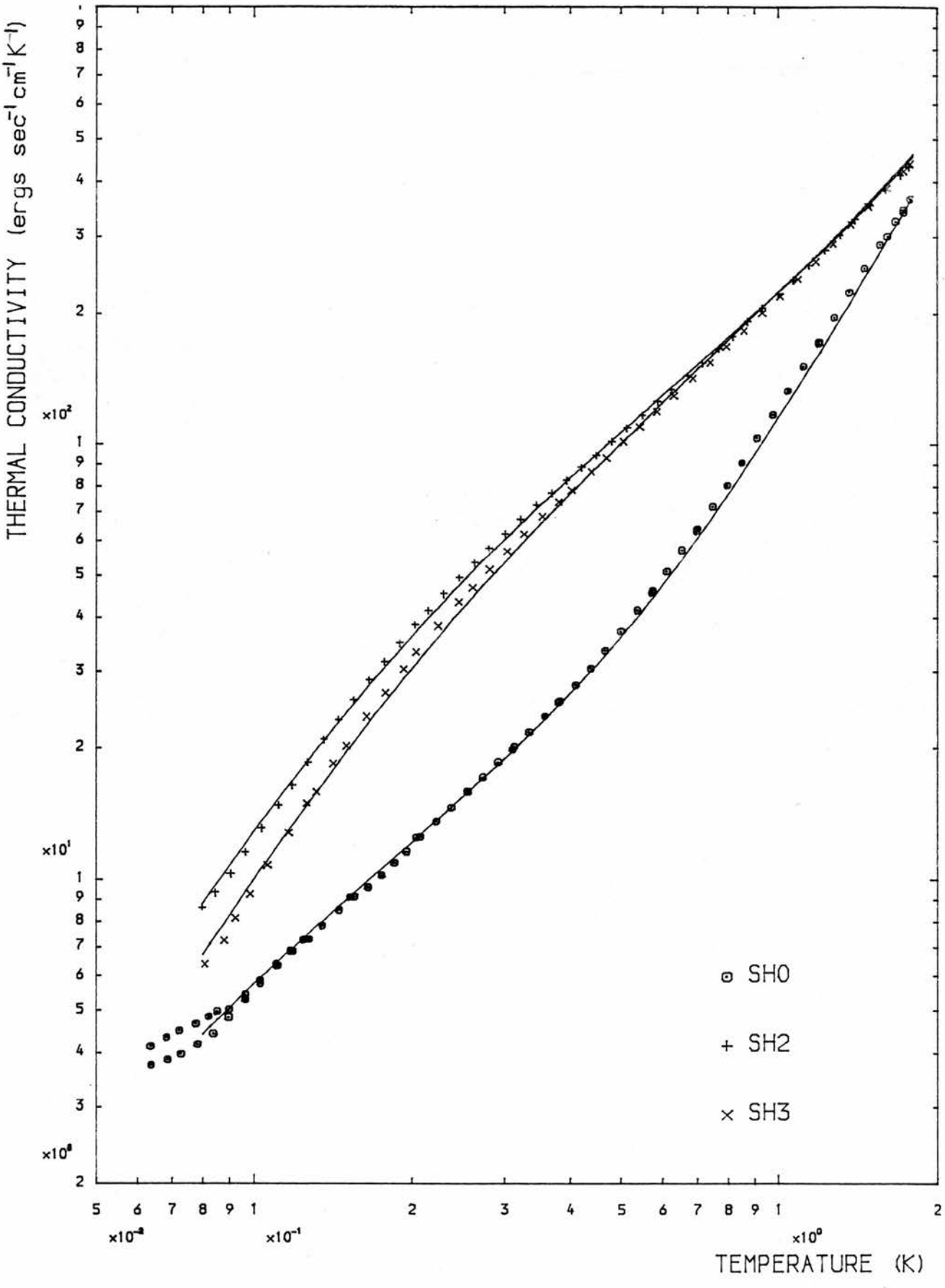

Figure 8.1

The theoretical conductivity curves obtained using the parameter values given in table 8.1. The points represent experimental values.

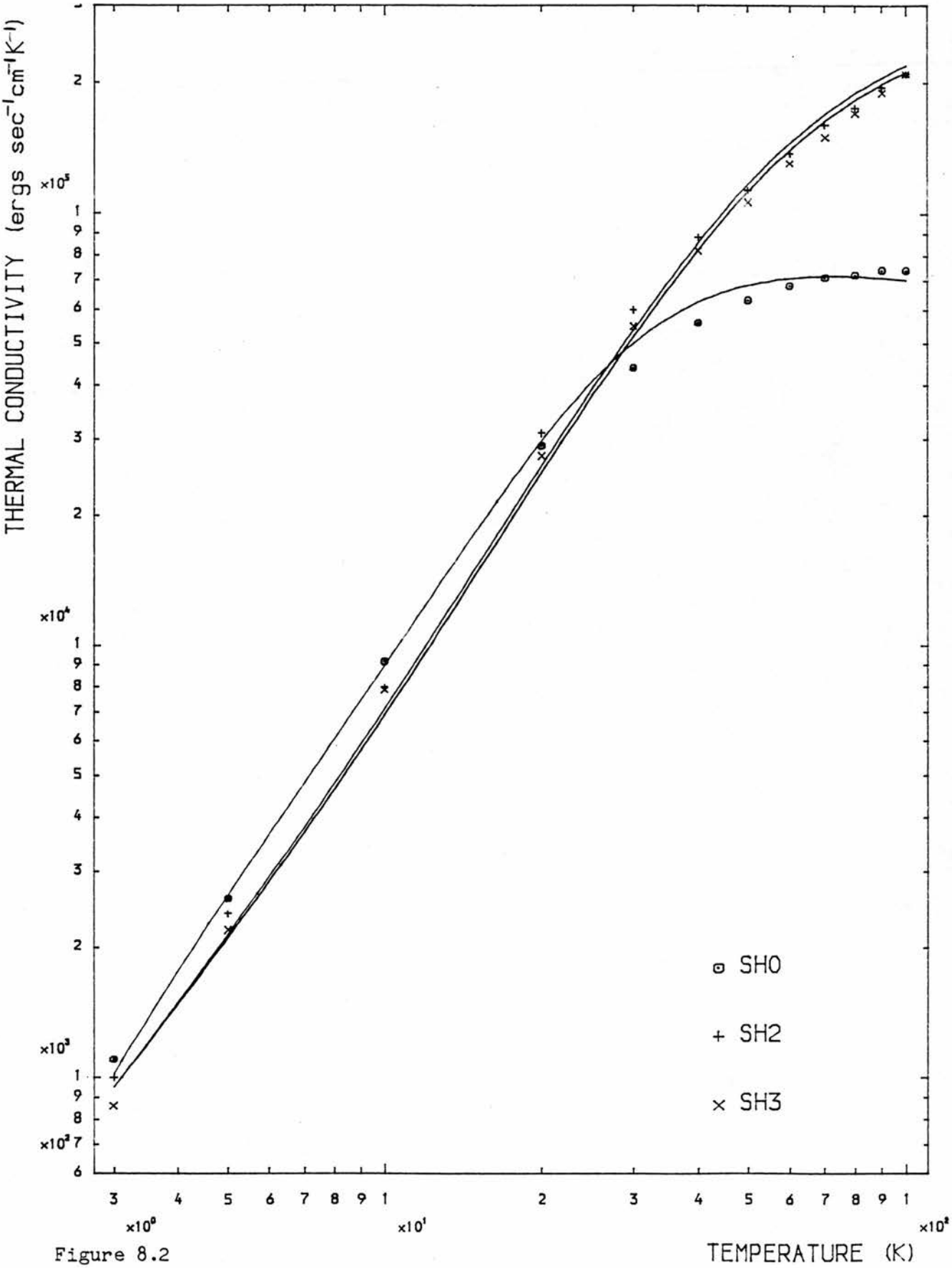

Figure 8.2

The theoretical conductivity curves obtained using the parameter values given in table 8.1. The points represent the experimental values obtained by Burgess & Greig (1975).

8.6 The Relationship between Correlation Length and Phonon Mean Free Path

Figures 8.3 to 8.5 essentially show the variation of the inverse relaxation time $[t_L(q)]^{-1}$ with wave number q for phonons with a longitudinal polarization. These curves will be referred to as relaxation curves. The axes have been calibrated in terms of the phonon mean free path $[L_L(q) = v_L t_L(q)]$ and phonon wavelength $[\lambda = 2\pi/q]$, so that the values of phonon wavelength, phonon mean free path and correlation length can easily be compared.

Figure 8.3 shows the relaxation curve associated with a conductivity curve obtained by Morgan & Smith (1974), which fits the experimentally observed values of conductivity obtained for selenium, a purely amorphous material. This curve was obtained using a combination of boundary scattering and structure scattering associated with correlation lengths a_L & a_S (see equation 2.3, section 2.5). Figures 8.4 & 8.5 show the relaxation curves obtained for samples SH0 & SH2 respectively, using the parameters given in table 8.1. The other curves shown in each figure are obtained for a single scattering process, such as tunnelling state scattering or the structure scattering associated with a single correlation length. The x axis coincides with the phonon mean free path due to boundary scattering. These processes combine to give the overall relaxation curve which is associated with the fitted conductivity curves. The relaxation curve associated with Umklapp scattering has not been included in figure 8.4, as this scattering process is not important at low temperatures.

The change in the mean free path, due to structure scattering associated with a particular correlation length a_x, is negligible for phonons whose wavelength is much longer than the correlation length. For $\lambda > 20a_x$, $L(q,a_x,\Delta_x^2) \propto \lambda^4$ so that structure scattering becomes rapidly more important as wavelength decreases. At shorter wavelengths the

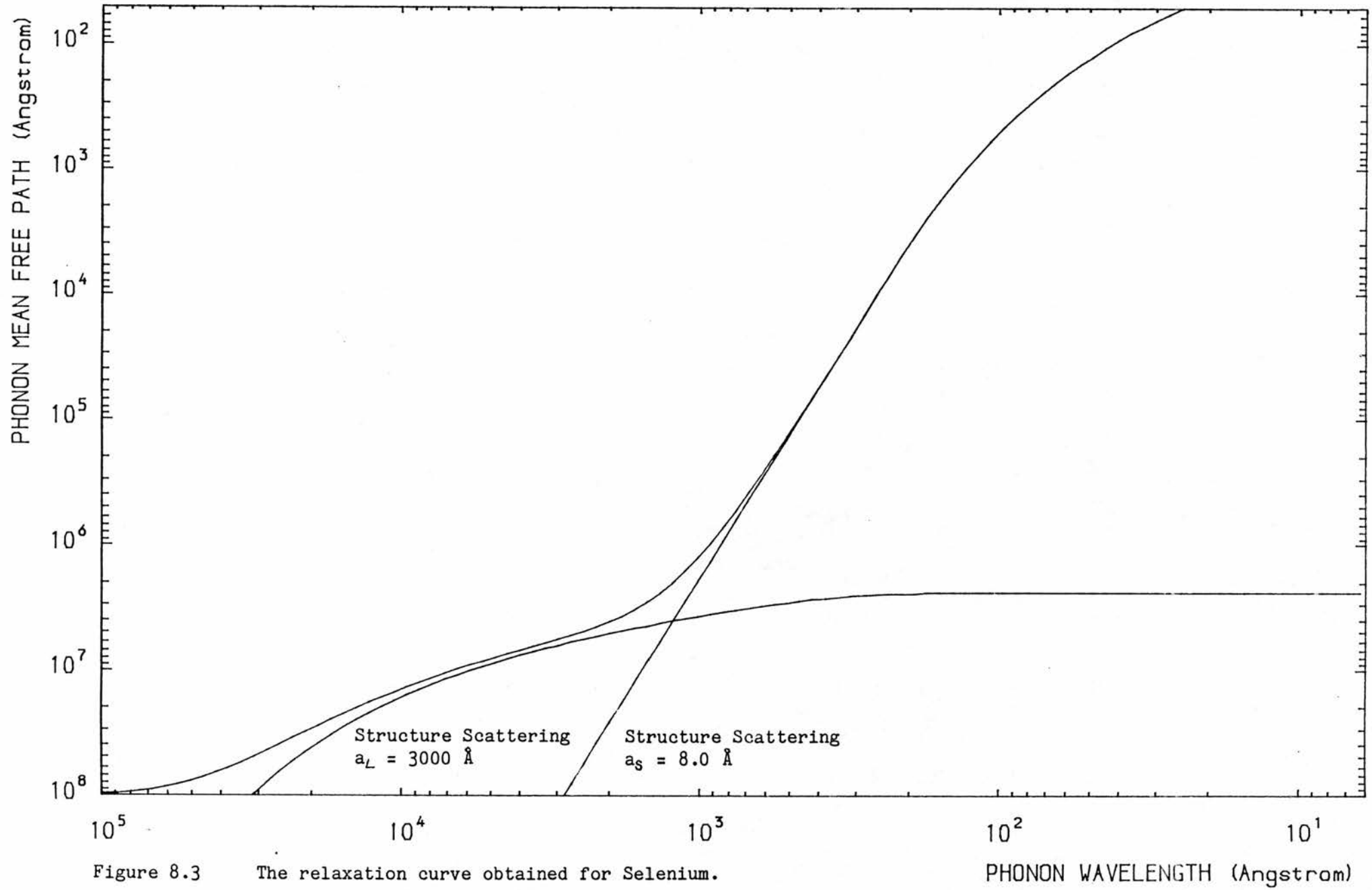

Figure 8.3 The relaxation curve obtained for Selenium.

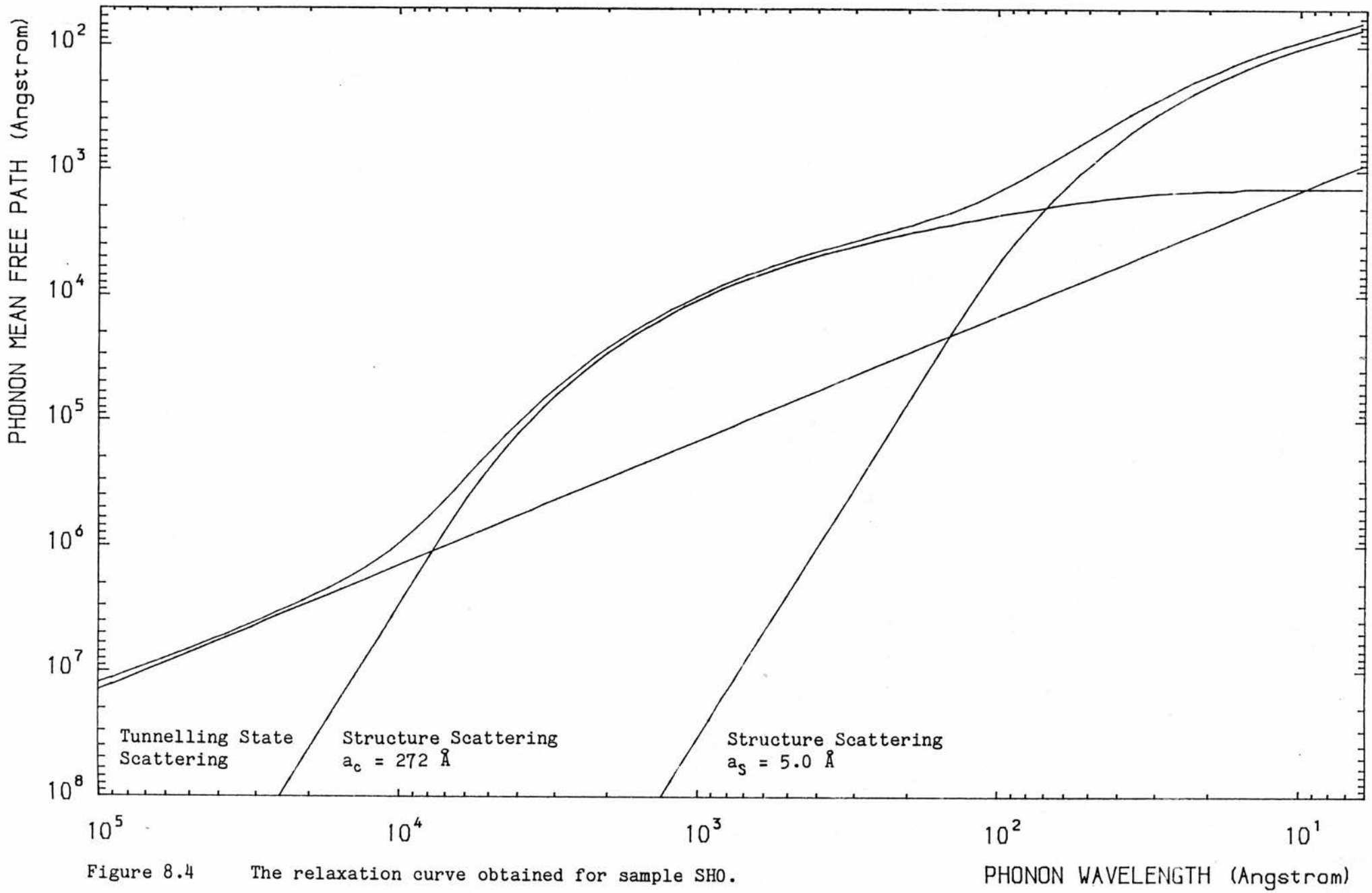

Figure 8.4 The relaxation curve obtained for sample SH0.

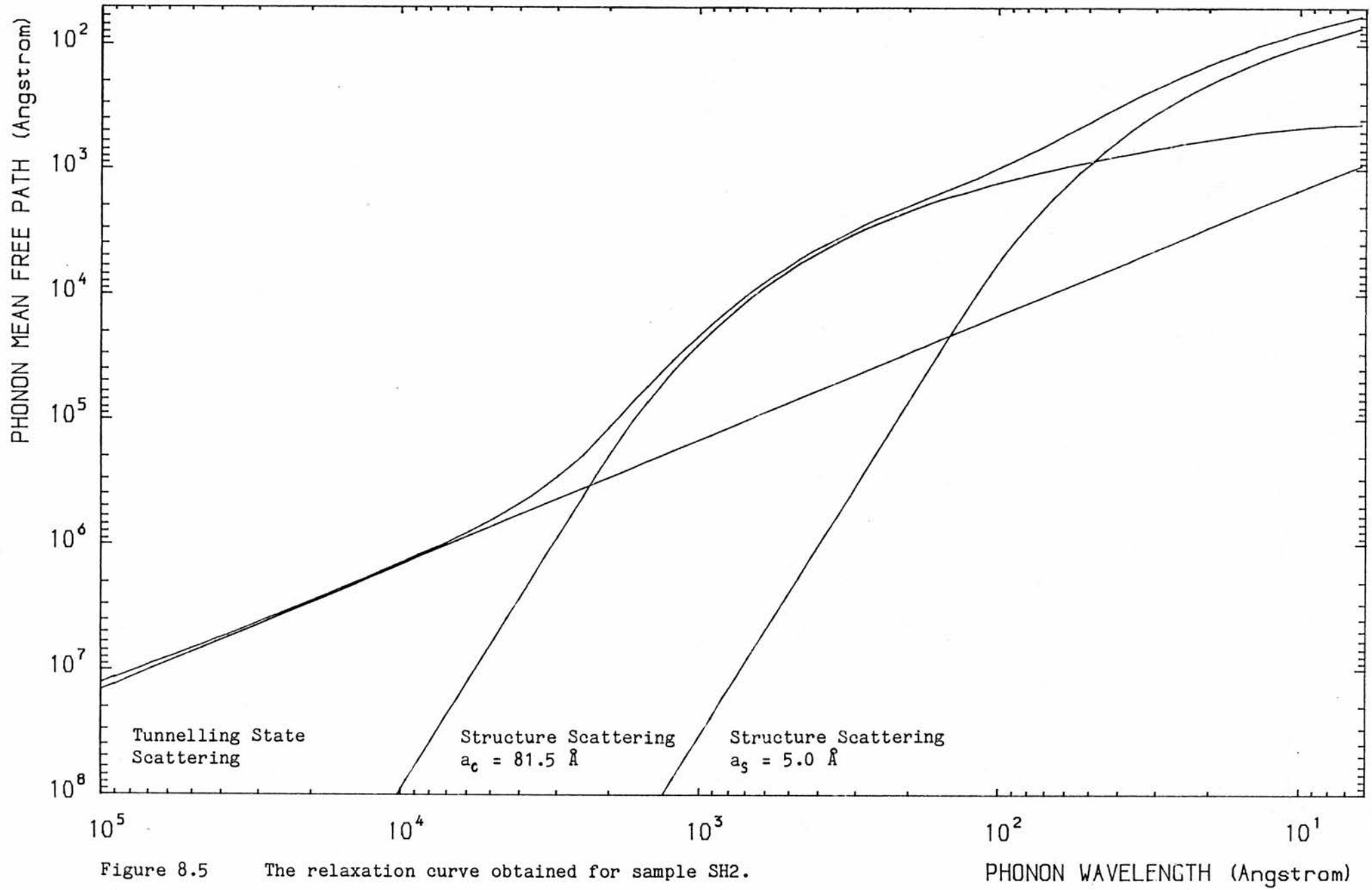

Figure 8.5 The relaxation curve obtained for sample SH2.

gradient of the relaxation curve decreases, until the mean free path becomes independent of wavelength. Thus for phonons with wavelengths shorter than the correlation length, structure scattering reaches a maximum; and the phonon mean free path reaches a minimum value, which for longitudinal phonons, is typically an order of magnitude larger than the relevant correlation length. Thus although a correlation length may be related to the separation of boundaries within a material, the effects of structure scattering are quite different to the effects of scattering at the sample boundaries, which gives rise to a constant mean free path equal to the separation of the sample boundaries.

The relationship between the relaxation curve obtained for a given value of correlation length and the MSUR curve (equation 8.5), can be written as follows: $t_p(q,a,\Delta^2) \propto \left(\frac{a}{\Delta^2}\right) F_p\left(\frac{2\pi a}{\lambda}\right)$. Thus if the value of a correlation length (a) is increased by a factor f, then a point on the relaxation curve with coordinates (λ, L) is shifted to the point $(f\lambda, fL)$; whereas if the parameter Δ^2 is increased by a factor g, then the point (λ, L) is shifted to the point $(\lambda, L/g)$. Thus it can be seen that altering the values of either the correlation length (a) or the associated parameter Δ^2, does not alter the shape of the relaxation curve associated with this correlation length; however the position of this curve relative to the curves associated with the other scattering mechanisms is altered, and so the shape of the relaxation curve obtained for the combined scattering processes is altered.

It can be seen from the relaxation curves obtained for the combined scattering processes, that the mean free path of a longitudinal phonon, varies between 100λ for long wavelength phonons ($\lambda \sim 10^5$ Å), and 10λ for short wavelength phonons ($\lambda \sim 10$ Å).

In the dominant phonon approximation, which is described in section 2.2, the thermal conductivity is given by $k(T) = \frac{1}{3} v.c(T).L(T)$, where c(T) is the Debye heat capacity so that $c(T) \propto T^3$ for $T < \theta_D$. The

phonon mean free path L(T), is associated with those phonons of wave number $q_{DOM} = \frac{4\ K_B T}{\hbar v_p}$, which are dominant in the specific heat capacity. Thus if $[L(q_{DOM})]^{-1} \propto q_{DOM}^{M} \propto T^{M}$, then $k(T) \propto T^{3-M}$, where m is the gradient of the relaxation curve plotted using logarithmic scales. Thus an increase (or a decrease) in the slope of the relaxation curve gives rise to a corresponding decrease (or an increase) in the slope of the conductivity curve.

The phonon mean free path associated with tunnelling state scattering is a function of both temperature and wave number. In order to obtain a relaxation curve, which can be related to a conductivity curve using the dominant phonon approximation, a fixed relationship between wavelength λ and temperature T has been assumed, such that a phonon of wavelength λ is dominant at temperature T. It follows that $L_{TS}(q,T) = L_{TS}(q) \propto q^{-1} \propto \lambda$, giving rise to a relaxation curve which is a straight line. It should be noted that the relaxation curve obtained for a fixed value of temperature, curves away from this straight line as wavelength increases, until $L_{TS}(q) \propto q^{-2}$.

It can be seen from figures 8.3 to 8.5, that the shape and gradient of the relaxation curve obtained for a combination of scattering processes, depends on the relative positions of the curves associated with the individual scattering processes. Different sets of parameter values can give rise to the same relative position of the components of the relaxation curve, and therefore to a conductivity curve with the same temperature dependence. Thus similarities in the temperature dependence of the conductivity of different materials, can be explained without assuming similarities in the microscopic structure of these materials.

For a purely amorphous material, scattering associated with only two correlation lengths a_L & a_S occurs, and it can be seen that the slope of the resulting relaxation curve changes significantly at the

It is interesting to note that the structure scattering associated with correlation length a_s, gives rise to a relaxation curve similar to that produced by the combination of Rayleigh scattering ($L(q) \propto q^{-4}$) and Kittel scattering ($L(q)=L_o$), which was proposed by Zaitlin & Anderson (1975a) and Walton (1974), to explain the behaviour of the conductivity of amorphous materials above 2K. The explanation of these relaxation curves is also similar; as in both cases the phonons are scattered by regions of short range order within the amorphous material, which in the latter case are assumed to behave like small crystals in a polycrystalline material.

A comparison of the relaxation curve obtained for sample SH0, with the curve obtained for sample SH2, reveals that the increase in the value of the correlation length a_c, shifts the curve associated with this correlation length to longer values of wavelength. Thus the steep section of the relaxation curve, which is associated with correlation length a_c, is shifted to longer wavelengths; and the corresponding section of the conductivity curve, which has an approximately linear temperature dependence, is shifted to lower temperatures.

In order to explain the features of the experimental conductivity curves obtained for polyethylene, an extra scattering mechanism must be introduced, in addition to those used to explain the conductivity curves obtained for purely amorphous materials. It can be seen from this discussion, that this extra scattering mechanism must give rise to a relaxation curve ($L(q) \propto q^{-n}$), with a gradient (n) which is greater than 2 for long wavelengths, and which decreases with decreasing wavelength. Thus scattering mechanisms which give rise to relaxation curves with constant gradients, such as tunnelling state scattering (n=1) or the structure scattering theory developed by Walton (1974) (n=1), cannot be used to provide this extra scattering mechanism.

The relaxation curve associated with correlation length a_c, intersects the curve associated with correlation length a_s at wavelength λ_{cs}, and intersects the curve associated with tunnelling state scattering at λ_{Tc} ;

where λ_{Tc}= 2300Å = $29a_c$ and λ_{cs}= 48Å = $0.59a_c$ = $9.6a_s$ for sample SH2;

while λ_{Tc}= 7700Å = $28a_c$ and λ_{cs}= 70Å = $0.26a_c$ = $14a_s$ for sample SH0.

Using the dominant phonon approximation, it can be deduced that scattering associated with correlation length a_c is the principal scattering mechanism over the temperature range $0.22K < T < 10.4K$ for sample SH2 and $0.065K < T < 7.2K$ for sample SH0.

At any given temperature, the heat current is carried by phonons with a range of different values of wave number, and therefore with a range of different values of mean free path taken from the relaxation curve. Consequently the conclusions obtained using the dominant phonon approximation are only qualitative.

The MSUR curves, which are appropriate to the transverse and longitudinal polarizations, are different; so that the relaxation curves obtained for transverse and longitudinal phonons are also different. Also the relationship between temperature and the wavelength of the dominant phonon, is different for transverse and longitudinal phonons, as it depends on the value of the velocity of sound. In general, longitudinal phonons are scattered less than the transverse phonons, so that the longitudinal phonons carry a larger heat current than the transverse phonons; even though the transverse phonons have a larger heat capacity than the longitudinal phonons. Thus the relationship between the features of the relaxation curve obtained for a single polarization, and the features of the conductivity curve obtained for all 3 polarizations, is closer for the longitudinal polarization than for the transverse polarization. For this reason, only the longitudinal phonons have been considered in this discussion, although this must be

regarded as an over-simplification.

8.7 The Relationship between the Values of Correlation Length and The Structure of Polyethylene

The correlation length a_S is related to the dimensions of the regions of order, which exist within an amorphous material. Using wide angle x-ray diffraction, Brown & Eby (1964) found that the dimensions of the unit cell within a polyethylene sample were 2.5Å x 4.9Å x 7.4Å. Frank (1970) notes that the cross-sectional area per chain in polyethylene is $18.2Å^2$, so that the diameter of the chain is typically 4.8Å. Thus the chosen value of the correlation length a_S (a_S=5Å) appears to be reasonable.

The correlation length a_C is related to the dimensions of the crystalline regions, which occur in both the isotropic and extruded polyethylene samples, in the form of lamellae. In the extruded samples, the lamellae are aligned with each other, and orientated at a fixed angle to the extrusion direction (Burgess & Greig 1975). Thus for phonons travelling parallel to the extrusion direction, the distance travelled within the lamella is fixed, and comparable to the thickness of the lamella, which is typically 100Å. In the isotropic sample, the lamellae form twisted ribbons, which radiate out from nucleating centres to form spherulites (Phillips 1971). Thus the lamellae are randomly orientated relative to the direction of phonon propagation, and some phonons travel distances within the lamellae, which are much larger than the thickness of the lamella. Thus it is to be expected that the chosen values of the correlation length a_C should be of the order of 100Å; and that the value obtained for the isotropic sample SH0 should be significantly greater than the values obtained for the extruded samples SH2 & SH3.

Hunklinger & Piché (1975), measured the variation of the velocity of sound within a borosilicate glass, and obtained the following values for the tunnelling state scattering constant: $\alpha_{TS} = 1.2 \times 10^{8}$ erg cm^{-3} for transverse waves and $\alpha_{TS} = 2.6 \times 10^{8}$ erg cm^{-3} for longitudinal waves. Thus the values of α_{TS} given in table 8.1, which were obtained for polyethylene by fitting the theoretical curves to the experimental conductivity data, are comparable to the values obtained for a purely amorphous material. This suggests that the scattering of long wavelength phonons within the amorphous regions of a semi-crystalline polymer is very similar to that within a purely amorphous material.

CHAPTER IX

CONCLUSION

The specific heat capacity of an isotropic polyethylene sample, and 3 extruded polyethylene samples, was measured over the temperature range 0.15K to 1.3K; and it was found that within the limits of experimental error, the specific heat capacity of the isotropic and extruded samples was the same. The temperature dependence of the specific heat capacity was found to be of the form $c(T) = aT + bT^3$, and was explained in terms of the heat capacity associated with phonons with a Debye density of states, and the heat capacity associated with the localised tunnelling states, proposed by Anderson et Al (1972) and Phillips (1972). Thus it was concluded that the density of the localised tunnelling states, within the amorphous regions of the semi-crystalline polymer, was not affected by extrusion.

The thermal conductivity of the isotropic polyethylene sample, and two of the extruded polyethylene samples, was measured over the temperature range 0.08K to 1.8K. It was found that the thermal conductivity of the isotropic sample, differed significantly both in magnitude and temperature dependence, from the thermal conductivity of the extruded samples. These conductivity curves have been explained by assuming that: the heat current is carried by phonons with a Debye density of states and acoustic velocities; and that the long wavelength phonons dominant at very low temperatures, are scattered by the localised tunnelling states which contribute to the heat capacity; while the phonons dominant at higher temperatures are scattered by the structure of the semi-crystalline polymer. The phonon mean free path due to structure scattering is obtained using the theory developed by Morgan & Smith (1974), which introduces correlation lengths a_s & a_c. The value of the correlation length a_s is related to the dimensions of the

structural units present within the amorphous regions of the semi-crystalline polymer; while the value of correlation length a_c is related to the dimensions of the crystalline lamellae. The differences between the conductivity curves obtained for the isotropic and extruded samples, have been explained using different values of the correlation length a_c, which have been related to the change in the orientation of the lamellae, which occurs as a result of extrusion. This explanation introduces 5 adjustable fitting parameters.

An alternative interpretation of the experimental data exists. The conductivity curves can be explained in terms of structure scattering alone, using correlation lengths a_L, a_c & a_s in the manner of Rogers (1980) (see equation 8.3, section 8.3). This explanation introduces 6 adjustable fitting parameters. This explanation of the thermal conductivity, can be reconciled with the explanation of the specific heat capacity in terms of tunnelling states, by assuming that the coupling between the phonons and the localised tunnelling states, is so weak that phonon scattering by these states can be neglected.

These alternatives also apply to purely amorphous materials. Tunnelling state theory provides an explanation of the temperature dependence, of both the specific heat capacity and the thermal conductivity, of amorphous materials at very low temperatures ($T<1K$). However some form of structure scattering must be introduced to explain the conductivity of amorphous materials, observed at higher temperatures (Zaitlin & Anderson 1975a, Walton 1974); so that at least 3 adjustable fitting parameters are introduced. Alternatively the conductivity of amorphous materials can be explained in terms of structure scattering theory alone, using 4 adjustable fitting parameters.

Thus structure scattering theory is essential to any explanation of the conductivity; and is particularly attractive, since only one type of scattering mechanism is required to explain the conductivity, of a

wide range of amorphous and semi-crystalline materials over a wide range of temperature (0.1K to 100K). However tunnelling state theory is essential to any explanation of the heat capacity of these materials. Consequently neither theory can be neglected.

BIBLIOGRAPHY

Anderson A.C., Folinsbee J.T. and Johnson W.L. (1971), J. Low Temp. Phys. 5, 591.

Anderson A.C. and Peterson R.E. (1970), Cryogenics 10, 430.

Anderson P.W., Halperin B.I. and Varma C.M. (1972), Phil. Mag. 25, 1.

Athougies A.D., Peterson B.T., Salinger G.L. and Swartz C.D. (1972), Cryogenics 12, 125.

Berman R. (1951), Phil. Mag. 42, 642.

Berman R. (1976), Thermal conduction in solids, Clarendon press, Oxford.

Brown R.G. and Eby R.K. (1964), J. Appl. Phys. 35, 1156.

Buhl A.J. and Giauque W.F. (1965), Rev. Sci. Instr. 36, 703.

Burgess S. and Greig D. (1975), J. Phys. C 8, 1637.

Chang G.K. and Jones R.E. (1962), Phys. Rev. 126, 2055.

Chapman A.J. (1974), Heat Transfer, 3rd Ed., Collier and Macmillan.

Choy C.L. and Greig D. (1975), J. Phys. C 8, 3121.

Choy C.L. and Greig D. (1977), J. Phys. C 10, 169.

Choy C.L., Hunt R.G. and Salinger G.L. (1970), J. Chem. Phys. 52, 3629.

Collan H.K., Heikkila T., Krusius M. and Pickett G.R. (1970), Cryogenics 10, 389.

Frank F.C. (1970), Proc. Roy. Soc. London A319, 127.

Gibson A.G., Greig D., Sahota M., Ward I.M. and Choy C.L. (1977), J. Polymer Sci., Polymer Lett. Ed. 15, 183.

Giles M. and Terry C. (1969), Phys. Rev. Lett. 22, 882.

Godratt E., Greenfield A.J. and Schlesinger Y. (1977), Cryogenics 17, 81.

Ho J.C., O Neal H.R. and Phillips N.E. (1963), Rev. Sci. Instr. 34, 782.

Ho J.C. and Phillips N.E. (1965), Rev. Sci. Instr. 36, 1382.

Hunklinger S. and Piche L. (1975), Solid St. Comm. 17, 1189.

Jackle J. (1972), Z. Physik 257, 212.

Keesom W.H. and Kok J.A. (1932), Commun. 219-C, Proc. Kon. Akad. Amsterdam, 35, 294.

Klemens P.G. (1951), Proc. Roy. Soc. A208, 108.

Klemens P.G. (1958), Solid St. Phys. (New York: Academic Press) 7, 1.

Kolouch R.J. and Brown R.G. (1968), J. Appl. Phys. 39, 3999.

Lasjaunias J.C., Picot B., Ravex A., Thoulouze D. and Vandorpe M. (1977), Cryogenics 17, 111.

Lasjaunias J.C., Ravex A., Vandorpe M. and Hunklinger S. (1975), Solid State Commun. 17, 1045.

Little W.A. (1959), Can. J. Phys. 37, 334.

Lounasmaa O.V. (1974), Experimental principles and methods below 1K, Academic press: London and New York.

Morgan G.J. (1968), J. Phys. C 1, 347.

Morgan G.J. and Smith D. (1974), J. Phys. C 7, 649.

Olsen J.L. and Renton C.A. (1952), Phil. Mag. 43, 946.

Phillips W.A. (1971), Phys. Rev. 3, 4338.

Phillips W.A. (1972), J. Low Temp. Phys. 7, 351.

Pohl R.O., Love W.F. and Stephens R.B. (1973), 5th Int. Conf. on Amorphous and Liquid Semiconductors, 1121 (Edited by Stuke and Brenig).

Reese W. (1969), J. Macromol. Sci. Chem. A3, 1257.

Reese W. and Tucker J.E. (1965), J. Chem. Phys. 43, 105.

Rochlin G.I. (1970), Rev. Sci. Instr. 41, 73.

Rogers J.N. (1980), The thermal conductivity of polyethylene at very low temperatures, Unpublished Ph.D. thesis.

Scott T.A., de Bruin J., Giles M.M. and Terry C. (1973), J. Appl. Phys. 44, 1212.

Sharma J.K.N. (1967), Cryogenics 7, 141.

Stephens R.B. (1973), Phys. Rev. B 8, 2896.

Stephens R.B. (1976), Phys. Rev. B 13, 852.

Stephens R.B., Cieloszyk G.S. and Salinger G.L. (1972), Phys. Letts. 38A, 215.

Tucker J.E. and Reese W. (1967), J. Chem. Phys. 46, 1388.

Walton D. (1974), Solid State Commun. 14, 335.

Zaitlin M.P. and Anderson A.C. (1975a), Phys. Rev. B 12, 4475.

Zaitlin M.P. and Anderson A.C. (1975b), Phys. Stat. Sol. B 71, 323.

Zavaritskii N.V. and Zeldovich A.C. (1956), Sov. Phys. Technical Phys. 1, 1970.

Zeller R.C. and Pohl R.O. (1971), Phys. Rev. B 4, 2029.